Structure-property relationship in waterborne poly(urethane urea)s containing small amounts of graphene derivatives of different nature and surface chemistry

Abir Tounici

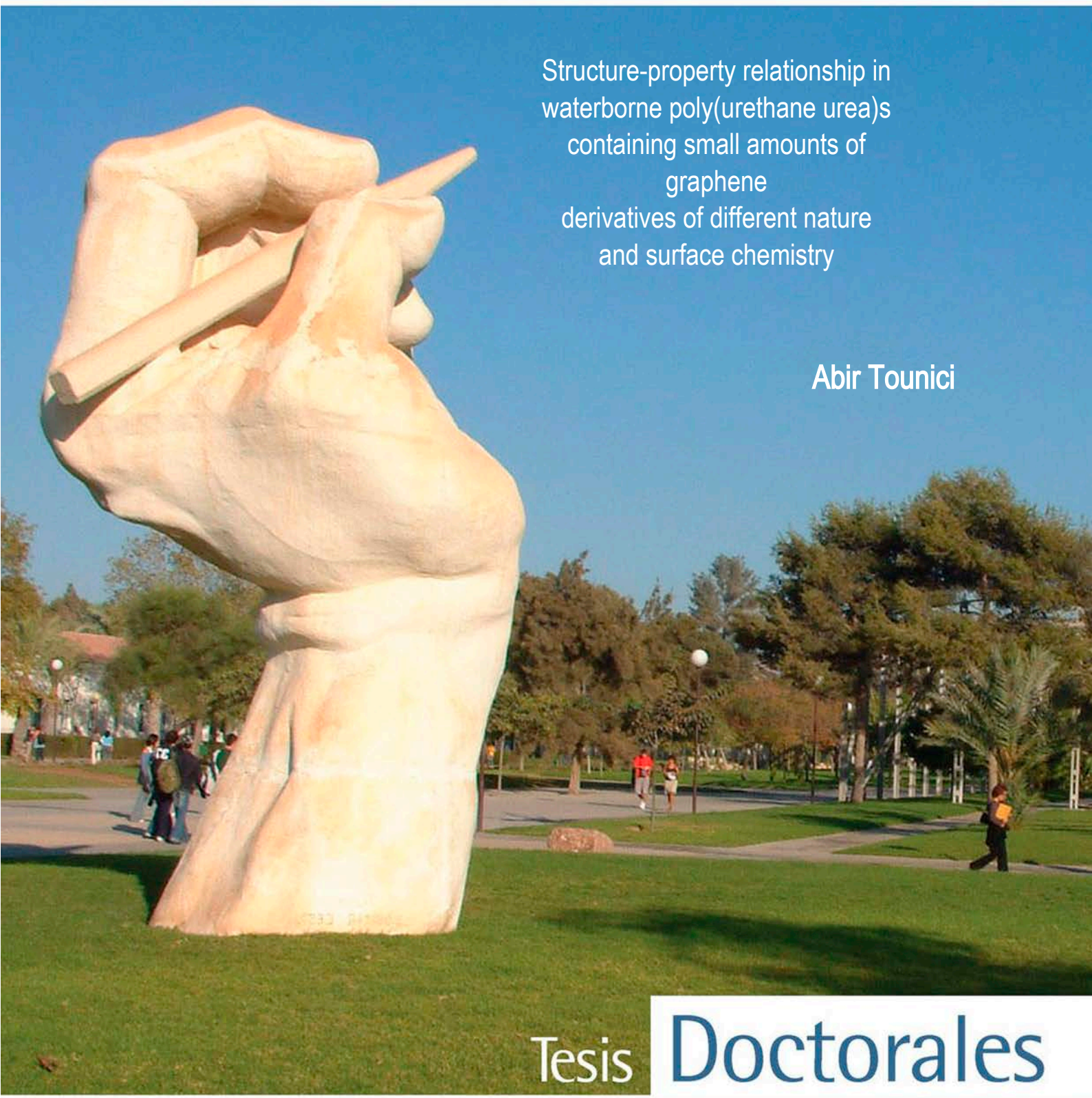

INSTITUTO UNIVERSITARIO DE MATERIALES DE ALICANTE
DEPARTAMENTO DE QUIMICA INORGANICA
FACULTAD DE CIENCIAS

Structure-property relationship in waterborne poly(urethane urea)s containing small amounts of graphene derivatives of different nature and surface chemistry

Abir Tounici

Tesis presentada para aspirar al grado de
DOCTORA POR LA UNIVERSIDAD DE ALICANTE
Mención de doctor internacional

Programa de Doctorado en Ciencias de Materiales

Dirigida por:
Prof. José Miguel Martín Martínez

José Miguel Martín Martínez, Catedrático de Química Inorgánica y responsable del Laboratorio de Adhesión y Adhesivos del Departamento de Química Inorgánica de la Universidad de Alicante.

HACE CONSTAR QUE

Que Abir Tounici ha realizado en el Laboratorio de Adhesión y Adhesivos del Departamento de Química Inorgánica de la Universidad de Alicante, bajo mi dirección, el trabajo de tesis doctoral titulado **"Structure-property relationship in waterborne poly(urethane urea)s containing small amounts of graphene derivatives of different nature and surface chemistry"** para aspirar al grado de Doctor en Ciencia de Materiales con Mención Internacional.

Alicante, 20 de diciembre de 2021

Fdo. José Miguel Martín Martínez

Laboratorio de Adhesión y Adhesivos

Departamento de Química Inorgánica

Universidad de Alicante

Index

Acknowledgments IX
Abbreviations XI
List of figures XIII
List of tables XVII
Summary XIX
Resumen XXIII
Structure of the thesis XXVII
Estructura de la tesis XXIX

First part. Summary and main achievements

1. Introduction 3
1.1 Waterborne polyurethane adhesives 3
1.2 Reagents used in the synthesis of waterborne polyurethane dispersions . 6
1.2.1 Polyol 6
1.2.2 Isocyanate 8
1.2.3 Internal emulsifier 9
1.2.4 Neutralization agent 10
1.2.5 Chain extender 11
1.3 Synthesis of the waterborne polyurethane dispersions 12
1.4 Graphene derivatives 14
1.4.1 Graphite 14
1.4.2 Graphene 15
1.4.3 Graphene oxide 19
1.4.4 Graphene nanoplatelets (GNPs) 21
1.5 Mixing methods in polyurethane-graphene oxide (PU-GO) blends 22
2. State of the art on waterborne polyurethane dispersions containing graphene derivatives 23
3. Objectives of the doctoral thesis 27
4. Experimental 28
4.1 Materials 28
4.2 Synthesis of the waterborne poly(urethane urea) dispersions (PUDs) 30
4.3 Experimental techniques 33
5. Main results and discussion 37

6. Conclusions 78
7. References 85
8. Future work 94

Second part. Copy of the published articles

1. "Addition of small amounts of graphene oxide in the polyol during the synthesis of waterborne polyurethane urea adhesives for improving their adhesion properties". Int. J. Adh. Adh. 2020; 104:102725 97

2. "Addition of graphene oxide in different stages of the synthesis of waterborne poly(urethane urea) adhesives and its influence on their structure, thermal, viscoelastic and adhesion properties". Materials. 2020; 13(13):2899. 99

3. "Influence of the surface chemistry of graphene oxide on the structure–property relationship of waterborne poly(urethane urea) adhesive". Materials. 2021,14:4377 101

4. "Structure and adhesion properties of waterborne poly(urethane ureas)s containing small amounts of different graphene derivatives". J. Adhes. Sci. Technol. 2021, 35(24), 2758-2789 103

Third part. Unpublished work

Electrical conductivities composites containing small amounts (less than 0.30 wt.%) of different graphene derivatives 107

1. Abstract 107
2. Introduction and objectives 107
3. Experimental 110
4. Results and discussion 113
5. Conclusions 120
6. References 120

Acknowledgments

During the development of this doctoral thesis, I have received great support and help. I would like to express my deepest gratitude to all people who have devoted a part of their time and dedication to the preparation of this doctoral thesis.

First and foremost, I am extremely grateful to my mentor and thesis supervisor Professor Jose Miguel Martín Martínez who has spent a lot of time researching and preparing this doctoral thesis as well as for his very interesting suggestions on how to direct the work. His immense knowledge and abundant experience encouraged me throughout my academic research, without him it would be impossible for me to complete my studies. I appreciate all of this.

I would like to express my deepest appreciation to Toñy for helping me whenever she could, for facilitating my laboratory work, and for taking care of me in the same way as I would be a part of her family.

I am deeply grateful to Dr. Mónica Fuensanta for her valuable support, which was really influential in my laboratory experiment methods.

My sincere thanks to all my colleagues in the LAA group (Carmen, Beatriz, Mari Carmen, Noemi, Sara) for helping me inside and outside the laboratory, and also for all their support in facilitating my stay and life at the university. Thanks for all the sweetest shared moments full of happiness.

I would like to thank Professor Maouche Naima for letting me stay in her laboratory even in the event of COVID-19, as well as for her advice and kindness. Furthermore, I would like to thank Amine for helping me during my stay in the laboratory.

I would like to thank Jaime Carpena for his help during my time in the LAA group.

My gratitude to Graphenea (San Sebastián, Spain), GrapheneTech (Zaragoza, Spain), and zEroCor/Carbon Upcycling (Calgary, Canada) for providing the graphene derivatives, and to Synthesia Technology (Barcelona, Spain) for supplying the polyol used in this study.

I dedicate this work to my father, Nour Eldine, my mother Faiza, my sisters Hadjer, Amira, and Romaissa, and my little brother, Hadj Mohamed, my aunt Soraya and her husband. They have always helped me, encouraged me, and led me to the right path by giving me will and confidence. God bless them. They have always been by my side with precious prayers which have pushed me for the better. Without their care and support from childhood to now, I would never have made it through this process in a successful way. I hope my work is a testament to my deepest gratitude and respect.

My special and big thanks to my husband Hocine for trusting me, making me believe I could do everything, and helping me all my life.

Abbreviations

IPDI	Aliphatic diisocyanate
DMPA	Dimethyl propionic acid
TEA	Triethylamine
HZ	Hydrazine
GO	Graphene oxide
r-GO	Reduced graphene oxide
A-GO	Amine-functionalized graphene oxide
GP	Graphene nanoplatelets
MG	Milled graphite
PUDs	Waterborne poly(urethane urea) dispersions
DBTDL	Dibutyltin dilaurate
XPS	X-ray photoelectron spectroscopy
XRD	X-ray diffraction
TGA	Thermal gravimetric analysis
TEM	Transmission electron microscopy
ATR-IR	Attenuated total reflectance Fourier transform infrared
DSC	Differential scanning calorimetry
TGA	Thermal gravimetric analysis
DMA	Dynamic mechanical thermal analysis
SEM	Scanning Electron Microscopy
PUs	Poly(urethane urea)s
T_g	Glass transition temperature
T_c(°C)	Cold crystallization temperature
$T_{m,ss}$	Melting temperature of the soft segments
$T_{m,hs}$	Melting temperature of the hard segments
$\Delta H_{m,ss}$	Melting enthalpy of the soft segments
G´	Storage modulus
CS	Cohesion failure of the substrate surface
CA	Cohesion failure of the adhesive
S	Rupture of substrate
C1s	Carbon 1s XPS spectra
E´	Storage modulus
DTGA	Differential thermogravimetric analysis

List of figures

First part. Summary and main achievements

Figure 1.1. Basic reaction of the synthesis of the polyurethanes. 3
Figure 1.2. Scheme of the segmented structure of polyurethanes. 4
Figure 1.3a. Scheme of the structure of one micelle/particle in the waterborne polyurethane dispersions. 5
Figure 1.3b. Scheme of the formation of the aggregation of the hydrophobic segments of the polyurethane chain in the center of the particle in the waterborne polyurethane dispersions. .. 6
Figure 1.4. Synthesis of polycaprolactone polyol (PCL). 8
Figure 1.5. Chemical structure of some aliphatic di-isocyanates. 8
Figure 1.6. Synthesis of isophorone diisocyanate. 9
Figure 1.7. Chemical structure of DMPA. 10
Figure 1.8. Stages of the synthesis of the waterborne polyurethane dispersions by using the acetone method. 13
Figure 1.9. Scheme of the formation of a polyurethane film from a waterborne polyurethane dispersion. 14
Figure 1.10. Structure of the graphite. 15
Figure 1.11. Structure of the graphene. 16
Figure 1.12. Different methods for obtaining graphene from graphite [35]. 17
Figure 1.13. Chemical functionalization of GO with different amine containing moieties [59,60]. (a) Melamine; (b) APTS: 3-aminopropyltriethoxysilane; (c) Dodecyl amine. 20
Figure 1.14. Structure of the graphene nanoplatelets (GNPs). 21
Figure 1.15. Different methods used for producing polyurethane-graphene oxide composites. 22
Figure 1.16. Stress-strain curves of GO/PU nanocomposites [68]. 24
Figure 1.17. Cross-hatch adhesion of graphene-sodium metaborate polyurethane composites on different substrates [78]. 25
Figure 1.18. T-peel adhesion of leather joints made with neat waterborne polyurethane and waterborne polyurethane nanocomposites [79]. 26
Figure 1.19. a. Hydrophobicity, and b. adhesion strength of waterborne polyurethane coating functionalized with graphene oxide [81]. 26
Figure 1.20. Scheme of the experimental system used for the synthesis of the waterborne poly(urethane urea) dispersions. 30
Figure 1.21. Mixing procedure of the graphene derivative and the polyol. 31
Figure 1.22. Dispersion of graphene oxide in acetone. 32
Figure 1.23. Dispersion of graphene oxide in water. 33
Figure 1.24a. Variation of the viscosity of the PUDs as a function of the shear rate. 38
Figure 1.24b. Variation of the viscosity at shear rate of 200 s^{-1} of the PUDs as a function of the amount of GO. 38
Figure 1.25. 1800-1600 cm^{-1} region of the ATR-IR spectra of the PUs. 39
Figure 1.26. Curve fitting of the carbonyl region (1800-1600 cm^{-1}) of the ATR-IR spectrum of the PU without GO. 39
Figure 1.27. 1800-600 cm^{-1} region of the Raman spectra of the PU and PU+GO materials. 40
Figure 1.28a. Variation of the weight as a function of the temperature for PUs. 42
Figure 1.28b. Variation of the derivative of the weight as a function of the temperature for PUs. . 42
Figure 1.29. Variation of the storage modulus (G´) as a function of the temperature for PU and PU+GO materials. 43
Figure 1.30. Confocal laser micrographs of the PU and PU+GO materials. 44

Figure 1.31. Variation of the water contact angle values on the PU and PU+GO materials as a function of the amount of GO. 45
Figure 1.32. Scheme of the interactions between the GO sheets and the end NCO groups of the prepolymer, and the intercalation of the GO nano-sheets during the phase inversion stage.. 46
Figure 1.33. Variation of the T-peel strength of plasticized PVC/PUD or PUD+GO dispersion/plasticized PVC joints as a function of the amount of GO measured 72 hours after joint formation. Locus of failure: CS - Cohesion failure of the substrate surface; CA - Cohesion failure of the adhesive; S - Rupture of a substrate. 47
Figure 1.34. Variation of the single lap-shear strength of stainless steel 304/PUD or PUD+GO/stainless steel 304 joints as a function of the amount of GO after 120 hours of joint formation. All joints show an adhesion failure to the stainless steel 304 substrate. 47
Figure 1.35. Synthesis of the waterborne poly(urethane urea) dispersions without and with 0.04 wt.% GO added in different stages of the synthesis. 48
Figure 1.36. Variation of the viscosity of PUD and PUD+0.04 wt.% GO dispersions as a function of the shear rate. 49
Figure 1.37a. 3600-2700 cm^{-1} region of the ATR-IR spectra of PU and PU+0.04 wt.% GO materials. 50
Figure 1.37b. 1400-900 cm^{-1} region of the ATR-IR spectra of PU and PU+0.04 wt.% GO materials. 50
Figure 1.38. X-ray diffractograms of PU and PU+0.04 wt% GO materials. 51
Figure 1.39. Variation of the storage modulus (G´) as a function of the temperature for PU and PU+0.04 wt% GO materials. Plate-plate rheology experiments. 53
Figure 1.40. Stress-strain curves of the PU and PU+0.04 wt% GO materials. 53
Figure 1.41. Variation of the viscosity of the PUDs without and with GO derivative as a function of the shear rate. 56
Figure 1.42a. 3500-2700 cm^{-1} region of the ATR-IR spectra of the PUs containing different GO derivatives. 56
Figure 1.42b. 1400-1000 cm^{-1} region of the ATR-IR spectra of the PUs containing different GO derivatives. 57
Figure 1.43. 1200-1000 cm^{-1} region of the Raman spectra of the PUs containing different GO derivatives. 58
Figure 1.44a. Variation of the weight of the PUs containing different GO derivatives as a function of the temperature. TGA experiment. 59
Figure 1.44b. Variation of the derivative of the weight of the PUs containing different GO derivatives as a function of the temperature. TGA experiment. 59
Figure 1.45a. Variation of the storage modulus (E′) as a function of the temperature for PUs containing different GO derivatives. DMA experiments. 61
Figure 1.45b. Variation of tan delta as a function of the temperature for PUs containing different GO derivatives. DMA experiments. 61
Figure 1.46. SEM micrographs of the fractured surfaces of the PUs containing different GO derivatives. 62
Figure 1.47. Scheme of the covalent linkages between the functional groups on the GO derivative surface and the end NCO groups of the prepolymer produced during PUD synthesis. 63
Figura 1.48. Variación de la viscosidad a 22 ºC de las PUDs que contienen diferentes derivados del grafeno en función de la velocidad de cizalla. 66
Figura 1.49a. Región de 3600-2700 cm^{-1} de los espectros IR-ATR de las PUs que contienen diferentes derivados del grafeno. 68
Figura 1.49b. Región de 1300-1200 cm^{-1} de los espectros IR-ATR de las PUs que contienen diferentes derivados del grafeno. 69
Figura 1.50. Región 1200-1000 cm^{-1} de los espectros Raman de las PUs que contienen diferentes derivados del grafeno. 70

Figura 1.51a. Variación del peso de las PUs que contienen diferentes derivados del grafeno en función de la temperatura. Experimentos TGA. 71
Figura 1.51b. Variación de la derivada del peso de las PUs que contienen diferentes derivados de grafeno en función de la temperatura. Experimentos TGA. 71
Figura 1.52a. Variación del módulo de almacenamiento (E ') en función de la temperatura para las PUs que contienen diferentes derivados del grafeno. Experimentos de DMA. 73
Figura 1.52b. Variación de tan delta en función de la temperatura para las PUs que contienen diferentes derivados del grafeno. Experimentos de DMA. 73
Figura 1.53. Curvas tensión-deformación de las PUs que contienen diferentes derivados del grafeno. 74
Figura 1.54. Micrografías de microscopía láser confocal de las PUs que contienen diferentes derivados del grafeno. 75
Figura 1.55. Micrografías SEM de las superficies fracturadas de las PUs que contienen diferentes derivados del grafeno. 76
Figura 1.56. Esquema de las interacciones entre los distintos derivados del grafeno y los segmentos duros y blandos de las poli(uretano urea)s. 77

Third part. Unpublished work

Figure 3.1. Scheme of the synthesis of the PUD/graphene derivative composites [16-19]. 111
Figure 3.2. Scheme of the four-point probe method for measuring the surface resistivity of the PU/graphene derivative composites. 112
Figure 3.3. Variation of the electrical conductivity of the PU/graphene oxide composites containing different amounts of GO as a function of the amount of GO. 114
Figure 3.4. Electrical conductivity of the PU/0.04 wt.% GO composites. Influence of the stage of addition of GO during synthesis. 115
Figure 3.5. Electrical conductivity of the PU/0.04 wt.% GO with different surface chemistry composites. 116
Figure 3.6. Electrical conductivity of the PU/graphene derivative composites. 117

List of tables

First part. Summary and main achievements

Table 1.1. Common polyols used in the synthesis of polyurethanes. 7
Table 1.2. Reagents used in the synthesis of the waterborne poly(urethane urea) adhesives. 29
Table 1.3. Relative contributions of the urethane and urea groups in the PU 40
Table 1.4. Some data obtained from the DSC traces of the PUs. Second heating run. 41
Table 1.5. Viscosities at 25 °C at different shear rates and pseudoplasticity index values of the PUDs. 49
Table 1.6. Some data obtained from the TGA thermograms of the PU and PU+0.04 wt% GO materials. At the end of TGA experiment, all PUs exhibit a residue of 2 wt.%. 52
Table 1.7. Some mechanical properties obtained from the stress-strain curves of the PU and PU+0.04 wt% GO materials. 52
Table 1.8. T-peel strength values of plasticized PVC/PUD or PUD+0.04 wt% GO/plasticized PVC joints. Locus of failure: CS - Cohesive failure of the substrate surface; CA - Cohesive failure of the adhesive; S - Rupture of a substrate. 54
Table 1.9. Atomic percentages of elements on the surface of the GO derivatives. XPS experiments. 54
Table 1.10. Binding energies and percentages of species on the surface on the GO derivatives. C1s spectra. 55
Table 1.11. Percentages of C=O species in the PUs containing different GO derivatives. Curve fitting of the carbonyl region of the ATR-IR spectra 57
Table 1.12. Some data obtained from the DSC traces of the PUs containing different GO derivatives. Second heating run. 58
Table 1.13. Water contact angle values at 25 ºC on the PUs containing different GO derivatives. 62
Table 1.14. T-peel strength values of the plasticized PVC/PUD or PUD+GO derivative/plasticized PVC joints obtained 72 hours after joint formation. Locus of failure: CS - Cohesion failure of the substrate surface; CA -Cohesion failure of the adhesive; S - Rupture of the PVC substrate. 64
Tabla 1.15. Cantidades de grupos funcionales de los derivados del grafeno. Experimentos TGA. 65
Tabla 1.16a. Porcentajes de elementos atómicos en la superficie de los derivados del grafeno. Experimentos de XPS. 65
Tabla 1.16b. Energía de enlace y porcentajes de especies de carbono en las superficies de los derivados del grafeno. Espectros C1s. 66
Tabla 1.17. Valores de las viscosidades (η) a 22 ºC a diferentes velocidades de cizalla e índice de adelgazamiento por cizalla de las PUDs que contienen diferentes derivados del grafeno 67
Tabla 1.18. Contribuciones relativas de los grupos uretano y urea libres y asociados en las PUs que contienen diferentes derivados del grafeno. Ajuste de la banda de carbonilo de los espectros IR-ATR. 69
Tabla 1.19. Algunos datos obtenidos de las curvas DSC de las PUs que contienen diferentes derivados del grafeno. 70
Tabla 1.20. Valores de fuerza de pelado de uniones PVC flexible/PUD/PVC flexible obtenidos 72 horas después de la formación de las uniones adhesivas. Tipos de fallos de las uniones: CS - Fallo de cohesión en la superficie del sustrato; CA - Fallo de cohesión del adhesivo; S - Rotura del sustrato. 77

Third part. Unpublished work

Table 3.1. Values of the electrical resistivity and the conductivity of the PU/graphene oxide composites containing different amounts of GO..... 113
Table 3.2. The percentage of associated urethane and urea groups in the PU/graphene oxide composites containing different amounts of GO. Curve fitting of the carbonyl band of the ATR-IR spectra [17]. 114
Table 3.3. Values of the electrical resistivity and conductivity of the PU/GO composites. Influence of the stage of addition of GO during synthesis..... 115
Table 3.4. Values of the electrical resistivity and conductivity of the PU/0.04 wt.% GO with different surface chemistry composites. 116
Table 3.5. Values of the electrical resistivity, the conductivity, the ratios of the intensities of the C-H stretching band with respect to the one of the C=O stretching (ATR-IR spectra) of the PU/graphene derivative composites......118
Table 3.6. Electrical conductivities of the PU/graphene composites in the existing literature and in this study. 119
Table 3.7. Variation of the electrical conductivities of the PU/graphene derivative composites with the time and temperature. 119

Summary

Waterborne poly(urethane urea) dispersions are an efficient and eco-friendly alternative to solvent-borne adhesives and coatings, but they have low viscosity, reduced tack, and limited mechanical properties. Several additives such as thickening agents, tackifiers, adhesion promoters, or fillers can be used for improving these properties. It has been shown that the addition of different carbon-based fillers (carbon nanotubes, activated carbon, carbon black) improved the thermal, rheological, and mechanical properties of different polyurethane adhesives. However, the addition of these fillers increased the viscosity and stiffness, and reduced the wettability of the polyurethane adhesives, so adding less filler amount without losing performance is desirable. The use of graphene derivative has the potential as a nanofiller for polyurethane adhesives and coatings, because of its high surface area, high aspect ratio, and efficient mechanical properties.

In this doctoral thesis, the influence of adding small amounts (i.e., less than 0.30 wt.%) of graphene derivatives of different nature and surface polarity, during the synthesis of waterborne poly(urethane urea) dispersions (PUDs). Affecting the properties of the PUDs mainly the adhesion properties, have been considered. This approach is novel in the existing literature and endorsed a better understanding of the structure-property relationship of PUDs containing graphene derivatives.

This doctoral thesis was written as a compendium of publications that were sequentially interrelated.

The first publication has explored the addition of different small amounts (0.01–0.10 wt.%) of graphene oxide (GO) during the synthesis of PUDs with the acetone method on their properties. GO was added to polyadipate of 1,4-butanediol polyol and the mixture was incorporated during prepolymer formation in the synthesis of the PUDs. The addition of 0.02–0.04 wt.% GO increased the T-peel strength, whereas the addition of 0.05–0.10 wt.% GO increased the single lap-shear strength. The improved adhesion of the PUDs containing GO was ascribed to the creation of covalent interactions between the surface groups on the GO surface and the NCO groups of the isocyanate during prepolymer formation, creating new urethane groups; during the phase inversion, the covalently bonded GO sheets were embedded between the polyurethane urea chains inside the PUD particles. As a consequence, the adhesion properties of the poly(urethane urea) containing GO films were different in the PU films containing 0.01–0.04 wt.% GO and the ones containing 0.05–0.10 wt.% GO.

The second publication has considered the addition of the "optimal" amount of GO (0.04 wt.%) in different stages of the synthesis of the PUDs, i.e., before prepolymer formation, after prepolymer formation, and during water addition. The addition of GO before and after prepolymer formation produced covalent bonds between the GO sheets and the NCO groups of the isocyanate, whereas the GO sheets were trapped between the polyurethane chains when added during the water addition stage. Depending on the stage of the PUD synthesis in which GO was added, the degree of micro-phase separation between the hard and soft segments changed differently. The addition of GO before prepolymer formation changed more efficiently the poly(urethane urea) structure. On the other hand, physical interactions between GO and the poly(urethane urea) chains were produced when GO was added to water during the synthesis, which is typical behavior of nanofiller polyurethanes.

In the third publication, the role of the surface chemistry of GO on the properties of PUDs containing 0.04 wt.% graphene derivative was assessed. Three different graphene derivatives were selected, graphene oxide – GO -, amine-functionalized GO – A-GO -, and reduced GO – r-GO -, and they were added before prepolymer formation during the synthesis of the PUDs. The addition of the graphene derivatives with different surface chemistry affected the structure of the poly(urethane urea)s differently. Due to the different extent of the covalent interactions between the surface groups on the graphene oxide derivatives and the end NCO groups of the prepolymer polyurethane, new urethane groups were formed. The GO and r-GO nano-sheets were covalently bonded to the urethane hard segments. On the other hand, the amine functional groups on the A-GO surface reacted preferentially producing new urea hard domains and because A-GO had thicker stacked graphene nano-sheets, a higher percentage of soft segments than in PU without GO derivative was produced. This led to a lower degree of phase separation in the poly(urethane urea). The addition of amine-functionalized graphene oxide and reduced graphene oxide altered the pH value of the waterborne poly(urethane urea)s, the viscoelastic properties of the PU films were also modified by adding 0.04 wt% graphene derivative. Depending on the functional group on the GO derivatives, the extent of shear-thinning of PUDs was reduced. However, the PU+GO showed lower thermal stability than other PUs; in addition, the toughness of the PU was improved by adding the GO derivatives. The addition of the GO derivative also affected the mechanical properties of the PUs, as the elongation-at-break increased although the tensile strength and the yield stress decreased. The addition of A-GO changed the wettability of the PU film due to the high polarity of the nitrogen functional groups. Furthermore, higher adhesion properties were obtained in the joints made with PUDs containing GO and r-GO.

In the fourth publication, small amounts (0.04-0-30 wt.%) of three different graphene derivatives - graphene oxide (GO), graphite nanoplatelets (GP), milled graphite (MG) - having different surface chemistry and number of stacked graphene sheets were added before prepolymer formation during the synthesis of the PUDs. The addition of graphene derivatives changed differently the degree of micro-phase separation of the poly(urethane urea)s depending on the balance between the number of covalent interactions due to the functional groups on the graphene sheets surface and the end isocyanate groups of the prepolymer, and the number of stacked graphene sheets. Whereas MG mainly intercalated between the soft segments showing a typical behavior of nanofiller, GP and, particularly, GO showed different degrees of micro-phase separation due to a higher number of covalent interactions with the poly(urethane urea) chains. The addition of graphene derivative decreased the glass transition temperature of the hard segments and increased the percentages associated by hydrogen bond urethane and urea groups, more noticeably by adding GP and MG. Lower temperatures of decomposition and higher amounts of urethane and urea hard domains, and soft domains were found in PU+GO and PU+MG, and they showed an additional structural relaxation at 11-16 ºC. PU and PU+GP had higher thermal stabilities than PU+GO and PU+MG and the addition of GP and, more markedly, GO imparted toughening to the poly(urethane urea). The T-peel strength values were higher in the joints made with PUD+GO, and the lap-shear strength of the joints made with PUD+MG and, to less extent, with PUD+GP noticeably increased.

In a visit to the Laboratory of Electrochemistry and Materials of the Department of Process Engineering of the University of Setif (Algeria), the electrical conductivity of the poly(urethane urea)s containing small amounts of different graphene derivatives was assessed. The addition of graphene derivatives increased the electrical conductivity and reduced the resistivity of the poly(urethane urea)s, and the electrical conductivity increased with the increase in the amount of GO. The electrical conductivity changed depending on the stage of the PUD synthesis in which GO was added. It was discovered that the highest electrical conductivity was obtained by adding GO in water. On the other hand, the different surface chemistry of the graphene oxide derivatives changed the electrical conductivity while the reduction of graphene oxide enhanced the transfer of electrons, this led to improved electrical conductivity of the poly(urethane urea). Additionally, the presence of functional groups on the GO surface reduced the electrical conductivity of the poly(urethane urea)s. Finally, the electrical conductivity of the poly(urethane urea)s containing various graphene derivatives was observed to be unstable over time, noticeably the highest electrical conductivity was obtained by adding milled graphite.

Resumen

Las dispersiones acuosas de poliuretano (PUDs) constituyen una alternativa eficiente y ecológica a los adhesivos y recubrimientos de poliuretano, pero su uso está limitado por su baja viscosidad, ausencia de tack y limitadas propiedades mecánicas. Para solventar estas limitaciones, se ha propuesto la incorporación de diferentes aditivos tales como agentes espesantes, agentes que imparten pegajosidad, promotores de adherencia y cargas/rellenos. Diferentes estudios previos han mostrado que la adición de diferentes rellenos a base de carbono (nanotubos de carbono, carbón activado, negro de carbón) mejoraban las propiedades térmicas, reológicas y mecánicas de diferentes adhesivos de poliuretano. Sin embargo, la adición de estos rellenos aumentaba la viscosidad y la rigidez, y reducían la mojabilidad de los adhesivos de poliuretano, por lo que sería deseable agregar menores cantidades de relleno sin que se perdieran las mejoras de las propiedades, el uso de derivados de grafeno tiene un gran potencial debido a su elevada superficie específica, alta relación de aspecto y buenas propiedades mecánicas.

En esta tesis doctoral se han adicionado diferentes pequeñas cantidades (0.01-0.30 % en peso) de distintos derivados del grafeno de diferente química superficial, polaridad, y número de nanoláminas de grafeno durante la síntesis de PUDs, para determinar sus propiedades, principalmente la adhesión. Este enfoque es novedoso en la literatura existente y permiten una mejor comprensión de la relación estructura-propiedades de las PUDs que contienen derivados del grafeno.

Esta tesis doctoral se ha realizado en la modalidad de compendio de publicaciones que se encadenan consecutivamente.

En la primera publicación se ha considerado la incorporación de diferentes pequeñas cantidades (0.01-0.10 % en peso) de óxido de grafeno (GO) en poliadipato de 1,4-butanodiol (poliol), y estas mezclas se han incorporado en la etapa de formación del prepolímero durante la síntesis de las PUDs. La adición de 0.02-0.04 % en peso de GO aumentó la fuerza de pelado en T, mientras que la adición de 0.05-0.10 % en peso de GO aumentó la fuerza de cizalla. La adhesión mejorada de los PUDs que contienen GO se atribuyó a la creación de interacciones covalentes entre los grupos superficiales en la superficie GO y los grupos NCO terminales del prepolímero, creando nuevos grupos uretano; durante la inversión de fases en agua, las nanoláminas de GO unidas covalentemente se intercalaron entre las cadenas de poli(uretano urea) entre las partículas

de PUD. Como consecuencia, las propiedades de adhesión de los PUDs que contienen GO fueron diferentes dependiendo de la cantidad de GO adicionada.

En la segunda publicación, se adicionó la cantidad “óptima” de GO (0.04 % en peso) en distintas etapas de la síntesis de las PUDs - antes de la formación del prepolímero, después de la formación del prepolímero, durante la adición de agua – determinando las propiedades de los mismos. La adición de GO antes y después de la formación del prepolímero produjo enlaces covalentes entre las nanoláminas de GO y los grupos NCO terminales del prepolímero, mientras que las nanoláminas de GO quedaron atrapadas entre las cadenas de poli(uretano urea) cuando se agregaban durante la etapa de adición del agua. En consecuencia, dependiendo de la etapa de la síntesis de la PUD en la que se añadió el GO, el grado de separación de microfases entre los segmentos duros y blandos cambió de manera diferente. La adición de GO antes de la formación del prepolímero cambió de manera más eficiente la estructura de las poli(uretano urea)s. Por otro lado, se produjeron únicamente interacciones físicas entre el GO y las cadenas de poli(uretano urea) cuando se añadió GO al agua durante la síntesis de las PUDs.

En la tercera publicación, se incorporó 0.04 % en peso de distintos GO con diferente química superficial - óxido de grafeno (GO), GO funcionalizado con amina (A-GO), GO reducido (r-GO) – durante la etapa de formación del prepolímero durante la síntesis de los PUDs. La adición de derivados de grafeno con diferente química superficial afectó de manera diferente a las propiedades estructurales de la poli(uretano urea), debido a la diferente extensión de las interacciones covalentes entre los grupos de superficie en los derivados de óxido de grafeno y los grupos NCO finales del prepolímero. Los nuevos grupos uretano se formaban por reacción entre los grupos C-O en la superficie de GO y r-GO con los grupos NCO finales del prepolímero. Las nano-hojas de GO y r-GO se unieron covalentemente a los segmentos duros de uretano. Por otro lado, los grupos amina en la superficie de A-GO reaccionaron preferentemente con el –NCO terminal del prepolímero produciendo nuevos dominios duros de urea; debido a que A-GO tenía nano-hojas de grafeno apiladas más gruesas, se produjo un porcentaje más alto de segmentos blandos que en PU sin derivado de GO. Esto condujo a un menor grado de separación de fases en la poli(uretano urea). La adición de óxido de grafeno funcionalizado con amina y óxido de grafeno reducido alteró el valor del pH de la dispersión de poli(uretano urea), así como modificó las propiedades viscoelásticas de las películas de poli(uretano urea) que contenían 0.04% en peso de derivado de GO. La adición del derivado de GO también afectó a las propiedades mecánicas de los PUs. La adición de A-GO cambió la mojabilidad de los PUs debido a la alta polaridad de los grupos nitrógeno, y las propiedades de

adhesión más altas se obtuvieron en las uniones realizadas con las PUDs que contenían GO y r-GO.

En la cuarta publicación, se incorporaron distintas cantidades (0.04-0.30 % en peso) de distintos derivados de grafeno de diferente polaridad y número de nanoláminas de grafeno apiladas - GO, nanoláminas de grafeno (GP), grafito molido (MG) – en la etapa de formación del prepolímero durante la síntesis de los PUDs. La adición de los distintos derivados de grafeno cambió de manera diferente el grado de separación de microfases de las poli(uretano urea)s dependiendo del equilibrio entre el número de interacciones covalentes entre los grupos funcionales superficiales de las nanoláminas de grafeno y los grupos isocianato terminales del prepolímero, y el número de nanoláminas de grafeno apiladas. Mientras que el MG se intercaló principalmente entre los segmentos blandos generando un comportamiento típico de un nanorrelleno, el GP y, en particular, GO mostraron diferentes grados de separación de microfases debido a un mayor número de interacciones covalentes con las cadenas de poli(uretano urea), de manera más marcada, al adicionar GO. La adición de los derivados de grafeno disminuyó la temperatura de transición vítrea de los segmentos duros y aumentó los porcentajes de grupos uretano asociados por enlace de hidrógeno y grupos urea libres, particularmente al adicionar GO y MG. PU+GO y PU+MG presentaban menores temperaturas de descomposición y mayor proporción de dominios duros y blandos, presentando una relajación estructural adicional a 11-16 ºC. PU y PU+GP presentaban mayores estabilidades térmicas que PU+GO y PU+MG, y la adición de GP y, sobretodo, GO impartió tenacidad a las poli(uretano urea)s. Las fuerzas de pelado en T fueron mayores en las uniones realizadas con PUD+GO y las fuerzas de cizalla fueron mayores en las uniones realizadas con PUD+MG y, en menor extensión, con PUD+GP.

En una visita al Laboratory of Electrochemistry and Materials del Department of Process Engineering de la Universidad de Setif (Argelia), se ha estudiado la conductividad eléctrica de las poli(uretano urea)s conteniendo diferentes pequeñas cantidades de distintos derivados de grafeno. La adición de los derivados de grafeno aumentó la conductividad eléctrica y redujo la resistividad de las poli(uretano urea)s, así como la conductividad eléctrica de las películas de poli(uretano urea) aumentaba al aumentar la cantidad de GO. Dependiendo de la fase de la síntesis de la PUD en la que se agregó GO, la conductividad eléctrica cambió, siendo mayor al adicionar el óxido de grafeno en agua. Por otro lado, los diferentes grupos superficiales de los derivados del óxido de grafeno cambiaron de manera distinta la conductividad eléctrica, la reducción del óxido de grafeno potenció la transferencia electrónica lo que mejoró la conductividad eléctrica en la poli(uretano urea)

que contenía r-GO. Por otro lado, la presencia de grupos funcionales en el GO redujo la conductividad eléctrica de las poli(uretano urea)s. Además, la conductividad eléctrica de las poli(uretano urea)s que contenían distintos derivados del grafeno era inestable con el tiempo, y la conductividad eléctrica más alta se obtuvo agregando grafito molido.

Structure of the thesis

The doctoral thesis is presented in the modality of compendium of publications, complying with the requirements established by the Internal Regulations of the Doctoral School of the University of Alicante.

The doctoral thesis is organized into three parts. The first part is dedicated to the summary of the doctoral thesis and consists of the main background of waterborne polyurethane dispersions, graphene derivatives, and the methods of mixing polyurethane-graphene materials. Then, the state of the art on the influence of the addition of graphene derivatives on the properties of waterborne polyurethanes has been described, followed by the objectives of the doctoral thesis. The description of the materials, the synthesis procedure, and the experimental techniques used in the doctoral thesis are summarized, followed by the summary of the main experimental results and the most relevant conclusions. At the end of the first part, the main references are given and the proposal for future works is described.

In the second part of the doctoral thesis, the four articles published in indexed journals are given. The first article focused on the addition of small amounts of graphene oxide in the polyol during the synthesis of waterborne poly(urethane urea) dispersions for improving their adhesion properties – *Addition of small amounts of graphene oxide in the polyol during the synthesis of waterborne polyurethane urea adhesives for improving their adhesion properties. Inter. J. Adh. Adh. 104, 102725 (2020)*. The second article focused on the addition of graphene oxide in different stages of the synthesis of the waterborne poly(urethane urea) dispersions and their influence on their structural, thermal, viscoelastic, and adhesion properties – *Addition of graphene oxide in different stages of the synthesis of waterborne poly(urethane urea) adhesives and its influence on their structure, thermal, viscoelastic and adhesion properties. Materials 13(13), 2899 (2020)*. The third article focused on the influence of the surface chemistry of graphene oxide on the properties of the waterborne poly(urethane urea) dispersions – *Influence of the surface chemistry of graphene oxide on the structure–property relationship of waterborne poly(urethane urea) adhesive. Materials 14, 4377 (2021)*. The fourth article focused on the structural and adhesion properties of the waterborne poly(urethane urea) dispersions containing different small amounts of different graphene derivatives – *Structure and adhesion properties of waterborne poly(urethane urea)s containing small amounts of different graphene derivatives. J. Adhes. Sci. Technol. 35, 24 (2021).*

In the third part of the doctoral thesis, the unpublished work related to the electrical conductivity of the waterborne poly(urethane urea)s containing different amounts of distinct graphene derivatives is given. This study was done during a visit to the Laboratory of Electrochemistry and Materials of the Department of Process Engineering of the University of Setif (Algeria).

Estructura de la tesis

La tesis doctoral se presenta en la modalidad de compendio de publicaciones, cumpliendo con los requisitos establecidos por el Reglamento Interno de la Escuela de Doctorado de la Universidad de Alicante.

El trabajo está estructurado en tres partes. La primera parte está dedicada al resumen del trabajo realizado incluyendo los conceptos básicos de poliuretanos, dispersiones acuosas de poliuretano, derivados del grafeno, y los métodos de mezcla de materiales poliuretano-grafeno. A continuación, se resume el estado del arte de la adición de derivados de grafeno a dispersiones acuosas de poliuretano, planteándose los objetivos de la tesis doctoral. Se describen los materiales empleados, los métodos de síntesis y las técnicas experimentales empleadas en la tesis doctoral, se resumen los principales resultados experimentales y las conclusiones más relevantes. Al final de la primera parte se enumeran las principales referencias utilizadas en el desarrollo de la tesis doctoral y se incluye una propuesta para futuros trabajos.

En la segunda parte de la tesis doctoral se recopilan los cuatro artículos publicados en revistas indexadas. El primer artículo trata de la adición de pequeñas cantidades de óxido de grafeno en el poliol durante la síntesis de adhesivos acuosos de poli(uretano urea) para mejorar sus propiedades de adhesión – *Addition of small amounts of graphene oxide in the polyol during the synthesis of waterborne polyurethane urea adhesives for improving their adhesion properties. Inter. J. Adh. Adh. 104, 102725 (2020)*. El segundo artículo trata de la adición de 0.04 % en peso de óxido de grafeno en diferentes etapas de la síntesis de los adhesivos acuosos de poli(uretano urea) y su influencia en su estructura, propiedades térmicas, viscoelásticas y de adhesión – *Addition of graphene oxide in different stages of the synthesis of waterborne poly(urethane urea) adhesives and its influence on their structure, thermal, viscoelastic and adhesion properties. Materials 13(13), 2899 (2020)*. El tercer artículo se centró en la influencia de la química superficial del óxido de grafeno en las propiedades de las dispersiones acuosas de poli(uretano urea) – *Influence of the surface chemistry of graphene oxide on the structure–property relationship of waterborne poly(urethane urea) adhesive. Materials 14, 4377 (2021)*. El cuarto artículo se centra en la estructura y propiedades de adhesión de dispersiones acuosas de poli(uretano urea) que contienen pequeñas cantidades de diferentes derivados del grafeno con distinta polaridad superficial y número de nanoláminas apiladas de grafeno – *Structure and adhesion properties of waterborne poly(urethane urea)s containing small amounts of different graphene derivatives. J. Adhes. Sci. Technol. 35, 24 (2021)*.

En la tercera parte de la tesis doctoral, se presenta el trabajo inédito relacionado con la conductividad eléctrica de las poli(uretano urea)s que contienen diferentes cantidades de distintos derivados del grafeno. Este estudio se realizó en una visita al Laboratorio de Electroquímica y Materiales del Departamento de Ingeniería de Procesos de la Universidad de Setif (Argelia).

First part. Summary and main achievements

1. Introduction

1.1 Waterborne polyurethane adhesives

Polyurethanes are polymers containing the urethane or carbamate group (-O-CO-NH -). Although they may also contain aliphatic or aromatic groups, as well as ester, ether, amide, etc, groups, their properties can be broadly tailored depending on the raw materials contained and synthesis parameters. Polyurethanes are basically synthesized by polyaddition or polycondensation reaction of isocyanates and compounds containing active hydrogen atoms, mainly hydroxyl groups (Figure 1.1).

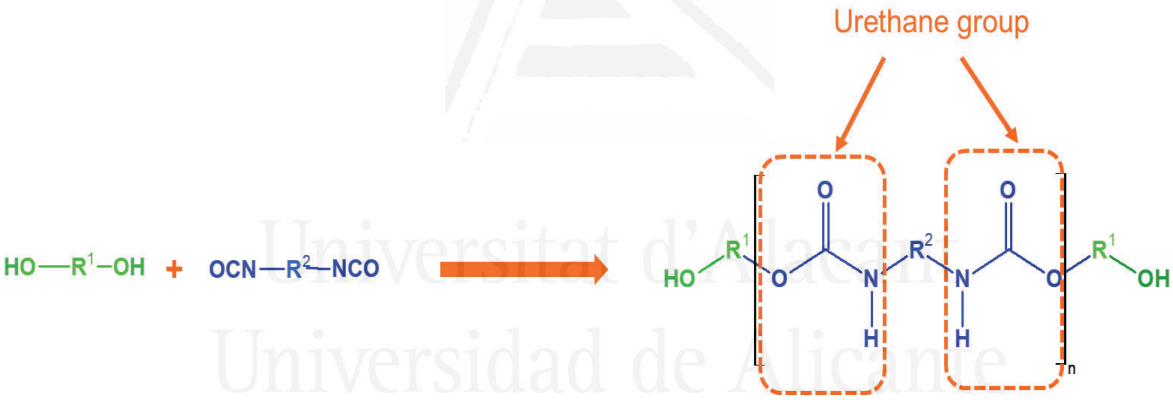

Figure 1.1. Basic reaction of the synthesis of the polyurethanes.

Isocyanates were first obtained in 1849 by Wurtz by reacting a salt of alkyl sulfuric acid with alkali metal cyanates, and the basic chemistry and technology of the polyurethanes were developed in 1937 by Otto Bayer and his coworkers at the laboratories of I.G. Farben in Leverkusen (Germany). Polyisocyanates were industrially available in 1952 and different polyester-polyisocyanate compounds were made by Bayer Company in 1952-1954. Polyurethane adhesives were developed in the mid-1970s and used in the automotive industry and, in 1984, Bostik produced the first polyurethane hot-melt adhesive [1].

Segmented polyurethanes can be considered as $(AB)_n$ block copolymers containing rigid (hard) and flexible (soft) segments, which are thermodynamically immiscible. The hard segments are made by reacting the diisocyanate with a low molecular weight diol or diamine

(chain extender), and they are polar and possess a high glass transition temperature (generally higher than 150 ºC). The soft segments are made of polyol (polyester, polyether, polyester, polycaprolactone, polycarbonate diol), and they are non-polar and have a low glass transition temperature (generally -30 to -70 ºC). The hard segments act as crosslinking centers and the soft segments as flexible structures. The degree of phase separation between the hard and soft segments determines the properties of the polyurethanes i.e., their structure-property relationships [2].

The crystallinity of the polyurethanes is generated by the formation of hydrogen bonds between the polyurethane chains (Figure 1.2) this contributes to the degree of phase separation and the creation of virtual cross-linking [3]. The hard segments significantly affect the mechanical properties of the polyurethanes, particularly their moduli, hardness, and tear resistance, while the soft segments affect their elasticity and flexibility [4]. In general, the increase of the degree of phase separation decreases the crystallization ability of the soft segments of the polyurethane adhesives. On the other hand, the crystallization of the hard segments restricts the ordered arrangement of long-chain diols and confines the crystallization ability of the soft segments [5].

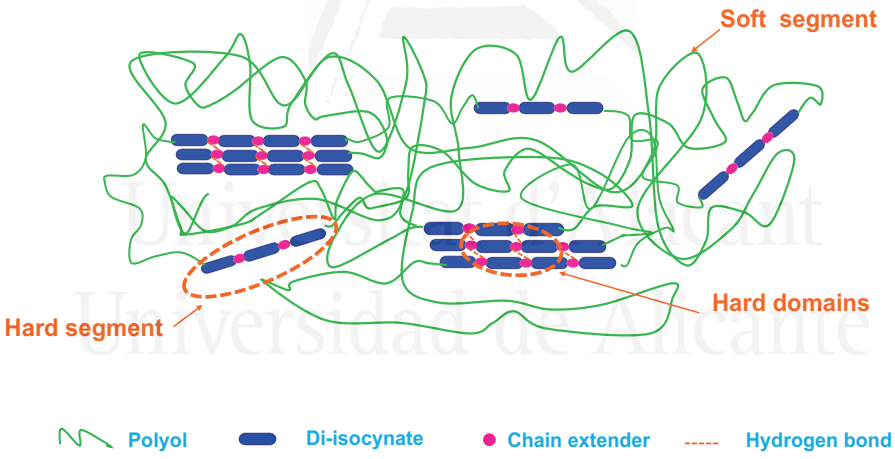

Figure 1.2. Scheme of the segmented structure of polyurethanes.

This doctoral thesis deals with waterborne polyurethane adhesives, therefore this introduction will focus on the understanding of the main aspects related to their composition, synthesis methods, and main structural features.

The ratio of the hard to soft segments (NCO/OH) determines the polyurethane properties, especially the adhesion properties, and affects the viscosity and particle size of the waterborne polyurethane adhesives [2,6,7]. On the other hand, the polyester soft segments

provide better mechanical properties and adhesive strength than the polyether ones. This affects the hydrolysis resistance and water-vapor permeability of the polyurethanes [8].

The polyurethane adhesives are certainly among the most versatile. A wide variety of urethane raw materials are commercially available, and, as a result, the bonding characteristics of the polyurethanes can vary widely. Polyurethane adhesives can be either flexible (thermoplastic) or rigid (thermoset), and they can be solvent-borne, waterborne, or 100 % solids. Although effective, during the last 20 years, the solvent-borne polyurethane adhesives have been replaced by more environmentally friendly and healthy polyurethane adhesives, the use of waterborne polyurethane adhesives is currently the most common alternative. However, the forced evaporation of water is an additional step needed for reaching an adequate adhesion, and they show low stability over time and under temperatures below 5 ºC.

Waterborne polyurethane adhesives are made of waterborne polyurethane dispersions (PUDs) containing a thickener (to increase the viscosity), a wetting agent, and an antifoaming agent. The water content in the waterborne polyurethane adhesives varies between 50 and 70 wt.%, and the major component is the PUD, which imparts their essential properties. Fillers are not commonly added in waterborne polyurethane adhesives because most of them are hydrophobic and produce phase separation. Waterborne polyurethane adhesives are commonly used in flooring, artificial skin, inks, shoes, decoration of textiles, membrane-press lamination, and outdoor applications, among others.

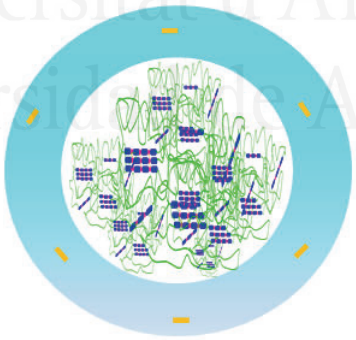

Figure 1.3a. Scheme of the structure of one micelle/particle in the waterborne polyurethane dispersions.

Aqueous polyurethane dispersions are colloidal binary systems in which the nanosized polyurethane micelles or particles are dispersed in water (Figure 1.3a). The stabilizing effect of the ionic centers during the ionomer dispersion process in water is due to the formation of tiny spheres or micelles due to the aggregation of the hydrophobic segments of the

polyurethane chain in the center of the particle which expose the ionic groups to the surface (Figure 1.3b). The shape and size of the micelles depend on the ionic strength, pH, temperature, and concentration. Since the polymer-water contact area is high, there is a tendency to produce the coalescence of micelles to minimize the contact surface between both phases which, by their nature, would be immiscible. The coalescence phenomenon is avoided because the micelles are structured in such a way that the ionic groups are directed outwards, physically integrated into water, constituting a double electrical layer that, due to electrostatic repulsion, keeps the micelles separate [9].

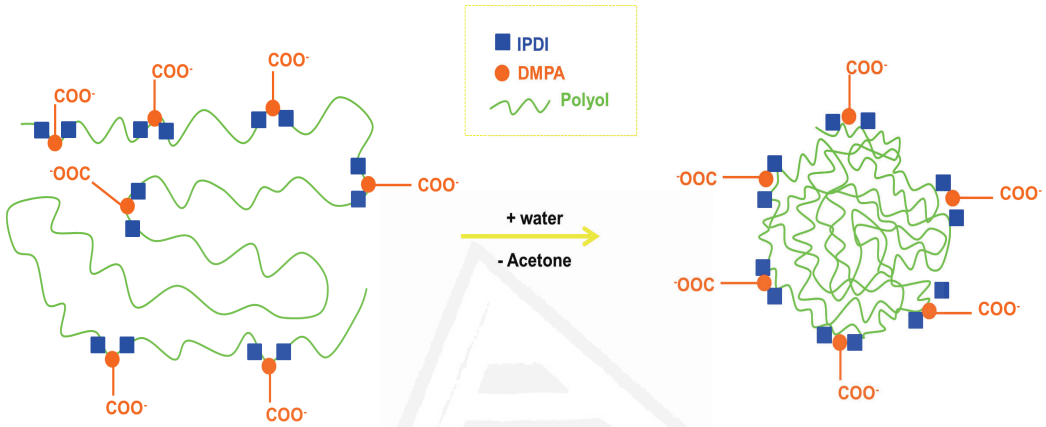

Figure 1.3b. Scheme of the formation of the aggregation of the hydrophobic segments of the polyurethane chain in the center of the particle in the waterborne polyurethane dispersions.

1.2 Reagents used in the synthesis of the waterborne polyurethane dispersions

Waterborne polyurethane dispersions are made by using different raw materials including polyol, isocyanate, internal emulsifier, neutralization agent, chain extender, and water. They are considered separately.

1.2.1 Polyol

Polyols are medium-high molecular weight (1000-8000 g mol^{-1}) macromolecules containing hydroxyl groups. Polyols constitute the soft segments of the waterborne polyurethane adhesives, conferring flexibility and toughness. There are different types of polyols depending on their chemical nature, molecular weight, and functionality. The most common

polyols used in the synthesis of polyurethanes are polyether and polyester polyols (Table 1.1).

Table 1.1. Common polyols used in the synthesis of polyurethanes.

Polyol		Chemical structure
Polyether	Poly (oxypropylene) (PPG)	$H(O\text{-}\underset{\displaystyle CH_3}{\underset{\vert}{CH}}\text{-}CH_2\text{-}O)_n\text{-}R\text{-}(O\text{-}CH_2\text{-}\underset{\displaystyle CH_3}{\underset{\vert}{CH}}\text{-}O)_mH$
	Tetramethylene oxide (PTMEG)	$H(O\text{-}(CH_2)_4\text{-})_mO\text{-}R\text{-}O\text{-}((CH_2)_4)_mH$
Polyester	Polyadipate	$HO\text{-}R\text{-}[\text{-}OOC\text{-}(CH_2)_4\text{-}COOR]_n\text{-}OH$
	Polycaprolactone	$HO\text{-}[\text{-}(CH_2)_5COO\text{-}]_m\text{-}R\text{-}[\text{-}OOC(CH_2)_5\text{-}]_n\text{-}OH$
	Polycarbonate diol	$HO\text{-}(\text{-}R\text{-}O\text{-}COO)_n\text{-}R\text{-}OH$

Polyether polyols are mainly polyalkylene glycols or polyalkylene oxides. These are synthesized by reacting epoxides with active hydrogen-containing reactants through polyaddition reaction via an anionic mechanism. Waterborne polyurethanes made with polyethers show improved water dispersion, high flexibility, and high hydrolytic resistance.

Polyester polyols are produced by reacting carboxylic acids and diols, and they have molecular weights between 400 and 6000 g mol^{-1}. The hydroxyl groups determine the functionality of the polyester polyols, and the decrease in the number of ester groups increases the hydrophobicity and the resistance to hydrolytic degradation of the polyurethanes. Furthermore, the polyurethanes made with polyester polyols show high mechanical strength under traction stresses and good color stability. Additionally, polyester polyols usually produce polyurethanes with higher mechanical properties and better oil resistance than the ones made with polyethers [10-12]. Polyesters are the most common polyols used in the synthesis of polyurethane adhesives due to their excellent balance between adhesion and cohesion properties.

Polycarbonate diol (PCD) polyols are considered as polyesters and they are obtained by condensation reactions between a dialcohol and a dialkyl carbonate using a catalyst that acts as Lewis acid. Polyurethanes made with PCD polyols have good heat, weathering, and hydrolytic resistance [10]. The polyurethanes made with PCD polyols exhibit higher hydrolytic stability than the ones made with polyester polyols because they absorb lower levels of moisture and they generate CO_2 upon hydrolysis without producing an acidic moiety; the acid moieties auto-catalyze the hydrolysis of the soft segments of the polyurethane. Although the polycarbonate diols are more expensive than other polyols, they are progressively used more in polyurethane coatings, adhesives, and elastomers requiring good strength and adequate resistance to aging.

Polycaprolactone polyols (PCL) are a special class of aliphatic polyester polyols, and they are prepared by ring-opening polymerization of ε-caprolactone in the presence of a catalyst (Figure 1.4). PCL-made polyurethane exhibits excellent hydrolysis resistance, and hydrophobic and biodegradable properties [13], therefore they are used in applications dealing with tissue engineering scaffolds, anti-biofilm materials, and biodegradable waterborne polyurethane dispersions [14]. Polyurethanes made with PCL polyols show high physical and mechanical properties.

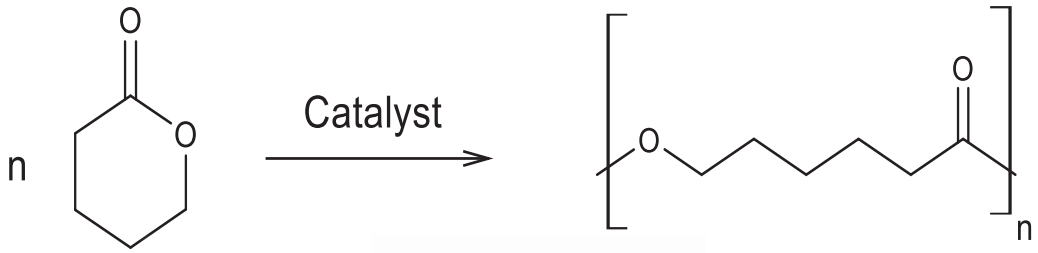

Figure 1.4. Synthesis of polycaprolactone polyol (PCL).

1.2.2 Isocyanate

The aliphatic, cycloaliphatic, or aromatic isocyanates containing two NCO groups are the most commonly used in the synthesis of the polyurethanes [15,16]. The most common aromatic isocyanates for adhesives, coatings, and sealants are toluene diisocyanate (TDI) and diphenylmethane diisocyanate (MDI), but they are scarcely used in the synthesis of waterborne polyurethane adhesives.

The most common aliphatic di-isocyanates used in the synthesis of the waterborne polyurethanes are isophorone diisocyanate (IPDI), hexamethylene diisocyanate (HDI), methylene dicyclohexyl diisocyanate and hydrogenated MDI - dicyclohexylmethane-4,4'diisocyanate (HMDI) (Figure 1.5) -, and polymeric versions of these diisocyanates are also utilized when light stability and/or reduced reactivity are needed.

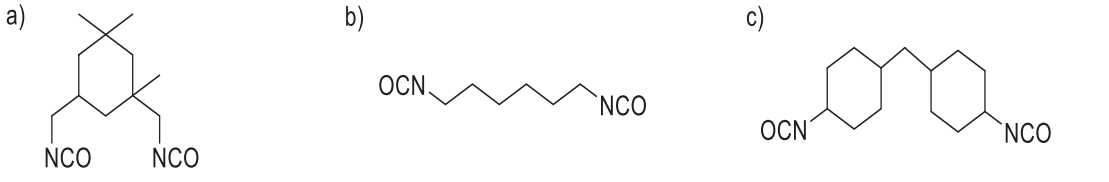

Isophorone diisocyanate (IPDI) | Hexamethylene diisocyanate (HDI) | Dicyclohexylmethane-4,4'diisocyanate (HMDI)

Figure 1.5. Chemical structure of some aliphatic di-isocyanates.

Isophorone diisocyanate (IPDI) is the most widely used di-isocyanate for the synthesis of waterborne polyurethane adhesives due to its low reactivity, which facilitates the control of the synthesis. Also, it produces stable adhesives [17]. IPDI is synthesized at the industrial level by phosgenation of isophorone followed by amination [18] -Figure 1.6.

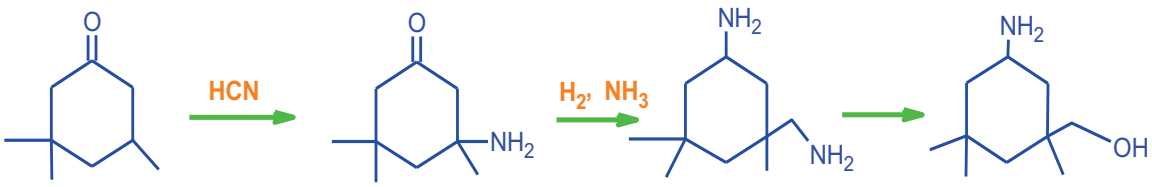

Figure 1.6. Synthesis of isophorone diisocyanate.

Isophorone diisocyanate is a colorless to yellowish liquid, which is pungent, smelly, and toxic. The low volatility of IPDI facilitates an easy and safe handle with respect to other isocyanates, in addition, it is insoluble in water and miscible with the most common organic solvents. IPDI exists in two forms, cis and trans, and is an asymmetric molecule with the secondary isocyanate group being less reactive than the primary isocyanate group. IPDI does not contain any groups that may oxidize or spontaneously ignite under ambient conditions [9].

1.2.3 Internal emulsifier

For the preparation of waterborne polyurethane dispersions, the presence of an internal surfactant or emulsifier is mandatory. A surfactant is characterized by having two groups with an opposite chemical nature in the same molecule, a hydrophobic group that repels water and a hydrophilic group with a good affinity for water. Aqueous polyurethane dispersions are prepared by adding internal emulsifiers or surfactants, and they have non-ionic centers such as polyethylene oxide or ionic centers such as anionic, cationic, and zwitterionic molecules. The polyurethane dispersions made with non-ionic internal emulsifiers contain a hydrophilic soft segment pendant group such as polyethylene oxide and they are colloidally stable in a wide range of pHs. The use of the internal emulsifier imparts adequate stability and good dispersion without applying high shear forces, and they allow the formation of particles or micelles with small particle size and high resistance to non-polar agents [19-21].

In waterborne polyurethane dispersions, the anionic internal emulsifier 2,2 bis(hydroxymethyl) propionic acid (DMPA) is the most commonly used (Figure 1.7). The chemical structure of DMPA consists of two hydroxyl groups capable of reacting with

isocyanate and one carboxylic acid. Due to its chemical nature, DMPA reduces the interfacial tension because it is placed between two media of different polarities. The DMPA concentration largely determines its solubility in water.

The mechanical, physical, and adhesive strength properties are affected by the nature and amount of the internal emulsifier. The increase in the amount of DMPA causes a decrease in the particle size of the waterborne polyurethane dispersion. In which case the increase in the ionic group content determines the interactions in the double electric layer of the particles [22,23].

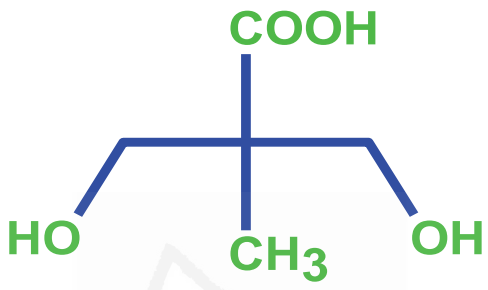

Figure 1.7. Chemical structure of DMPA.

The particle size of the waterborne polyurethane dispersion decreases with the increase in the stabilization of the micelles, which was ascertained by the homogeneity of the distribution of the ionic units. The presence of ionic groups in the hard segment has a considerable effect on its physical properties [24,25]. The anionic waterborne polyurethane dispersions made with DMPA have a small particle size and their stabilities are good. On the other hand, the addition of DMPA in different stages during the synthesis of the waterborne polyurethane changes its structure and properties, because the length of the prepolymer changes as well as the viscosity and the mean particle size. This is higher when DMPA is added after prepolymer formation [23].

1.2.4 Neutralization agent

During the synthesis of the waterborne polyurethanes, after prepolymer formation and before the chain extension stage, the neutralization stage is carried out; the neutralization step involves mono-ionic species to form hydrophilic sites to help the polyurethane to disperse in water. The protons of the ionic internal emulsifier need to change by a bulky counter-ion in order to impart stability.

Several neutralization agents with different counter-ions have been proposed for the synthesis of waterborne polyurethanes, including ammonia (NH_3), lithium hydroxide (LiOH),

sodium hydroxide (NaOH), potassium hydroxide (KOH), and tertiary amines such as triethylamine (TEA). In this study, triethylamine (TEA) was used as a neutralization agent, it produces ammonium carboxylate anion ($-COO^- HN^+ (C_2H_5)_3$) in the waterborne polyurethanes containing carboxylic groups (such as DMPA) [26]. Due to excellent water solubility and lack of active hydrogen atoms in TEA, the waterborne polyurethane dispersion neutralized with TEA shows good mechanical properties and gives high adhesive strength. On the other hand, the particle size of the waterborne polyurethane dispersion decreases with the increase of the degree of neutralization.

1.2.5 Chain extender

Chain extenders are usually low molecular weight (<400 g/mol) symmetric diols or diamines. They react with isocyanate-ended prepolymers to build polyurethane or polyurea molecules and in so doing increase the length of the hard segments [27]. In the synthesis of the waterborne polyurethane dispersions, the chain extension should be performed before the dispersion step, in order to avoid the competition of the isocyanate groups with water.

Generally, if a diol chain extender is used, the urethane group (NH-CO-O-) is obtained, while if a diamine chain extender is used, the urea group (-HN-CO-NH-) is formed, in this case, poly(urethane-urea)s are obtained. The absence of a chain extender in the synthesis of polyurethane leads to poor physical properties, as well as the absence of microphase separation. The chain extenders can be either aliphatic or aromatic. Their structure determines the rigidity of the hard segments and the extent of hydrogen bonding and virtual cross-linking [6].

Diamine chain extenders exhibited higher mechanical properties than diol ones [28] and favour the cohesion forces between the urea groups compared with the ones of the urethane linkages [29], in the case of the diol chain extender it provides a higher degree of crystallinity in the polyurethane structure and better adhesion properties [30].

The use of diamines in the synthesis of the aqueous polyurethane dispersions is widespread due to their greater reactivity with the isocyanate group with respect to diols, which allows chain extension in water. The most common diamines used as chain extenders in the waterborne polyurethanes are hydrazine (HD), ethylene diamine (EDA), 1,4-butane diamine (BDA), ethylene diamine (EDA), diethylene triamine (DETA), and triethylene tetramine (TETA). The different diamine chain extenders give different properties and structures of the hard domains in the waterborne polyurethanes [31].

1.3 Synthesis of the waterborne polyurethane dispersions

The synthesis of the waterborne polyurethane dispersions is mainly based on the reaction of a polyol (polyester or polyether polyol with terminal hydroxyl groups), a diisocyanate, and a chain extender (short-chain diamine). Furthermore, the addition of an internal emulsifier is required to impart dispersibility in water. There are four different methods for synthesizing waterborne polyurethane dispersions: pre-polymer mixing, acetone process, hot-melt, and ketimine-ketazine.

The prepolymer mixing process consists of the synthesis of a hydrophilically modified prepolymer with free isocyanate groups which is mixed with water. Chain extension with amines in the aqueous phase is then accomplished.

In the hot-melt process, a low viscous prepolymer in solution is reacted with urea or ammonia to form a capped oligomer with terminal biuret groups. Chain extension with amines in the aqueous phase is then accomplished.

In the ketamine/ketazine process, the isocyanate prepolymer is blended with a blocked amine (ketamine) or hydrazine (ketazine) and dispersed in the aqueous phase. In contrast to the prepolymer mixing process, the liberated amine is homogeneously distributed in the dispersed particles.

The most common procedures used in the manufacture of waterborne polyurethane dispersions are the acetone and the prepolymer mixing methods, and, in this study, the acetone method for the synthesis of the waterborne poly(urethane urea) was used.

The acetone method allows the homogeneous synthesis of the waterborne polyurethane dispersions, with high control of the molecular weight (a necessary condition to obtain good adhesive properties) and the ionic groups of the poly(urethane-urea) chains are properly oriented during the dispersion in water [32]. In this method, the polyol, the internal emulsifier and the diisocyanate react for forming a prepolymer with terminal -NCO groups (Figure 1.8). The process continues through the addition of the organic solvent (acetone) to reduce the viscosity of the prepolymer. Then, the protons of the internal emulsifier are neutralized by adding a tertiary amine, and the polymer formation takes place by adding the chain extender followed by the addition of water to produce the phase inversion. By distillation, the organic solvent (acetone) is removed rendering the waterborne polyurethane dispersion with small particle sizes. Depending on the content of the ionic groups, the particle size and stability of the waterborne polyurethane dispersions vary.

The study of the stability of the waterborne polyurethane dispersions is of great importance to prevent their impairment during the storage since they are thermodynamically unstable systems that tend to coalesce under freezing conditions or excessive temperature. The

stability of the waterborne polyurethane dispersions is determined by the pH, the presence of electrolytes, mechanical stresses, and temperature.

The thermal, mechanical, electrolytical properties and pH stability of the waterborne polyurethane dispersions depend on the internal stabilization system used in their syntheses. The increase of the pH could increase the viscosity of the waterborne polyurethane dispersions, and strong acidic conditions normally cause precipitation or coagulation. Also, the presence of electrolytes in the waterborne polyurethane dispersion can cause stability problems, so the presence of electrolytes must be controlled and double-distilled and deionized water should be used during the synthesis.

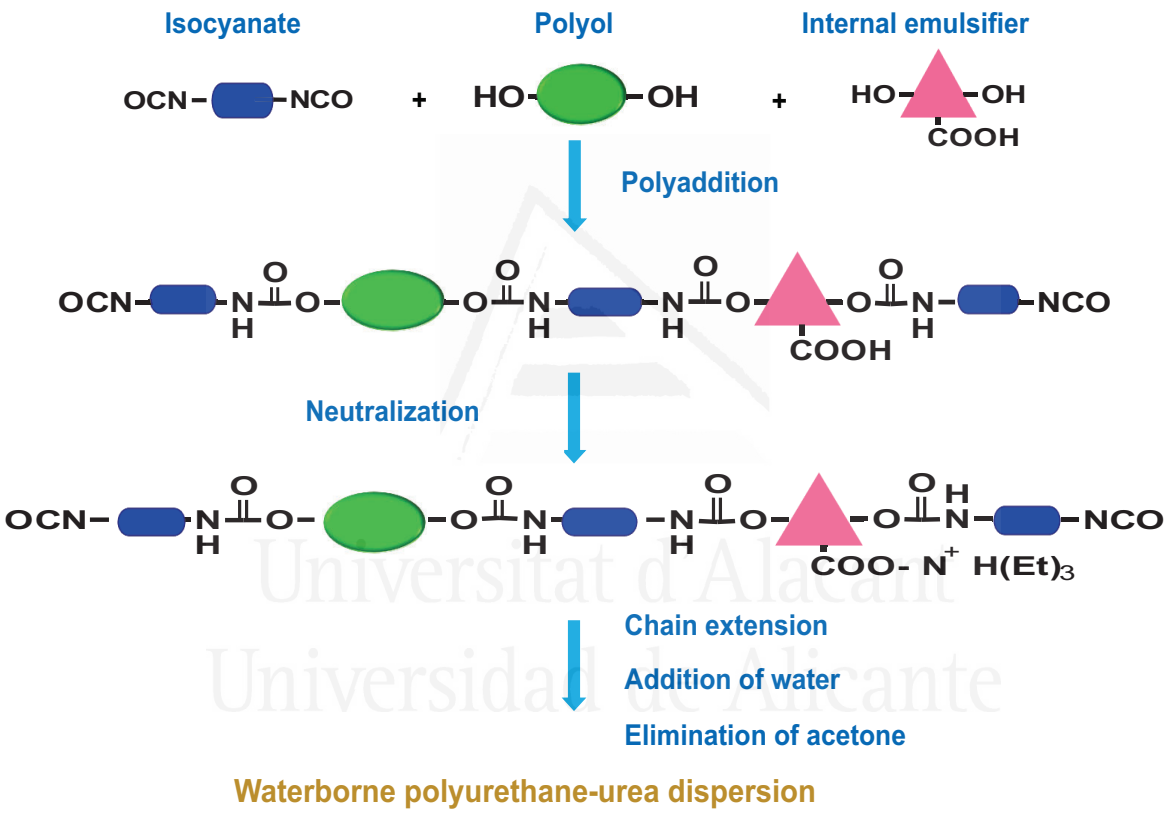

Figure 1.8. Stages of the synthesis of the waterborne polyurethane dispersions by using the acetone method.

The process of forming solid polyurethane films from the waterborne polyurethane dispersions is crucial for adequate performance and is summarized in Figure 1.9. The polyurethane films are formed by a coalescence process, in which the individual polymer particles coalesce as water is lost during drying. Consequently, the particles are deformed and eventually interdiffusion at the molecular scale.

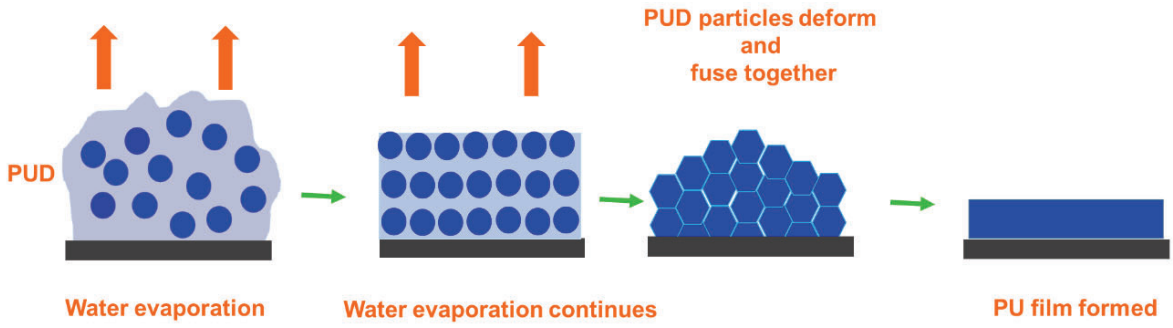

Figure 1.9. Scheme of the formation of a polyurethane film from a waterborne polyurethane dispersion.

The coalescence process of the waterborne polyurethane dispersions is highly dependent on different parameters, being aided by the decrease of the particle size, the decrease of the glass transition temperature (T_g), the addition of co-solvent, the absence of crosslinking, etc. On the other hand, the increase of the solids content is a way to decrease the drying time of the waterborne polyurethane dispersion, mainly on non-porous substrates.

In ionomeric polyurethanes, the domain structure is stabilized by hydrogen bonds and reinforced by coulombic interactions between the ionic groups. The existence of small amounts of water in the film acts as a plasticizer because it interacts with the polar groups of the polyurethane, blocking the formation of the structure of the domains. As a result, the structure is totally stable when the water is completely removed, which only happens after several days at room temperature.

1.4 Graphene derivatives

In this doctoral thesis, several graphene derivatives have been used. Their main features are given separately below.

1.4.1 Graphite

Before 1565, graphite was used for marking sheep in Borrowdale Parish (Cumbria, England), and was also used as a refractory material to line molds, and for cannonballs and softballs of the English Navy. This particular deposit of graphite in Borrowdale Parish was very pure and soft, and could be cut into sticks. In 1789, Abraham Gottlob Werner (a German geologist) named the material as "graphite" which means writing stone because it

was used in the manufacture of pencils, although the terms Plumbago and black lead were also used.

Graphite is a common allotrope of carbon and the most stabilized form of carbon. The carbon atoms are arranged in hexagonal sheets (Figure 1.10), giving a honeycomb lattice with a C-C distance of 0.142 nm and a distance between the graphite sheets of 0.335 nm. Every hexagonal sheet of carbon atoms is called graphene in which the carbon atoms possess sp^2 hybridization and their bond angle is 120°. The van der Waals forces holding the layers of graphene are caused by the polarization of the carbon molecules. Graphite has a giant covalent structure in which each carbon atom is joined to three other carbon atoms by covalent bonds imparting high thermal and electrical conductivity, and it is highly refractory and chemically inert. Furthermore, graphene is flexible and shows extraordinary mechanical properties.

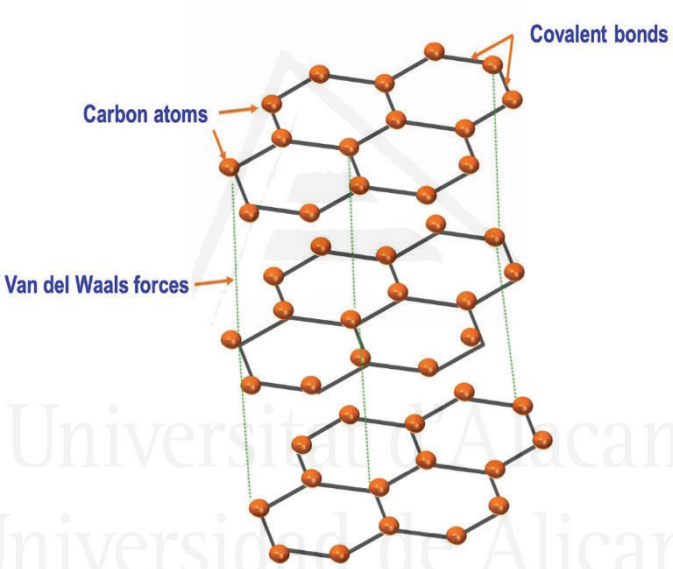

Figure 1.10. Structure of the graphite.

The milling process of the graphite changes its particle size as well as helps in the ordering of the graphitic sheets. Furthermore, the milling improves the chemical reactivity and increases the specific surface area of the graphite, but also a disorder at the atomic scale is produced [33,34].

1.4.2 Graphene

Graphene is the building block of graphite, i.e., one atom thick layer of graphite (Figure 1.11). It is the structural element of other allotropes of carbon, including graphite, carbon nanotubes, and fullerenes.

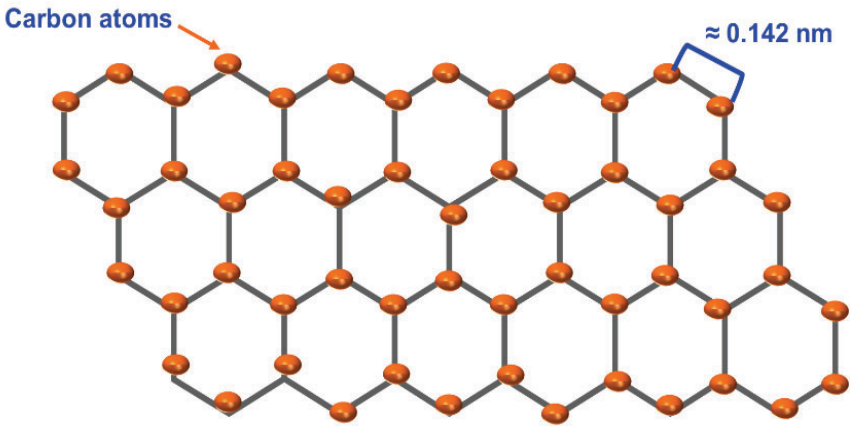

Figure 1.11. Structure of the graphene.

Graphene is the strongest, thinnest element known to exist, with a 2-dimensional (2D) structure. It was discovered and isolated at room temperature by Andre Geim and Konstantin Novoselov in 2004, although was first mentioned in 1946. Chemically, graphene is the most reactive form of carbon. Graphene burns at relatively low temperatures and the carbon atoms at the edges own special chemical reactivity. Graphene is the strongest material ever measured and up to 150 times stronger than the comparable weight of steel, it is flexible as rubber and remarkably lightweight, and has great electrical conductivity.

Graphene can be obtained from graphite by using different methods, which are summarized in Figure 1.12.

- Micromechanical cleavage or micromechanical exfoliation: This process was used by Andre Geim and Konstantin Novoselov. An adhesive tape is pressed onto the graphite and exfoliated away (Figure 1.12(a)); this tape is applied onto the surface of a substrate and peeled off, then transferred onto a thin SiO_2 wafer [35].
- Anodic bonding: It is commonly used in the microelectronics industry to bond Si wafers to glass, to preserve them from humidity and/or contamination. Graphite is first pressed onto a glass substrate; a high voltage is used between the graphite and a metal back connection (Figure 1.12(b)). The glass substrate is then heated. If a positive voltage is connected to the top contact, a negative charge grows in the glass side facing the positive electrode, then a few layers of graphite stick to the glass by electrostatic interaction [36].
- Laser ablation and photoexfoliation: The laser can be used to ablate/exfoliate graphite flakes (Figure 1.12(c)). By harmonizing the laser energy density, the accurate patterning of the graphene can be produced. The ablation of a determined number of layers can be obtained by exploiting the laser energy density window. The laser ablation method is yet in its infancy and needs further development [37].

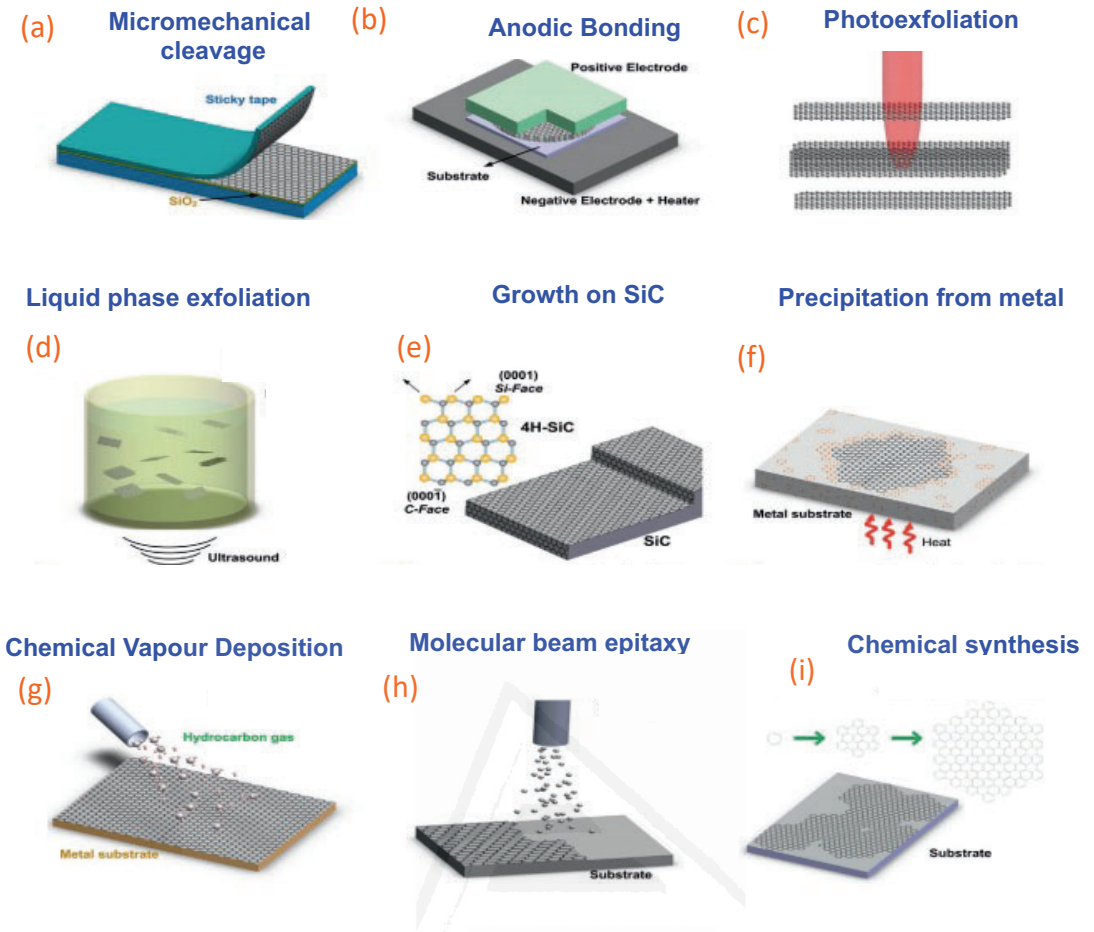

Figure 1.12. Different methods for obtaining graphene from graphite [35].

- Liquid-phase exfoliation (LPE): Graphite can be exfoliated in individual layers with ultrasounds in a liquid environment (Figure 1.12(d)) [35]. The liquid-phase exfoliation process generally involves different steps, including the dispersion of graphite in a solvent, the exfoliation, and the purification. A different step is necessary to separate the exfoliated from the non-exfoliated flakes and is usually carried out by ultracentrifugation. This process increases the interlaminar distance of the graphite, thus reducing the interactions between graphene layers which are lately separated by ultrasounds [38].
- Growth on silicon carbide (SiC): This method produces epitaxial graphene with dimensions conditioned by the size of the wafer on which silicon is evaporated after heat treatment of SiC. The surface polarity of the SiC highly determines the thickness of the graphene, the heating of SiC at high temperatures under low pressure causes its reduction to graphene (Figure 1.12(e)) [39].
- Growth on metals by precipitation: Graphene can also be obtained from carbon overfilled molten Fe during the production of steel. In this method, Fe is supersaturated with carbon, and the excess carbon precipitates render the so-

called “Kish graphite” (Figure 1.12(f)). In order to eliminate the competition between the formation of carbide and graphite/graphene growth, the use of non-carbide forming metals, such as Cu, Ni, Au, Pt, or Ir, is preferred. The graphite film thickness depends on the metal, and the solubility of the carbon in that metal. The growth of graphene by precipitation requires a careful control of the metal thickness, the temperature, the annealing time, the cooling rate, and the metal microstructure [40].

- Chemical vapor deposition (CVD): A process generally used to deposit thin films from solid, liquid or gas precursors (Figure 1.12(g)). The method of deposition of solid material over a heated substrate throughout decomposition or chemical reaction of compounds in the gas passing over the substrate is called chemical vapor deposition [41]. CVD is a widely used bottom-up method for synthesizing low-layer and single-layer graphene films. There are many different CVD methods for synthesizing graphene-based materials, and the choice depends on the processing parameters (wall/substrate temperature, nature of the precursor, pressure, temperature, etc). The most common method is the CVD hot wall in which the reaction chamber is fully heated in the oven to provide sufficient energy for the solidification of the growth substrate and the subsequent decomposition of the feedstock. In the CVD cold wall method, the growth substrate is heated directly to the required growth temperature in the chamber. In the plasma-enhanced CVD (PECVD), the high-frequency voltage ignites the plasma in a low-pressure gas (hydrocarbon) stream and the collisions in the reactor led to the formation of reactive species required for graphene deposition [42].
- Molecular beam epitaxy (MBE): Molecular beam epitaxy (MBE) is widely used and well suited for the deposition and growth of semiconductors (Figure 1.12(h)), and it has been utilized to grow graphitic layers with high purity. However, these graphitic layers have a large domain of defective crystals, because MBE relies on atomic beams of elements impinging on the substrates, so it is hard to prevent carbon from being deposited on areas where graphene already has grown [35].
- Chemical synthesis: Graphene can also be chemically produced from polycyclic aromatic hydrocarbons (PAHs) by surface-mediated reactions (Figure 1.12(i)). Two approaches can be utilized consisting of a dendritic precursor transformed by cyclo-dehydrogenation and planarization, or in PAH pyrolysis. Chemical synthesis is promising for obtaining graphene but needs development at a large scale [35,43,44].

1.4.3 Graphene oxide

Graphene oxide (GO) is a single-atomic layered material produced by the strong oxidation of graphite following the methods proposed by Brodie, Hummers, and Staudenmaeir [45,46]. Brodie was the first who discover the ability to oxidize graphite in 1859. Staudenmaier [45] developed Brodie´s method with the addition of concentrated sulfuric acid and potassium perchlorate in multiple aliquots over the course of the reaction rather than in a single addition. In 1957, Hummers and Offeman discovered a new quicker, and more efficient method for synthesizing GO, in which a mixture of sulfuric acid (H_2SO_4), sodium nitrate ($NaNO_3$), and potassium permanganate ($KMnO_4$) was used [46]. This process is commonly used in producing GO, often with some modifications.

Graphene oxide consists of two-dimensional sheets of single carbon atoms arranged in a honeycomb structure in which the carbon has sp^2 hybridization. GO has a multilayer structure containing oxygenated hydrophilic sheets, these oxygenated functional groups consist of phenolic hydroxyl (-OH), epoxy (C-O-C), carboxyl (-COOH), and carbonyl (-C=O) groups [47]. Also, the GO can be produced in high volumes and is hydrophilic, the GO nanosheets can easily be dispersed into polymers, and can be chemically functionalized (for example, by oxygen removal). Due to their planar structure, the GO sheets can be easily self-assembled to create an ordered macroscopic structure. Moreover, the hydrogen bond in GO plays a major role in improving the mechanical properties of several materials. For example, the action of the strong H-bonds is the primary factor in the remarkable extensibility and tensile strength of several polymers containing GO [48].

Graphene oxide (GO) is a carbon-based nanomaterial that has attracted the interest of researchers due to its unique properties including high specific surface area (~2630 $m^2\ g^{-1}$) [49], high intrinsic mobility (up to $2x10^5\ cm^2\ V^{-1}\ s^{-1}$) [50], high Young modulus (~1 TPa) [51], high mechanical stiffness (>10^3 GPa) [52], and exceptionally high thermal conductivity [53]. The presence of oxygen-containing groups increases the interlayer space in the GO.

A significant part of the oxygen-containing functional groups can be easily removed from the basal plane of the GO nano-sheets due to their great surface reactivity; this produced the so-called reduced graphene oxide (r-GO). The r-GO is usually obtained by thermal and chemical methods. The thermal methods consist of heating or irradiation (infrared-visible, ultraviolet (UV), or microwave) methods in an inert, vacuum, or reduced pressure atmosphere [54]. On the other hand, the chemical reduction can be produced with hydrazine, sodium borohydride, hydrogen sulfide, hydroquinone, sodium borohydride, hydrohalic acid, or ascorbic acid, the most common is hydrazine [55]. In general, the chemical method is preferred because no special equipment is needed hence reduced

expenses [56]. GO can be functionalized with small molecules or by polymer intercalation [57] - functionalized graphene oxide. Non-covalent functionalization of GO involves hydrogen bonding, van der Waals forces, π-π or π-cation interactions [48]. Several functional groups produce different characteristics, and the covalent functionalization happens on the carboxylic or epoxide groups of the GO nano-sheets.

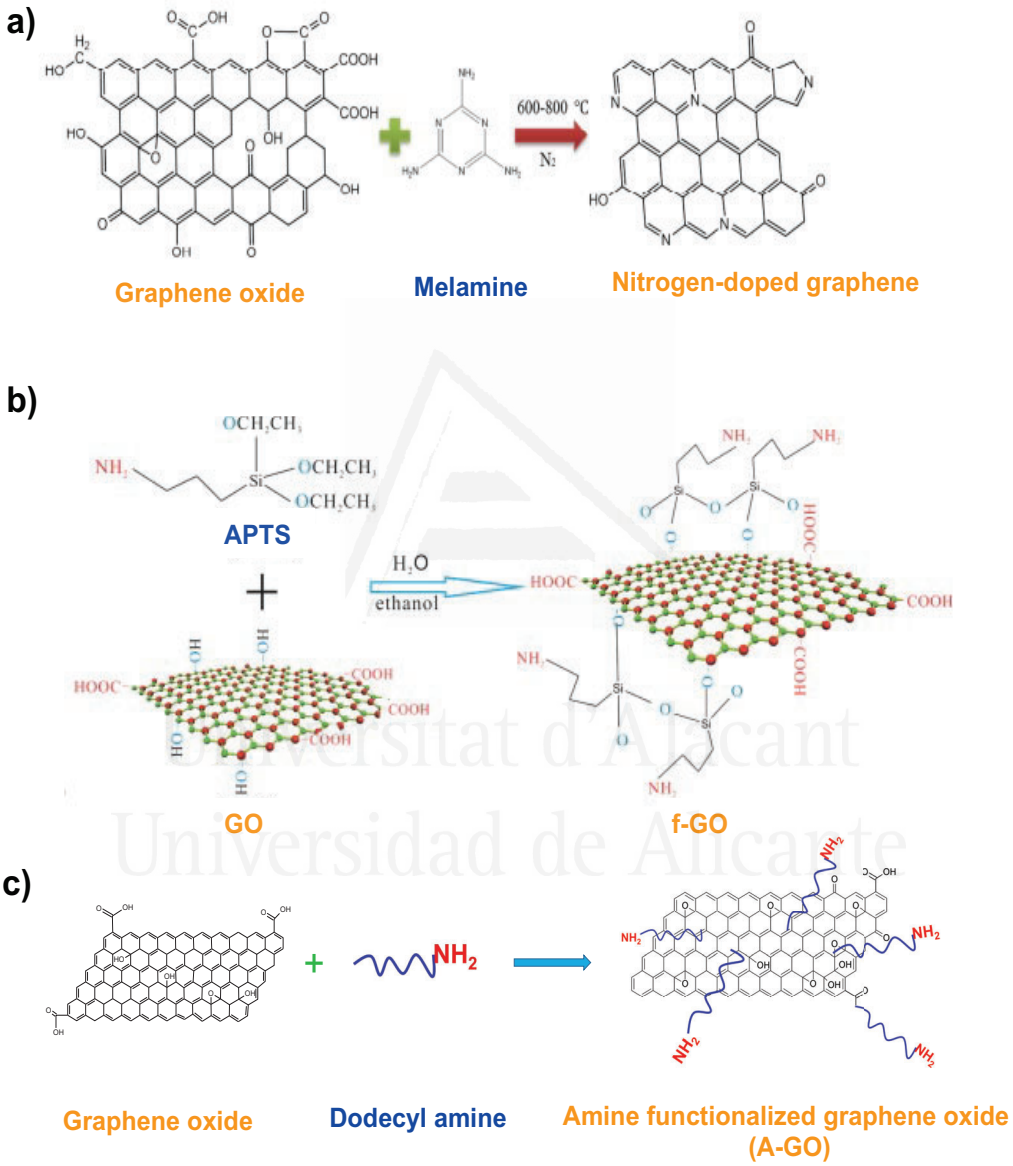

Figure 1.13. Chemical functionalization of GO with different amine containing moieties [59,60]. (a) Melamine; (b) APTS: 3-aminopropyltriethoxysilane; (c) Dodecyl amine.

Different studies [58-61] have been devoted to the functionalization of GO with organic or inorganic substances and molecules. The organic covalent functionalization of GO is

generally carried out by using two methods: formation of covalent bonds between free radicals or dienophiles and C=C bonds from pristine GO, and the creation of covalent bonds between the organic functional groups in the precursor and the surface oxygen groups of GO. On the other hand, GO can be grafted with polymeric chains containing reactive species like hydroxyl and amines, such as poly(ethylene glycol), polylysine, polyallylamine, poly(vinyl alcohol), and polyurethane [58]. Nitrogen functional groups can be grafted onto the GO surface by treatment with amines (Figure 1.13 (a) and (b)) [59,60], the higher nucleophilic properties of nitrogen with respect to oxygen may facilitate the reaction with several polymers [61]. In this study, a commercial amine grafted GO made by reaction with dodecylamine was used (Figure 1.13 (c)).

1.4.4 Graphene nanoplatelets (GNPs)

Graphene nanoplatelets (GNPs) are two-dimensional carbon structure materials made of multi-graphene layers interacting by van der Waals forces and strong π-π interactions [62]. GNPs can be produced from graphite through chemical exfoliation, thermal shock, and shear stresses, or in a plasma reactor.

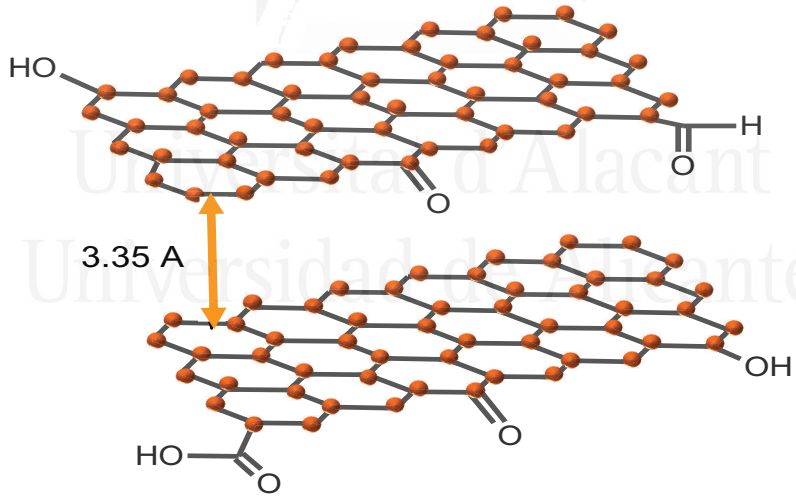

Figure 1.14. Structure of the graphene nanoplatelets (GNPs).

GNPs have become a low-cost alternative to graphene with adequate properties and mass production potential. GNPs have a small number of layers of graphene (usually 5 to 20 layers) and can be envisioned as stacks of parallel sheets of hexagonal carbon atoms (Figure 1.14), the thickness varies between 0.7 and 100 nm. The use of GNPs can replace conventional nanoparticles, expanding their applications, and they are widely used as nanomaterials in polymers, concrete, metals, etc.

Typically, the addition of GNP enhances the mechanical and tribological behavior, increases the barrier properties, the thermal and electrical conductivity, and may act as a flame retardant in several polymers [63].

1.5 Mixing methods of polyurethane-graphene oxide (PU-GO) blends

Three different common methods have been proposed to improve the dispersion of graphene oxide (GO) in polyurethanes (Figure 1.15).

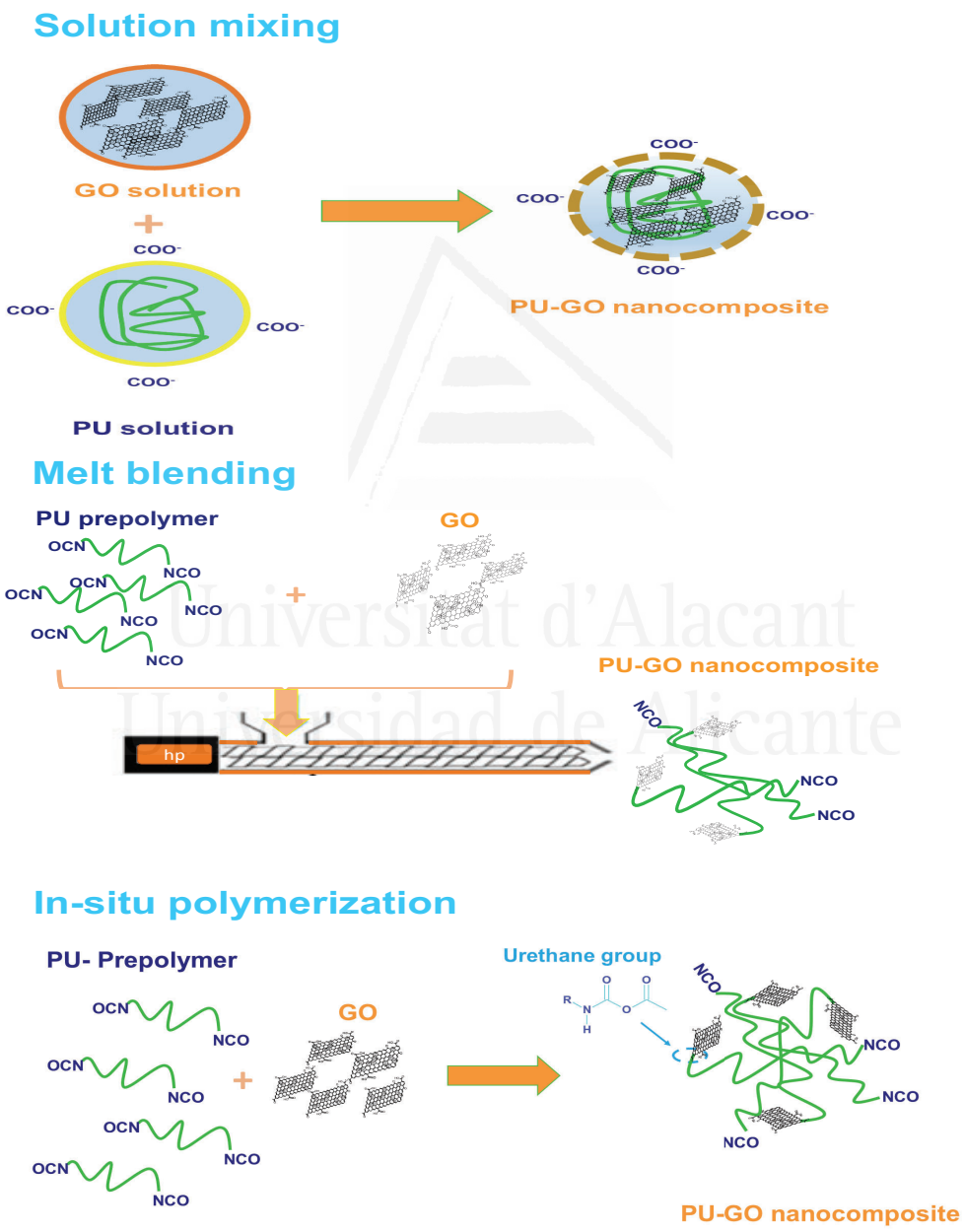

Figure 1.15. Different methods used for producing polyurethane-graphene oxide composites.

The mixing solution method consists of the dispersion of the GO in an organic solvent solution of the polyurethane. The physical mixing is produced followed by the removal of the organic solvent.

In the melt blending method, the polyurethane and the GO are heated and mechanically assisted in an extruder until melting of the polymer.

The in-situ polymerization method requires the mixing of the urethane monomers with GO in the presence of a surfactant, then the polymerization is accomplished by adjusting the temperature and the time (Figure 1.15). Covalent bonds between the prepolymer functional groups (mainly isocyanate groups) and the surface functional groups on the GO sheets are produced, urethane groups are generally produced.

2. State of the art on waterborne polyurethane dispersions containing graphene derivatives

Waterborne poly(urethane urea) dispersions (PUDs) are currently used as flexible coatings and adhesives due to environmental regulations concerning the organic solvents emissions. Several studies have revealed the advantages of adding carbon nanofillers to solvent-borne thermoplastic polyurethanes, i.e., polyurethanes dissolved in organic solvents [64–66]. However, few studies have considered the use of graphene derivatives into waterborne polyurethanes [67–69], mainly due to the poor ability of the graphene to disperse in water, in which it tends to agglomerate.

The addition of graphene derivatives to waterborne polyurethanes for obtaining composites with improved properties has been previously studied. Thus, Wu et al. [70] have added 0.1–1 wt.% amine-functionalized GO to waterborne polyurethane dispersions to improve their mechanical and thermal properties. An improvement in tensile strength of 73 %, an increase in the storage modulus of 973 %, and an increase in the degradation temperature of 40 °C were found. On the other hand, Kim and Kim [71] have synthesized and characterized GO-silanized waterborne polyurethane nanocomposites made with polycaprolactone polyol, isophorone diisocyanate (IPDI), dimethylol butanoic acid, and (3-aminopropyl) triethoxysilane, containing 0.5 to 1.5 wt.% GO. They found an increase in the contact angle values, the glass transition temperature (T_g), the hardness, and young's modulus.

Different methods have been proposed for improving the dispersion of the graphene derivatives in the polymers. Kaur et al. [72] prepared graphene-polyurethane composites by using solution mixing, melt processing, and in situ methods, and their properties were

compared. The solution mixing method consisted of the dispersion of graphene in 20 mL tetrahydrofuran (THF) under sonication for 30 minutes; afterward, 1.9 g polyurethane was added to the solution, the mixture was stirred for several hours until the polymer was completely dissolved. Then, THF was evaporated at 60 °C under vacuum (~ 10 mbar) to obtain the composites. In the melt processing method, the polyurethane was mixed with graphene and melted at 190 °C under stirring at 200 rpm for 2-3 minutes. The in-situ polymerization method consisted of the mixing of the polyurethane with graphene at 80 °C under nitrogen in a furnace. This study showed that the solution mixing method imparted the highest electrical conductivity and the best mechanical properties. On the other hand, it has been shown that the mechanical and toughness properties of polyurethanes were increased by adding 1-4 wt.% GO (Figure 1.16) [68].

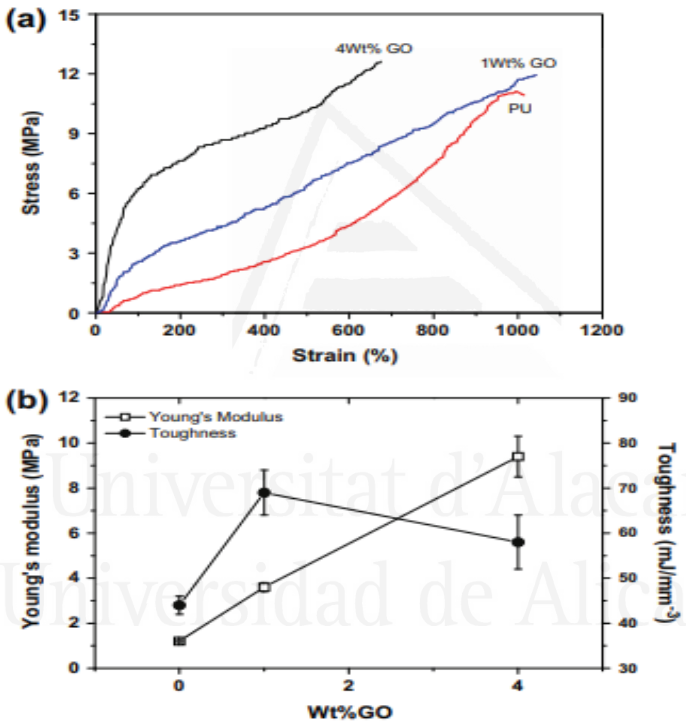

Figure 1.16. Stress-strain curves of GO/PU nanocomposites [68].

Lee et al. [73] have shown increased degradation temperature of waterborne polyurethanes containing different amounts of functionalized graphene, the improvement was ascribed to the enhanced crystallization of the soft segments and decreased interactions between the hard segments of the polyurethane. Zhang et al. [74] have added amine-modified GO to improve the water-resistance, thermal, and mechanical properties of waterborne polyurethanes. Christopher et al. [75] prepared waterborne polyurethane coatings with polyvinyl alcohol modified GO/zinc oxide (GO/ZnO) or functionalized carbon black/ZnO to

enhance their corrosion resistance. The performance of the coating containing GO was better than the one made with carbon black. Hu et al. [76] found improved thermal, mechanical, and hydrophobic properties of waterborne polyurethane/amine functionalized-graphene oxide nanocomposites, the improvement was ascribed to enhanced interfacial interactions between the polyurethane and the functionalized GO. In the same direction, Yadav and Cho [77] have prepared polyurethane nanocomposites with 0.5-2 wt.% graphene nanoplatelets (GP) and f-GP by in situ polymerization. Both fillers improved the thermal stability, crystallinity, modulus, and tensile strength.

There are few studies considering the influence of adding graphene derivatives on the properties of adhesives. Nine et al. [78] prepared graphene composite by the growth of sodium metaborate crystals between the graphene layers during GO reduction intended as fire-retardant polyurethane coatings for metal and glass. They found good cross-hatch adhesion and high mechanical strength (Figure 1.17), the enhanced adhesion was ascribed to strong binding between the native oxide layer on the metal surface and the borate groups. Kale et al. [79] mixed a commercial waterborne polyurethane with 0.2 wt.% graphene oxide and silica nanocomposites intended for leather coatings and improved mechanical and thermal properties, flexibility, and adhesion (Figure 1.18) were obtained. The enhanced adhesion was ascribed to improved interfacial interactions. On the other hand, Araldite 2011 epoxy adhesive has been reinforced by adding different amounts of reduced graphene oxide (r-GO), the addition of 0.5 wt.% r-GO enhanced the tensile strength, and an increase of 27 % in the single lap shear strength was obtained [80].

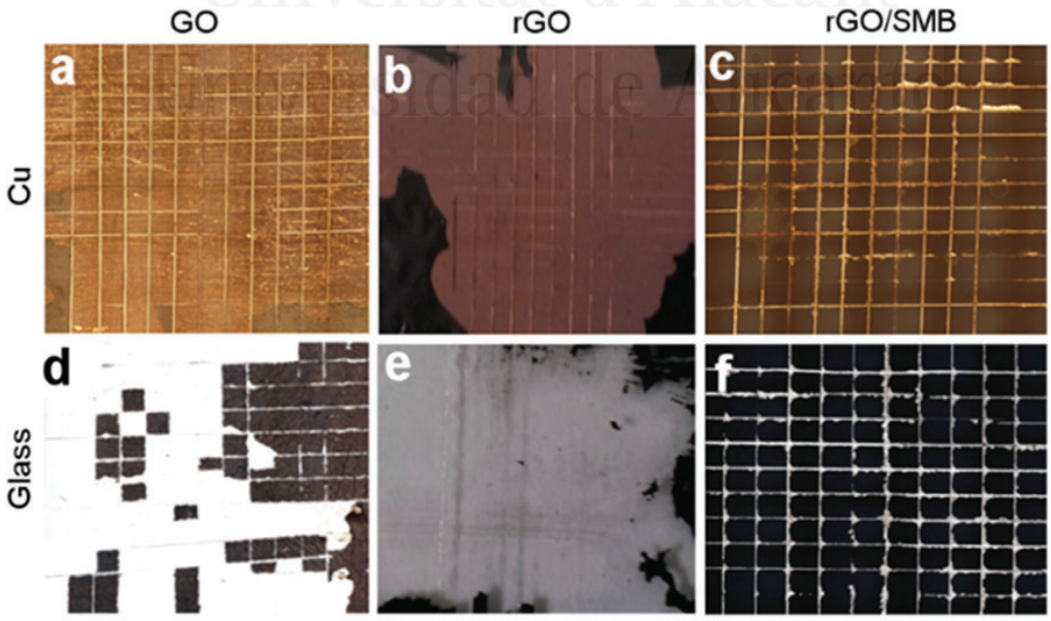

Figure 1.17. Cross-hatch adhesion of graphene-sodium metaborate polyurethane composites on different substrates [78].

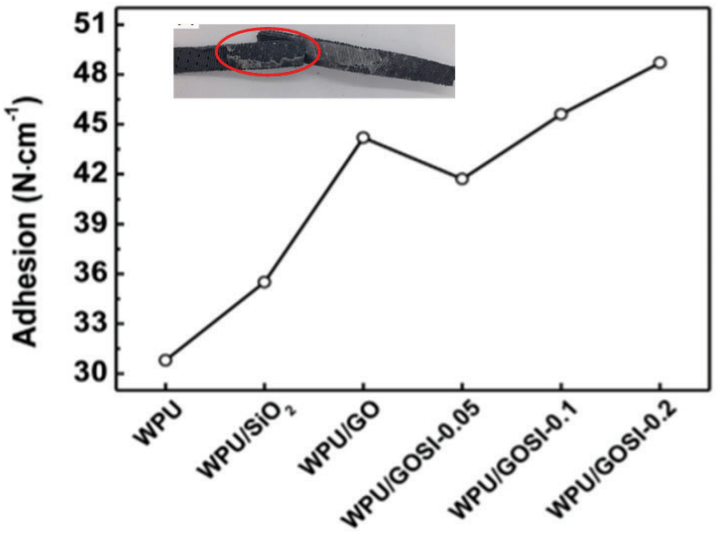

Figure 1.18. T-peel adhesion of leather joints made with neat waterborne polyurethane and waterborne polyurethane nanocomposites [79].

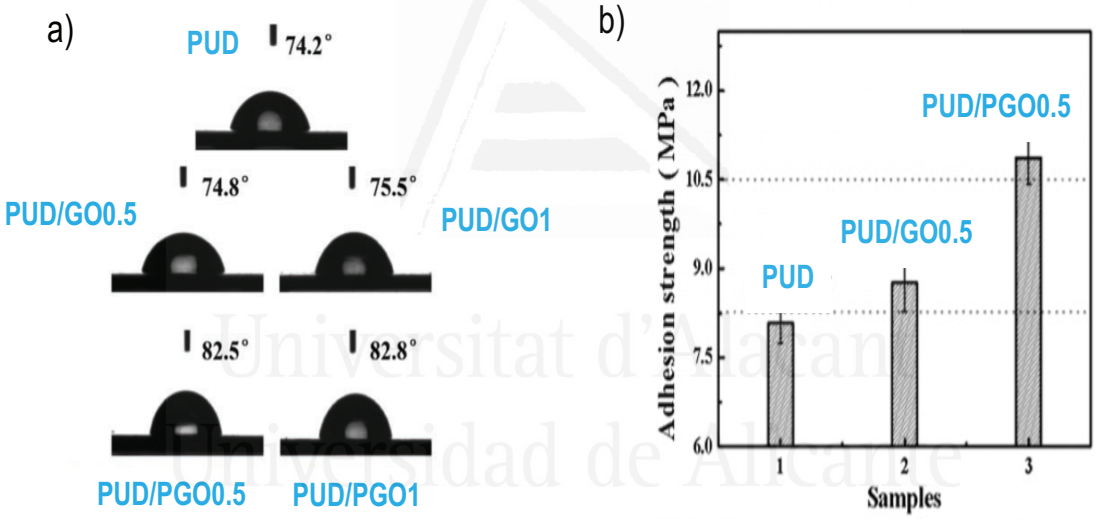

Figure 1.19. a. Hydrophobicity, and **b.** adhesion strength of waterborne polyurethane coating functionalized with graphene oxide [81].

Most studies on the improved adhesion of polyurethanes by adding graphene derivatives have been devoted to coatings. Thus, Zhao et al. [81] have prepared waterborne polyurethane coatings containing 0.1–1 wt.% polydopamine functionalized graphene by solution blending. The coatings made with 0.5 wt.% functionalized graphene imparted improved corrosion resistance, good adhesion, and hydrophobicity (Figure 1.19). Furthermore, Yang et al. [82] developed waterborne polyurethane coatings containing cellulose nanocrystals and graphene to improve their hardness, abrasion resistance, thermal conductivity, and adhesion. Cristofolini et al. [83] have added mixtures of 0.01 wt.%

carboxyl functionalized GP and 0.1-1 wt.% GO to commercial PUD by vigorous mixing and they found increased peel strength.

3. Objectives of the doctoral thesis

Graphene derivatives are promising additives in polymers because of their high specific surface areas and high aspect ratios, these allow the modification of their properties by adding small amounts. Previous studies [48,60,68] in the existing literature have demonstrated that the addition of 1 to 5 wt.% graphene derivative increases the thermal stability, controls the wettability, and increases the thermal and electrical conductivity of different polymers, including polyurethanes.

Although the properties of the waterborne polyurethane dispersions are adequate, however, their mechanical properties are not sufficient for some applications. One way to increase the mechanical properties of the waterborne polyurethane dispersions is the addition of nanofillers such as nanosilicas, carbon nanotubes, or exfoliated clays. However, most of these fillers are hydrophobic and not miscible in water, these issues lead to phase separation. Although graphene is also hydrophobic, graphene oxide is hydrophilic, it is a promising nanofiller for waterborne polyurethane dispersions.

Some previous studies [73-83] have been devoted to analyzing the properties of waterborne polyurethane dispersions containing different types and amounts of graphene derivatives, but only a few ones have been devoted to analyzing their adhesive properties. On the other hand, the sedimentation is a limitation in the addition of graphene derivatives to waterborne polyurethane dispersions, this has been solved by sonication of the graphene derivatives in solvents and/or by adding surfactants. In this study, a different approach was used, which consists in adding very small amounts of graphene derivative (less than 0.30 wt.%) during the synthesis of the waterborne polyurethane dispersions to increase their properties with particular focus on their adhesion properties. Therefore, the main general objective of this doctoral thesis is the addition of less than 0.30 wt.% graphene derivative to enhance the properties, including adhesion, of the waterborne polyurethane adhesives. The structural, thermal, rheological, viscoelastic, and, particularly, the adhesion properties of the waterborne polyurethane dispersions without and with different amounts of graphene derivatives of different nature were determined, paying particular focus to the structure-property relationship. The optimal method of addition of the graphene derivative during the synthesis of the waterborne polyurethane dispersions was studied and different amounts of graphene oxide were added. Furthermore, different graphene oxide derivatives (reduced

graphene oxide, amine-functionalized graphene oxide) and graphene derivatives (graphene nanoplatelets, milled graphite) were studied. All these approaches are novel in the existing literature and allow a better understanding of the structure-property relationship of the waterborne polyurethane dispersions containing graphene derivatives, including the adhesion properties.

The specific objectives of this doctoral thesis are the following:

- Study the influence of the addition of small amounts (0.01-0.10 wt.%) of graphene oxide (GO) during the synthesis of the waterborne poly(urethane urea) dispersions (PUDs) by the acetone method on their structure and properties, particularly adhesion.
- Optimize the method of addition of a given GO amount (0.04 wt.%) during the synthesis of the waterborne poly(urethane urea) dispersions (PUDs) (before prepolymer formation, after prepolymer formation, during the water addition stage) to obtain optimal properties.
- Determine the influence of the surface chemistry of the graphene oxide (GO, amine-functionalized GO, reduced GO) on the structure and properties of the waterborne poly(urethane urea) dispersions (PUDs).
- Determine the influence of the nature and morphology of the graphene derivative (graphene oxide (GO), graphite nanoplatelets (GP), milled graphite (MG)) added by in-situ polymerization on the structure and properties of the PUDs.
- Determine the electrical conductivity of PUDs containing different amounts of graphene derivatives of different nature.

4. Experimental

4.1 Materials

In this doctoral thesis, the reagents used in the synthesis of the waterborne poly(urethane urea) dispersions were aliphatic isophorone diisocyanate (IPDI), polyadipate of the 1,4-butanediol polyol with a molecular weight of 2000 g/mol, dimethyl propionic acid (DMPA) internal emulsifier, triethylamine (TEA) neutralization agent, hydrazine (HZ) chain extender, acetone co-solvent, and de-ionized water. Their main characteristics are given in Table 1.2. Several graphene derivatives were used in the synthesis of the waterborne poly(urethane urea) dispersions:

- Graphene oxide (GO) slurry in water containing 3.1 wt.% GO supplied by Graphenea (San Sebastián, Spain). GO slurry has a pH of 2.4 and more than 95 % monolayer graphene content. The GO slurry was dried to remove water for obtaining the GO powder. 21 g GO slurry was placed in the oven at 80 ºC overnight. Afterwards, the dried GO was crushed with mortar for obtaining the GO powder.
- Reduced graphene oxide (r-GO) powder supplied by Graphenea (San Sebastián, Spain). Chemical reduction was carried out and r-GO contains 13-19 % oxygen groups.
- Amine-functionalized graphene oxide (A-GO) powder was obtained by treatment of GO with a dodecyl amine and was supplied by Graphenea (San Sebastián, Spain).
- Graphene nanoplatelets (GP) were supplied by GrapheneTech (Zaragoza, Spain). GP has 97 wt.% carbon, a BET surface area of 500 m^2/g, and the nano-sheets have a length of 5-10 µm and lateral size of 0.04-0.2 µm.
- Milled graphite (MG) was supplied by zEroCor/Carbon Upcycling (Calgary, Canada). Its specific BET surface area is 188 m^2/g and contains 96 at.% carbon and 4 at.% oxygen.

All graphene derivatives were dried in an oven at 80 ºC overnight and kept in the oven at 80 ºC until use.

Table 1.2. Reagents used in the synthesis of the waterborne poly(urethane urea) adhesives.

Nomenclature	Role	Supplier	Reagent name/Purity
Polyol	Polyol	Synthesia (Barcelona, Spain)	Polyadipate of 1,4-butanediol of molecular weight 2000 Da
IPDI	Isocyanate	Sigma Aldrich (Barcelona, Spain)	Isophorone diisocyanate (98 wt.% purity)
DMPA	Internal emulsifier	Sigma Aldrich (Barcelona, Spain)	2,2 bis(hydroxymethyl) propionic acid (98 wt.% purity)
TEA	Neutralization agent	Sigma Aldrich (Barcelona, Spain)	Trimethylamine 99 wt.% purity) as neutralizing agent
HZ	Chain extender	Sigma Aldrich (Barcelona, Spain)	Monohydrated hydrazine (60 wt.% purity)
DBTDL	Catalyst	Sigma Aldrich (Barcelona, Spain)	Dibutyl dilaurate (95 wt.% purity)
Acetone	Co-solvent	Sigma Aldrich (Barcelona, Spain)	2-butanone (99.5 wt.% purity)
De-ionized water	Solvent	Technical Services – University of Alicante	Ultrapure water

4.2 Synthesis of the waterborne poly(urethane urea) dispersions (PUDs)

The synthesis of the waterborne poly(urethane urea) dispersions (PUDs) with and without graphene derivative was carried out in a 500 mL jacketed glass reactor provided with a lid having four connections. A Frigiterm 6000382 water bath (Selecta, Niles, IL, USA) was fitted to control the temperature during the synthesis process. Nitrogen (50 mL/min) was used for maintaining an inert atmosphere throughout the synthesis and entered the reactor through one of the lateral connections. Another connection was used for a thermocouple to control the temperature during the synthesis, and the remaining connection was used for adding the reagents (Figure 1.20).

The nitrogen gas stream used in the synthesis circulates through three desiccators to ensure an inert and dry atmosphere within the reactor during the synthesis. The first desiccator contains zeolites (4 Å pore size) to retain the moisture in the nitrogen gas, the second desiccator contains concentrated sulfuric acid to remove the even residual moisture, and the third desiccator is empty to avoid over-pressure (Figure 1.20) [9].

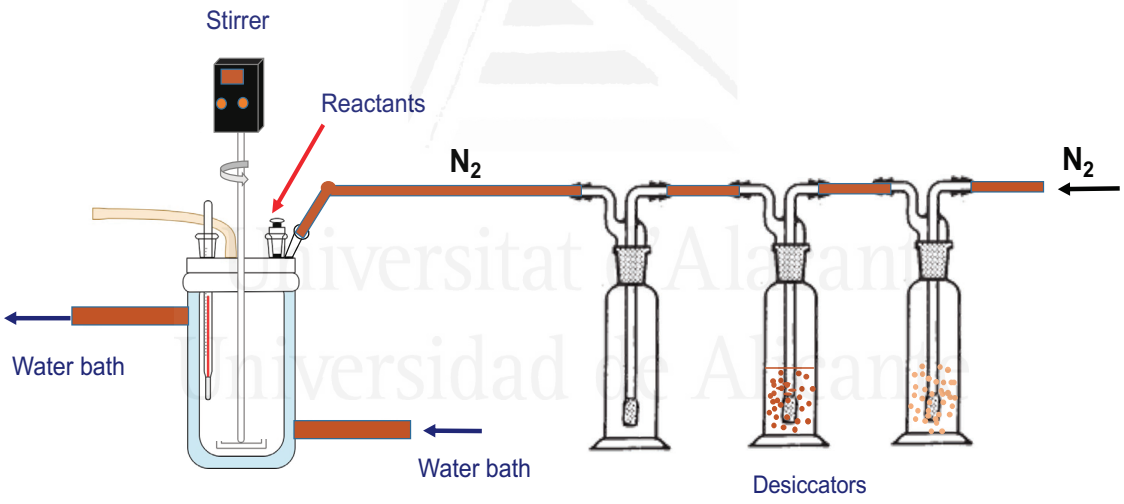

Figure 1.20. Scheme of the experimental system used for the synthesis of the waterborne poly(urethane urea) dispersions.

The waterborne poly(urethane urea) dispersion without graphene derivative (PUD) was synthesized by using the acetone method. 5 wt.% DMPA was used, the targeted solids content was 40 wt.%, and an NCO/OH ratio of 1.5 was set (the OH groups of the polyol and DMPA were considered in the calculations). PUD was synthesized by following different consecutive steps:

- ❖ Synthesis of the prepolymer: The polyol, 5 wt.% DMPA (with respect to the total amount of prepolymer) and DBTDL catalyst were added into the reactor at 80 °C under stirring at 450 rpm for 30 minutes. Then, IPDI was added slowly at 80 °C under stirring at 450 rpm for 2 hours 35 min.
- ❖ Dissolution of the prepolymer in acetone: The temperature was lowered to 42 °C and 70.2 g acetone was added to dissolve the prepolymer, maintaining the stirring at 450 rpm for 30 minutes.
- ❖ Neutralization of the ionic groups: For neutralizing the protons of DMPA in the prepolymer, TEA in 25 mL acetone was added at 40 °C under stirring at 450 rpm for 30 minutes.
- ❖ Chain extension: HZ was added at 40 °C under stirring at 450 rpm for 30 minutes.
- ❖ Dispersion in water: The stirring speed was increased to 900 rpm and water was added maintaining the stirring at 40 °C for 30 minutes.
- ❖ Distillation of the acetone: The residual acetone was removed in rotavapor (Büchi B-210, Flawil, Switzerland) at 50 °C and 300 mbar for 1 hour.

The graphene derivatives were added in different stages of the PUD synthesis.

Addition of the graphene derivative together with the polyol

The mixture of polyadipate of 1,4-butanediol and graphene derivatives (GO, r-GO, A-GO, MG, GNP) was carried out in a Speed Mixer double orbital centrifuge (Hauschild Engineering, Hamm, Germany) operating at 2500 rpm for 150 seconds. Afterward, to remove the potential residual water, the mixture was heated at 75 ºC for 30 minutes (Figure 1.21) and kept in the oven at 80 ºC until it was added into the reactor.

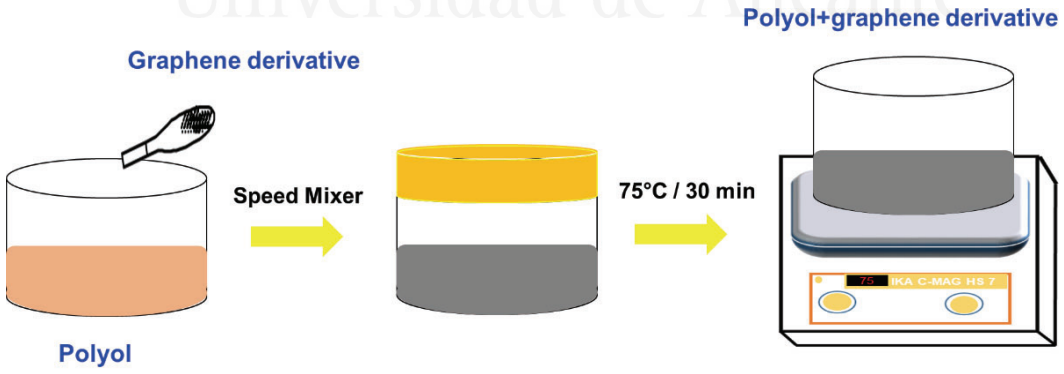

Figure 1.21. Mixing procedure of the graphene derivative and the polyol.

The polyol + graphene derivative mixture was added to the reactor together with the DMPA internal emulsifier and DBTDL catalyst at 80 ºC under stirring at 450 rpm for 30 minutes.

Then the isocyanate (IPDI) was added slowly at 80 ºC under stirring at 450 rpm for 2 h 30 minutes. 80 g prepolymer with an NCO/OH ratio of 1.5 was prepared. The remaining stages of the synthesis were the same as the ones in the PUD without the graphene derivative.

Addition of graphene oxide (GO) during prepolymer formation

GO powder was placed in a polypropylene container and heated at 75 ºC for 30 minutes to remove the potential residual water. After cooling down to 60 ºC, 70.2 g acetone was added and mixed with dried GO in a Speed Mixer double orbital centrifuge (Hauschild Engineering, Hamm, Germany) operating at 2000 rpm for 150 seconds (Figure 1.22).

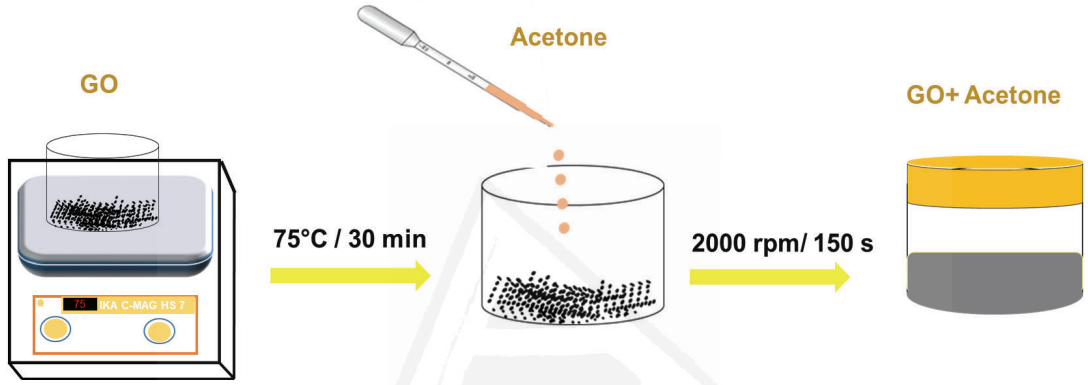

Figure 1.22. Dispersion of graphene oxide in acetone.

The polyol, 5 wt.% DMPA (with respect to the total amount of prepolymer), and DBTDL catalyst were added into the reactor at 80 °C under stirring at 450 rpm for 30 minutes. Then, IPDI was added slowly at 80 °C under stirring at 450 rpm for 2 hours 30 min. The temperature was lowered to 40 °C and a 70.2 g acetone+GO mixture was added to dissolve the prepolymer, allowing the reaction of the surface functional groups on the GO surface with the end NCO groups of the prepolymer, maintaining the stirring at 450 rpm for 30 minutes. The remaining stages of the synthesis were the same as in the PUD without the graphene derivative. Thus, in-situ polymerization of GO surface groups with the terminal NCO groups of the prepolymer was expected.

Addition of graphene oxide (GO) after prepolymer formation

GO and 120.7 g of water were mixed in a glass container placed in a magnetically stirred IKA C-MAG HS 7 stirrer (IKA, Staufen, Germany) at 40 ºC for 30 minutes (Figure 1.23).

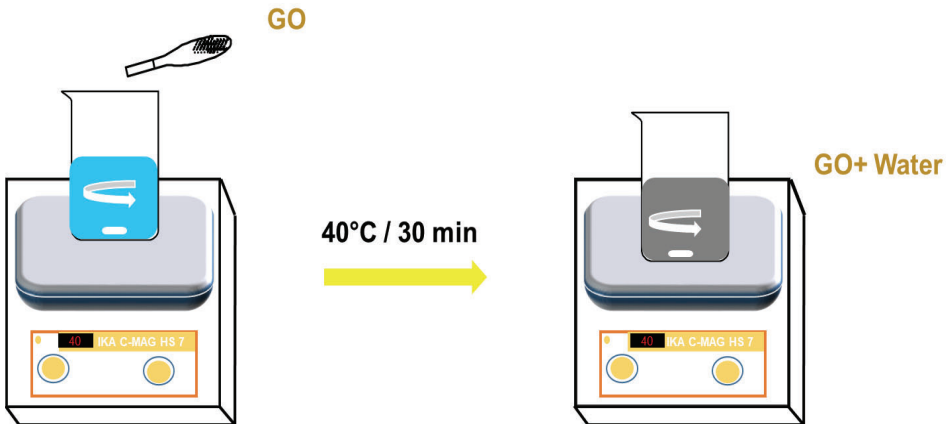

Figure 1.23. Dispersion of graphene oxide in water.

The remaining stages of the synthesis of the waterborne poly(urethane urea) dispersion containing GO added during the water addition stage were the same as in the PUD without graphene derivative, but instead of adding water, the GO+water mixture was added after the chain extension stage. This method will allow the GO sheets to be occluded between the poly(urethane urea) chains during the phase inversion stage in which the particles are formed (solution mixing method).

4.3 Experimental techniques

Characterization of the graphene derivatives

Raman spectroscopy. The chemical structure of the graphene derivatives was analyzed in a Raman spectrometer, Jasco NRS-5100 (Jasco, Madrid, Spain) by using an excitation wavelength of 532 nm (HeNe source). The exposure time was 40 seconds and the power was 0.7 mW.

X-ray photoelectron spectroscopy (XPS). The elemental chemical compositions and the amounts of the surface functional groups on the graphene derivatives were determined by XPS. A Surface Science SSX-100 ESCA spectrometer (Thermo Ficher Scientific - Waltham MA, USA) with an Al-Kα X-ray source (1486.6 eV) was used. Prior to analysis, the residual pressure was lower than 2.10^{-6} Torr, and to avoid sample charging, the flood gun/screen technique was used. XPS survey spectra were collected in the range of binding energies between 0 and 1200 eV, using a spot size of 600 µm and a pass energy of 150 eV. High-resolution C1s, O1s, and N1s spectra of the graphene derivatives were obtained over a 20 eV range. The binding energies were corrected by fitting the peak position for the main hydrocarbon peak at 285.0 eV.

Thermal gravimetric analysis (TGA). The amount of functional groups of the graphene derivatives was determined by TGA Q500 equipment (TA Instruments, New Castle, DE, USA). 10-15 mg samples were placed in a platinum crucible and heated under nitrogen (flow rate: 100 mL/min) from room temperature up to 800 °C, by using a heating rate of 10 °C/min.

X-ray diffraction. The crystallinity of the graphene derivatives was determined by X-ray diffraction (XRD) on Bruker D8-Advance equipment (Bruker, Ettlingen, Germany) provided with Kristalloflex K 760-80F X-ray generator (3000 W, 20-60 kV, current of 5-80 mA). A voltage of 40 kV and the wavelength of copper kα (1.5418 Å) were used.

Transmission electron microscopy (TEM). The morphologies of the graphene derivatives were determined by a Jeol JEM-1400 Plus instrument (Jeol, Tokyo, Japan) by using an acceleration voltage of 120 kV. Before analysis, the graphene derivative was diluted in 2-propanol and the solution was placed in an ultrasonic bath for 60 seconds.

Characterization of the waterborne poly(urethane urea) dispersions (PUDs) without and with graphene derivatives

Solids content. The solids content of the PUDs with and without graphene derivatives were determined by DBS 60 thermo balance (Kern &Sohn GmbH, Balingen, Germany). About 0.5 g of PUD was spread on an aluminum foil plate of 9 cm diameter and heated at 105 ºC for 15 minutes, then at 120 ºC until a constant weight was obtained. Five replicates were carried out and averaged.

pH measurement. The pH values of the PUDs with and without graphene derivatives were measured on a pH-meter PC-501 (XS Instruments, Carpi, Italy) equipped with an XC-PC510 electrode. About 25 cm^3 of each PUD was placed in a beaker and the pH value was measured at 25 °C. Three replicates were measured and averaged.

Viscosity. The viscosities of the PUDs with and without graphene derivatives were measured in a DHR-2 rheometer (TA Instruments, New Castle, DE, USA) at 25 °C using coaxial cylindrical geometry (cylinder dimensions: 42 m height and 28 mm internal diameter) according to DIN 53019 standard. The gap was set at 2 mm. The viscosities of the PUDs were measured as a function of the shear rate in the range of 0.1–1000 s^{-1}.

Characterization of the solid poly(urethane urea)s (PUs) without and with graphene derivatives.

Attenuated total reflectance Fourier transform infrared (ATR-IR) spectroscopy. The chemical structure of the poly(urethane urea)s with and without graphene derivative was studied in a Tensor 27 FT-IR spectrometer (Bruker Optik GmbH, Ettlinger, Germany) by

using a Golden Gate single reflection diamond ATR accessory. 64 scans with a resolution of 4 cm^{-1} were recorded and an averaged incident angle of the IR beam of 45º was used.

Raman spectroscopy. The chemical structure of the poly(urethane urea)s with and without graphene derivative was recorded in a Raman spectrometer Jasco NRS-5100 (Jasco, Madrid, Spain) by using an excitation wavelength of 532 nm (HeNe source). The exposure time was 40 seconds and the power was 0.7 mW.

Differential scanning calorimetry (DSC). The degree of phase separation in the poly(urethane urea)s with and without graphene derivative was assessed by differential scanning calorimetry (DSC) on TA DSC Q100 V6.2. equipment (TA Instruments, New Castle, DE, USA). Aluminum pans containing 10–15 mg samples were heated from −80 to 110 °C under a nitrogen atmosphere (flow rate: 50 mL/min), the heating rate was 10 °C/min. Then a cooling run from 110 ºC to -80 ºC was carried out by using a cooling rate of 10 ºC/min, and finally, a second DSC heating run from -80 to 250 ºC was carried out by using a heating rate of 10 ºC/min. From the second DSC heating run, the glass transition temperatures (T_gs) and the thermal events of the PU films were obtained.

X-ray diffraction. The crystallinity of the poly(urethane urea)s without and with graphene derivative were determined by X-ray diffraction (XRD) on Bruker D8-Advance equipment (Bruker, Ettlingen, Germany) provided with a Kristalloflex K 760-80F X-ray generator (3000 W, 20-60 kV, current of 5-80 mA). A voltage of 40 kV and the wavelength of copper kα (1.5418 Å) were used.

Thermal gravimetric analysis (TGA). The structure and the thermal properties of the poly(urethane urea)s without and with graphene derivative were carried out on TGA Q500 equipment (TA Instruments, New Castle, DE, USA). 10-15 mg samples were placed in a platinum crucible and heated under nitrogen (flow rate: 100 mL/min) from room temperature up to 800 °C, by using a heating rate of 10 °C/min.

Plate-plate rheology. The rheological properties of the poly(urethane urea)s without and with graphene derivative were measured in a DHR-2 rheometer (TA Instruments, New Castle, DE, USA) by using parallel plates (upper plate diameter = 20 mm) geometry. The PU was placed on the bottom plate heated at 150 °C and, once it was melted, the upper plate was lowered for setting a gap of 400 µm. Then, the temperature was increased to 200 °C and the excess dough was carefully trimmed off with a spatula. Experiments were performed in the region of linear viscoelasticity by decreasing the temperature from 200 to 25 °C by using a cooling rate of 5 °C/min.

Dynamic mechanical thermal analysis (DMA). The viscoelastic properties of the poly(urethane urea)s without and with graphene derivative were measured on the DMA-Q800 equipment (TA Instruments, New Castle, DE, USA) by using the single cantilever

mode. Poly(urethane urea) films with dimensions 18 mm × 13 mm × 1 mm were used and they were heated from −100 to 70 °C under nitrogen atmosphere (flow: 100 mL/min) by using a heating rate of 5 °C/min. All experiments were carried out at a frequency of 1 Hz, an amplitude of 20 μm, and a strain of 0.5 %.

Stress-strain tests. The mechanical properties of the poly(urethane urea)s without and with graphene derivative were assessed by stress-strain tests according to ISO 37 standard. Dog-bone test specimens were cut and the stress-strain tests were carried out in an Instron 4411 universal testing machine (Instron, Buckinghamshire, UK) provided with a mechanical extensometer, a pulling rate of 100 mm/min was used. Five replicates were measured and averaged.

Confocal laser microscopy. The degree of agglomeration of the graphene derivatives in the poly(urethane urea) films was studied using a Leica TCS SP2 microscope (Leica, Heidelberg, Germany). A drop of PUD was placed on a glass microscope slide (dimensions of 76 mm ×26 mm) and then covered with a small glass cover slide, allowing it to evaporate the water at room temperature for four days followed by heating at 40 °C for 8 hours.

Scanning Electron Microscopy (SEM). The poly(urethane urea) films were immersed in liquid nitrogen for 2 minutes and mechanically fractured immediately after being taken out. The fractured surfaces of the poly(urethane urea)s were analyzed using a Jeol JSM-840 SEM microscope (Jeol, Tokyo, Japan). The samples were secured onto a copper mount by using silver paint and they were gold coated in a high-resolution Polaron sputtering coater. The energy of the electron beam was 10 kV.

Adhesion properties of the waterborne poly(urethane urea) dispersions (PUDs) without and with graphene derivatives.

T-peel tests of plasticized PVC/PUD/plasticized PVC joints. Adhesive strengths (under peeling stresses) of the joints made with the PUDs with and without graphene derivatives were obtained from T-peel tests of plasticized poly(vinyl chloride) (PVC)/PUD/plasticized PVC joints. The plasticized PVC test samples had dimensions of 30 mm × 150 mm × 5 mm and they were methyl ethyl ketone wiped for plasticizer removal, allowing the solvent to evaporate for 10 minutes under the open air. Then, 0.90 g PUD was applied by brush to each PVC strip to be joined and, after water evaporation at 25 °C for 1 hour, the adhesive film was heated suddenly at 80 °C for 10 seconds under infrared radiation (reactivation process). The PVC strips were immediately placed in contact and a pressure of 0.8 MPa was applied for 10 seconds to achieve a suitable joint. The T-peel strength was measured 1 and 72 hours after joint formation in an Instron 4411 universal testing machine (Instron Ltd., Buckinghamshire, UK). A crosshead speed of 100 mm/min was used. Five replicates

were measured and averaged. The loci of failure of the joints were assessed by visual inspection.

Single lap-shear test of stainless steel 304/PUD/stainless steel 304 joints. The adhesion (under shear stresses) of the PUDs with and without graphene derivative was determined by single lap-shear tests of stainless steel 304/PUD/stainless steel 304 joints. Stainless steel 304 specimens with dimensions of 30 mm x 150 mm x 1 mm were used. They were mechanically abraded with a green fiber scouring pad (Scotch Brite®) followed by wiping with isopropanol, leaving it to evaporate at room temperature for 30 minutes. To make the joints, 0.2 g PUD was placed with a Pasteur pipette on 1.5 cm x 3 cm side surface of one of the stainless-steel specimens, leaving it to evaporate at room temperature for 15 minutes; then, the other stainless-steel specimen was placed on top, applying a pressure of 0.16 kPa at room temperature for 5 days (120 hours). The single lap-shear tests were carried out on an Instron 4411 universal testing machine (Instron Ltd., Buckinghamshire, UK). A crosshead speed of 10 mm/min was used. At least five replicates for each adhesive joint were determined and averaged. The loci of failure of the joints were assessed by visual inspection.

5. Main results and discussion

Influence of adding different small amounts (0.01-0.10 wt.%) of GO on the properties of the PUDs

The variation of the viscosity at 25 ºC of the PUDs as a function of the shear rate is given in Figure 1.24a. The viscosity of the PUD without GO decreases by increasing the shear rate, i.e., shear-thinning, is shown, and the viscosity measured at a shear rate of 200 s^{-1} is low (42 mPa.s). The addition of 0.01-0.05 wt.% GO decreases the viscosity at 200 s^{-1} (at this shear rate, the viscosity is not dependent on the shear rate) of the PUDs (Figure 1.24b) and the extent of shear-thinning is much less marked – PUD+0.04 wt% GO is an exception. Because the shear thinning in the PUD can be associated with the ionic interactions between the micelles/particles, the interactions between the GO particles and the poly(urethane urea) chains in the micelles may decrease the ionic forces among the micelles. However, the addition of 0.10 wt.% GO increases noticeably the viscosity and the shear thinning of the PUD, this may indicate an agglomeration of the GO particles inside the micelles which increases the interactions between the PUD micelles.

Figure 1.25 shows the carbonyl region of the ATR-IR spectra of the poly(urethane urea)s (PUs). The carbonyl region is somewhat similar in all PUs, but differences in the 1650-1720

cm^{-1} region corresponding to the associated by hydrogen bond (H-bonded) urethane and urea groups are distinguished. In order to quantify the percentages of the different C=O species in the PUs, the curve fitting of the carbonyl region of the ATR spectra has been carried out.

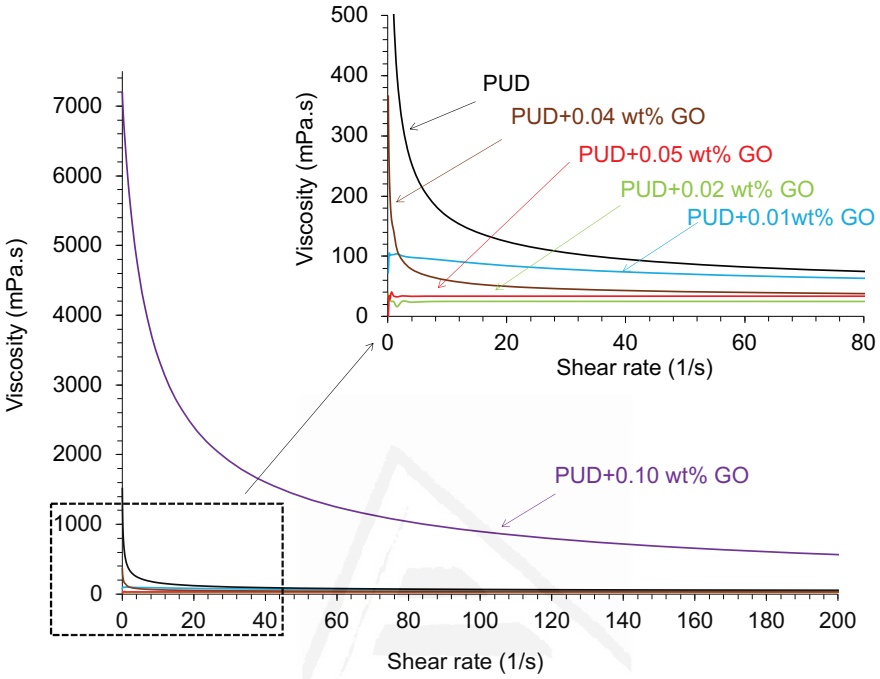

Figure 1.24a. Variation of the viscosity of the PUDs as a function of the shear rate.

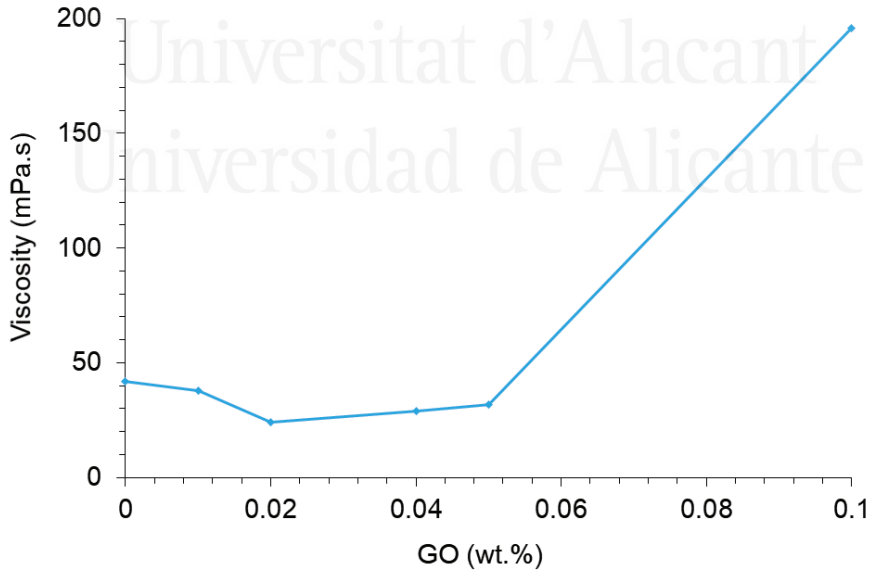

Figure 1.24b. Variation of the viscosity at shear rate of 200 s^{-1} of the PUDs as a function of the amount of GO.

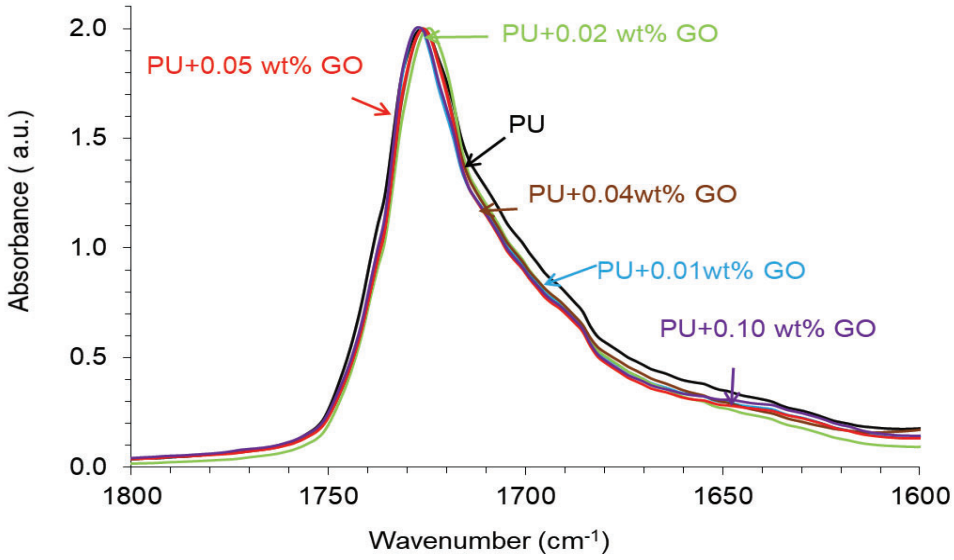

Figure 1.25. 1800-1600 cm^{-1} region of the ATR-IR spectra of the PUs.

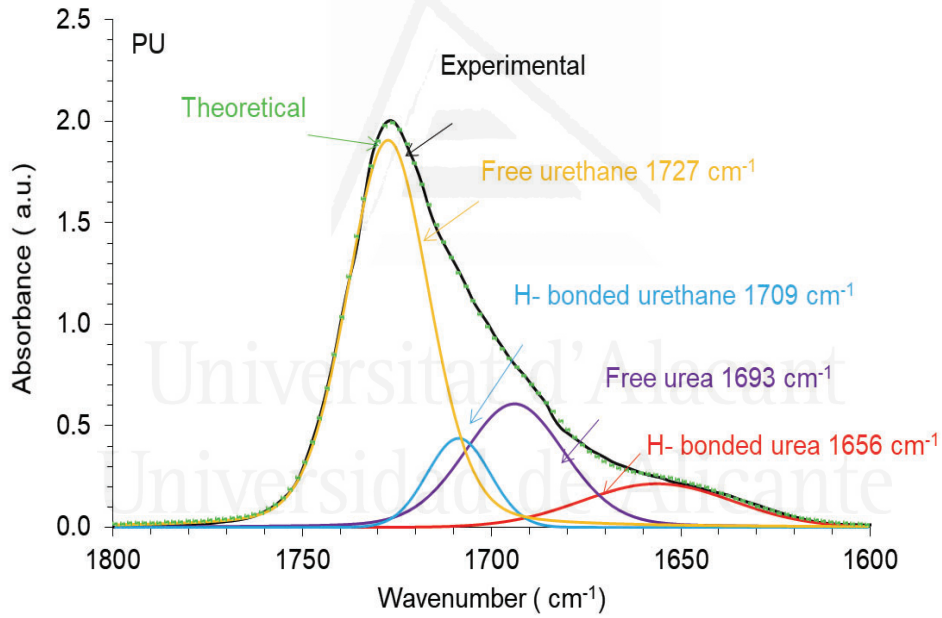

Figure 1.26. Curve fitting of the carbonyl region (1800-1600 cm^{-1}) of the ATR-IR spectrum of the PU without GO.

Figure 1.26 shows, as a typical example, the curve fitting of the PU without GO in which four contributions due to free urethane (1727 cm^{-1}), H-bonded urethane (1709 cm^{-1}), free urea (1693 cm^{-1}), and H-bonded urea (1656 cm^{-1}) can be distinguished. Table 1.3 shows that the addition of GO enhances the percentages of H-bonded urethane and H-bonded urea groups due to the interactions between the oxygen surface groups on the GO nano-sheets and the hard segments of the PU, this anticipates a higher degree of micro-phase

separation. The addition of up to 0.04 wt.% GO increases steadily the percentages of free and H-bonded urethane groups in detriment of the ones of free and H-bonded urea groups, this is due to different GO-poly(urethane urea) interactions. On the other hand, the addition of 0.05 and 0.10 wt.% produces the reverse trend, i.e., less free and H-bonded urethane, and more free and H-bonded urea groups than in the PU without GO, likely due to some agglomeration of the GO nano-sheets. As a result, the addition of less or more than 0.05 wt.% GO produces different structures in the PUs. The addition of 0.04 wt.% GO causes the highest percentages of free and H-bonded urethane and the lowest ones of free and H-bonded urea groups, this PU should have the highest degree of micro-phase separation.

Table 1.3. Relative contributions of the urethane and urea groups in the PU

Poly(urethane urea)	Relative contribution of species (%)			
	Wavenumber (cm^{-1})			
	1727-1725 (free urethane)	1712-1709 (H-bonded urethane)	1693-1686 (free urea)	1658-1653 (H-bonded urea)
PU	58	9	22	11
PU+0.01 wt% GO	40	20	13	27
PU+0.02 wt% GO	40	29	12	19
PU+0.04 wt% GO	45	35	9	11
PU+0.05 wt% GO	42	31	8	19
PU+0.10 wt% GO	43	23	15	19

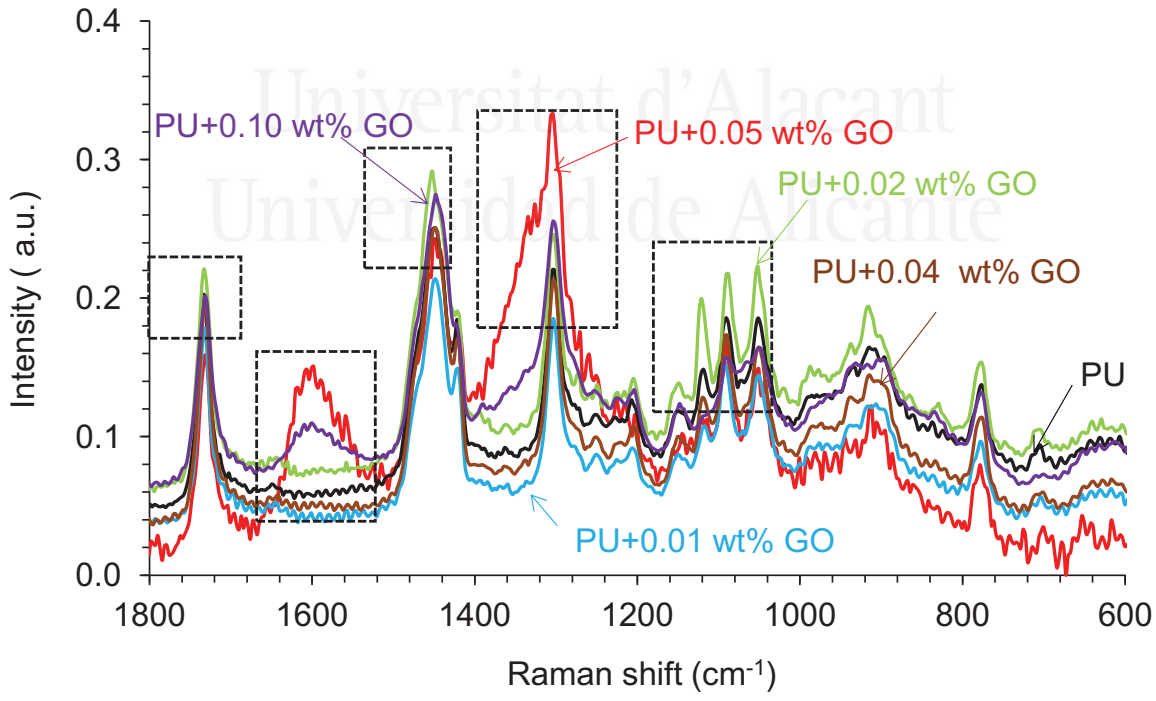

Figure 1.27. 1800-600 cm^{-1} region of the Raman spectra of the PU and PU+GO materials.

Figure 1.27 shows the 1800-600 cm^{-1} region of the Raman spectra of the PUs. The addition of GO does not produce new bands in the Raman spectra of the PUs containing up to 0.04 wt.% GO, but the Raman spectra of PU+0.05 wt.% GO and PU+0.10 wt.% GO show a new shoulder at 1306 cm^{-1} due to CH_2 bending and a new band at 1609 cm^{-1} due to C–N stretching. Furthermore, there are changes in the intensities of the bands at 1125, 1090, and 1054 cm^{-1} due to C–N, C–O–C, and C–C groups respectively. Therefore, the interactions between the hard and soft segments in the PUs are altered by adding 0.05–0.10 wt.% GO.

The degree of phase separation in the PUs can be assessed by DSC. The thermal events obtained from the DSC traces (second heating run) of the PUs are given in Table 1.4. The DSC trace of the PU without GO shows the glass transition temperature (T_g) of the soft segments at -49 ºC and the addition of GO slightly shifts the T_g of the soft segments to (-51) – (-54) ºC. The DSC traces of the PUs containing 0.02 and, more markedly, 0.04 wt.% GO exhibit the melting of the crystalline hard segments at 206-216 ºC, but the T_g of the hard segments is not shown, this agrees with the increase of the percentage of H-bonded urethane groups evidenced by ATR-IR spectroscopy. This structural change could be attributed to the gathering of the GO nano-sheets around the hard segments via hydrogen bonding. On the other hand, the PU with 0.05 wt.% GO shows the T_g of the hard segments at 193 ºC and PU+0.10 wt% GO shows additionally a cold crystallization at 26 ºC followed by the melting of the soft segments at 45 ºC, due to stronger interactions between the soft segments induced by agglomeration of the GO nano-sheets.

Table 1.4. Some data obtained from the DSC traces of the PUs. Second heating run.

Poly(urethane urea)	T_{g1} (°C)	T_{g2} (°C)	$T_{m,hs}$ (°C)	T_c (°C)	ΔH_c (J/g)	$T_{m,ss}$ (°C)	$\Delta H_{m,ss}$ (J/g)
PU	-49	-	-	-	-	-	-
PU+0.01 wt% GO	-54	-	-	-	-	-	-
PU+0.02 wt% GO	-51	-	206	-	-	-	-
PU+0.04 wt% GO	-52	-	216	-	-	-	-
PU+0.05 wt% GO	-53	193	-	-	-	-	-
PU+0.10 wt% GO	-54	194	-	26	1	45	2

The thermal stability and structure of the PUs were studied by TGA. Figure 1.28a shows the variation of the weight as a function of the temperature of the PUs. The thermal stabilities of the PUs increase by adding GO - PU+0.04 wt% GO is an exception –, and similar thermal stabilities are found in all PU+GO films, irrespective of the amount of GO. The values of temperature at which 50 wt.% is lost ($T_{50\%}$) in the PUs increase in 14-20 ºC - PU+0.04 wt%

GO is an exception -, indicating improved thermal stability due to the interactions between the GO surface groups and the poly(urethane urea) chains.

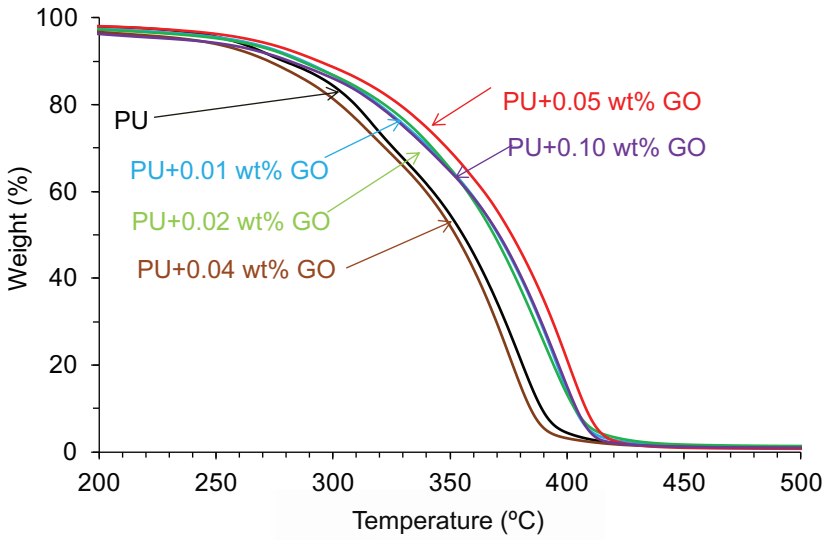

Figure 1.28a. Variation of the weight as a function of the temperature for PUs.

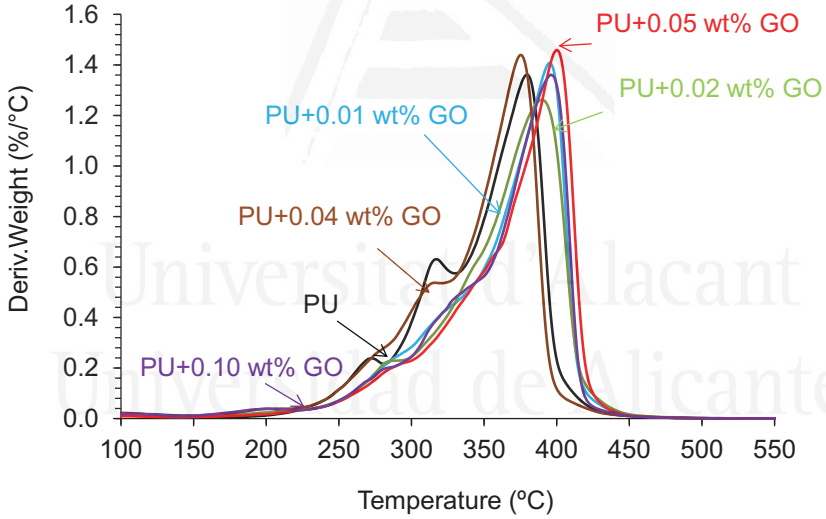

Figure 1.28b. Variation of the derivative of the weight as a function of the temperature for PUs.

The structural changes in the PUs caused by adding GO can be better distinguished in the derivative TGA plots (Figure 1.28b). Only PU and PU+0.10 wt% GO show a small thermal decomposition at 111-114 ºC due to residual moisture. The PU without GO shows three thermal decompositions due to the urethane hard domains (270 ºC), urea hard domains (315 ºC), and soft domains (380 ºC). All PU+GO materials show an additional thermal decomposition at 198-229 ºC with weight losses of 3-4 wt.% which can be ascribed to the thermal rupture of the GO-polyurethane interactions; this thermal decomposition is displaced to lower temperature by increasing the GO content, this is an indication of the

existence of lower interaction between the GO surface groups and the poly(urethane urea) chains by adding more GO. Furthermore, the addition of GO increases the temperatures of the thermal decompositions of the urethane and urea hard domains, and the soft segments of the PUs, additional evidence of the existence of GO-polyurethane interactions.

Figure 1.29 shows the variation of the storage modulus (G′) as a function of the temperature for the PUs. The addition of GO reduces the storage modulus of the PUs, and similar rheological plots are obtained in the PUs containing 0.01–0.05 wt.% (PU+0.02 wt.% GO is an exception), confirming the interactions between the GO surface and the poly(urethane urea) chains. These interactions are less important in PU+0.10 wt.% GO because the decrease in the G′ values by increasing the temperature is less marked than in the other PU+GO materials. Although an increase of the storage modulus of the PU can be expected by adding GO, in this study the addition of GO modifies the degree of micro-phase separation.

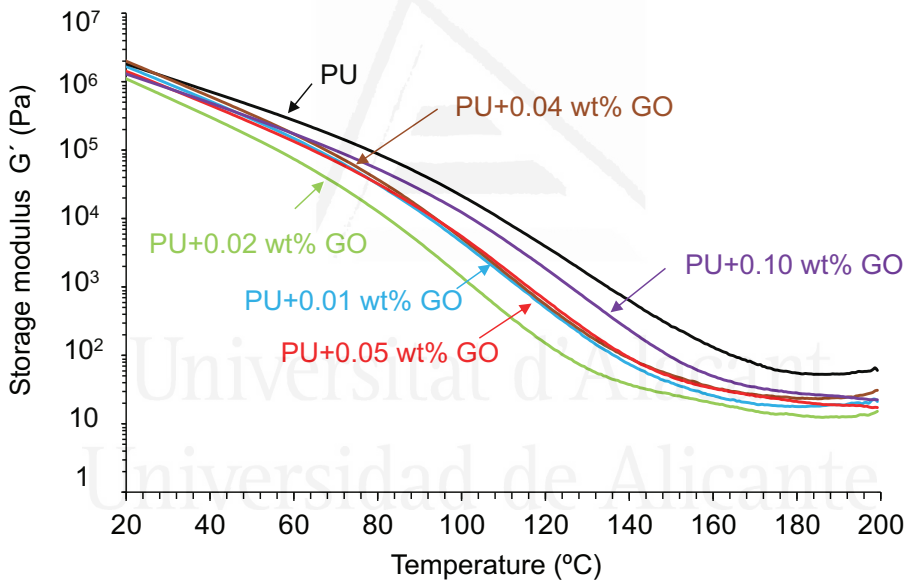

Figure 1.29. Variation of the storage modulus (G´) as a function of the temperature for PU and PU+GO materials.

The dispersion of the GO nano-sheets into the poly(urethane urea) matrix was assessed by confocal laser microscopy. Figure 1.30 shows that the GO particles are well dispersed into the PU matrix in the PUs containing 0.01-0.05 wt.% GO. The particle size of the GO nano-sheets is similar (10-15 μm) in all PU+GO materials. Furthermore, well-dispersed small GO particles with a size lower than 1 μm can also be distinguished, more abundant by increasing the GO content in the PU. The number of smaller GO particles is more important in the PU+0.04 wt.% GO film. This justifies its different properties evidenced by ATR-IR spectroscopy, DSC, and TGA. On the other hand, the extent of the dispersion of

the GO nano-sheets into the PU matrix is not so good in the PU+0.10 wt% GO film as some small agglomerates of GO sheets can be noticed, this is consistent with the lower improvement in the properties evidenced above.

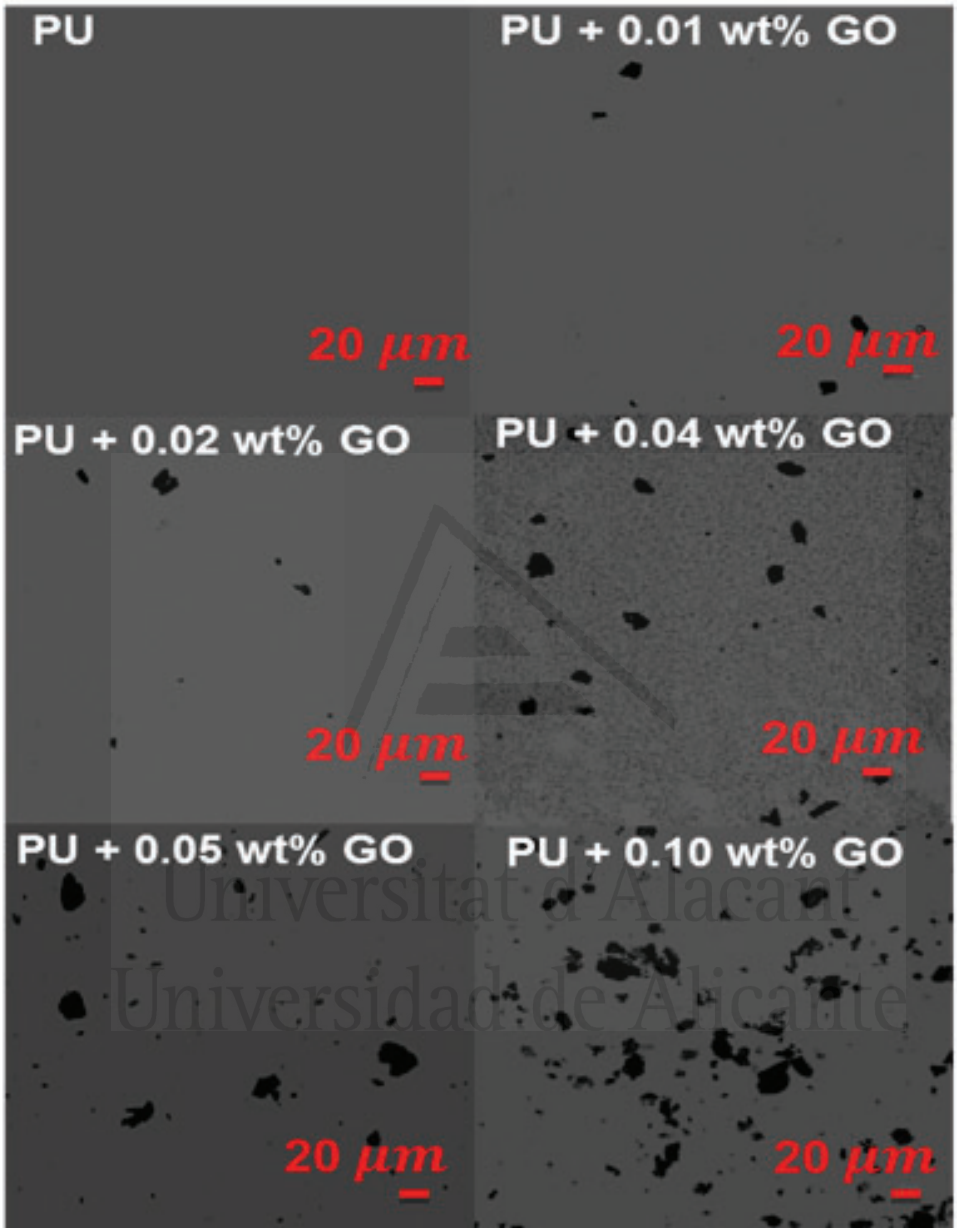

Figure 1.30. Confocal laser micrographs of the PU and PU+GO materials.

Figure 1.31 shows that the water contact angle on the PU without GO is 40º, and the addition of GO increases steadily the water contact angle value up to 53º. The higher is the amount of GO, the higher is the water contact angle value of the PU, the more noticeable increase corresponds to PU+0.10 GO wt.%. As a result, the addition of GO reduces the polarity of the PU, but the wettability of the PU+GO materials is reasonable.

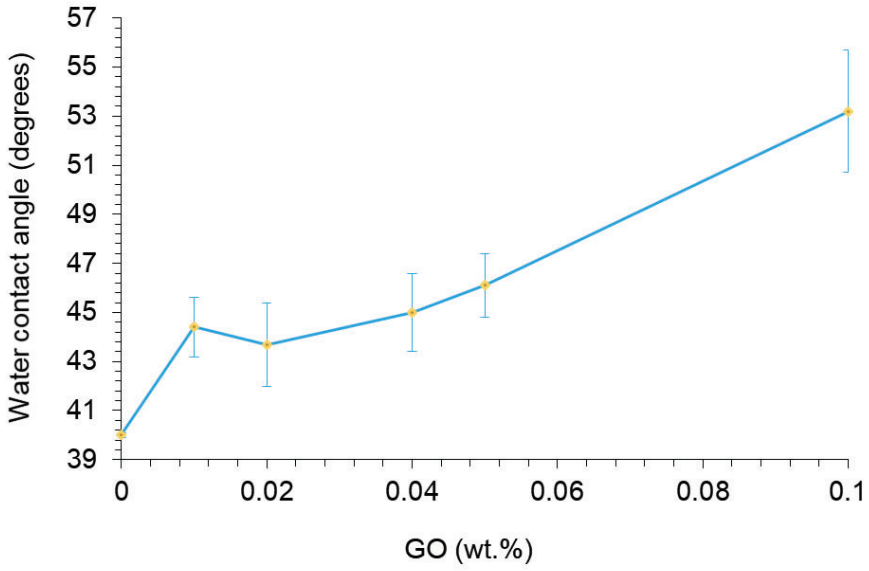

Figure 1.31. Variation of the water contact angle values on the PU and PU+GO materials as a function of the amount of GO.

The improvement of the properties of the PUs obtained by adding GO can be explained by the existence of interactions between the functional groups on the GO nano-sheets surface and the NCO groups of the isocyanate during their syntheses. During prepolymer formation, some end NCO groups of the prepolymer will react with the OH groups on the edges of the GO nano-sheets, creating new urethane groups which will covalently bond the GO surface groups to the prepolymer backbone (Figure 1.32). During the phase inversion stage, the covalently bonded GO nano-sheets will be embedded between the poly(urethane urea) chains, this will change the degree of micro-phase separation between the hard and the soft segments. This justifies the improved thermal and viscoelastic properties of the PU+GO materials. However, for amounts of GO higher than 0.04 wt.%, some GO particles cannot react with the end NCO groups and won´t be covalently bonded to the prepolymer, they will be "trapped" between the poly(urethane urea) chains during the phase inversion stage and an agglomeration of the GO nano-sheets will be produced (Figure 1.32). As a consequence, the properties of the PU+GO materials are different when they contain 0.01-0.04 wt.% GO and 0.05-0.10 wt.% GO.

Figure 1.33 shows the variation of the T-peel strength values of plasticized PVC/PUD or PUD + GO/plasticized PVC joints as a function of the amount of GO measured 72 h after joint formation. The addition of 0.01–0.04 wt.% GO increases the T-peel strength due to the GO-poly(urethane urea) interactions, but the T-peel strength decreases in the joints made with the PUDs containing 0.05–0.10 wt.% GO, this can be ascribed to the existence of some agglomerates of GO nano-sheets. Mixed loci of failure are found in all joints, the cohesive

failure of the PVC substrate is major in the joints made with the PUDs containing 0.01–0.04 wt.% GO, confirming an excellent adhesion.

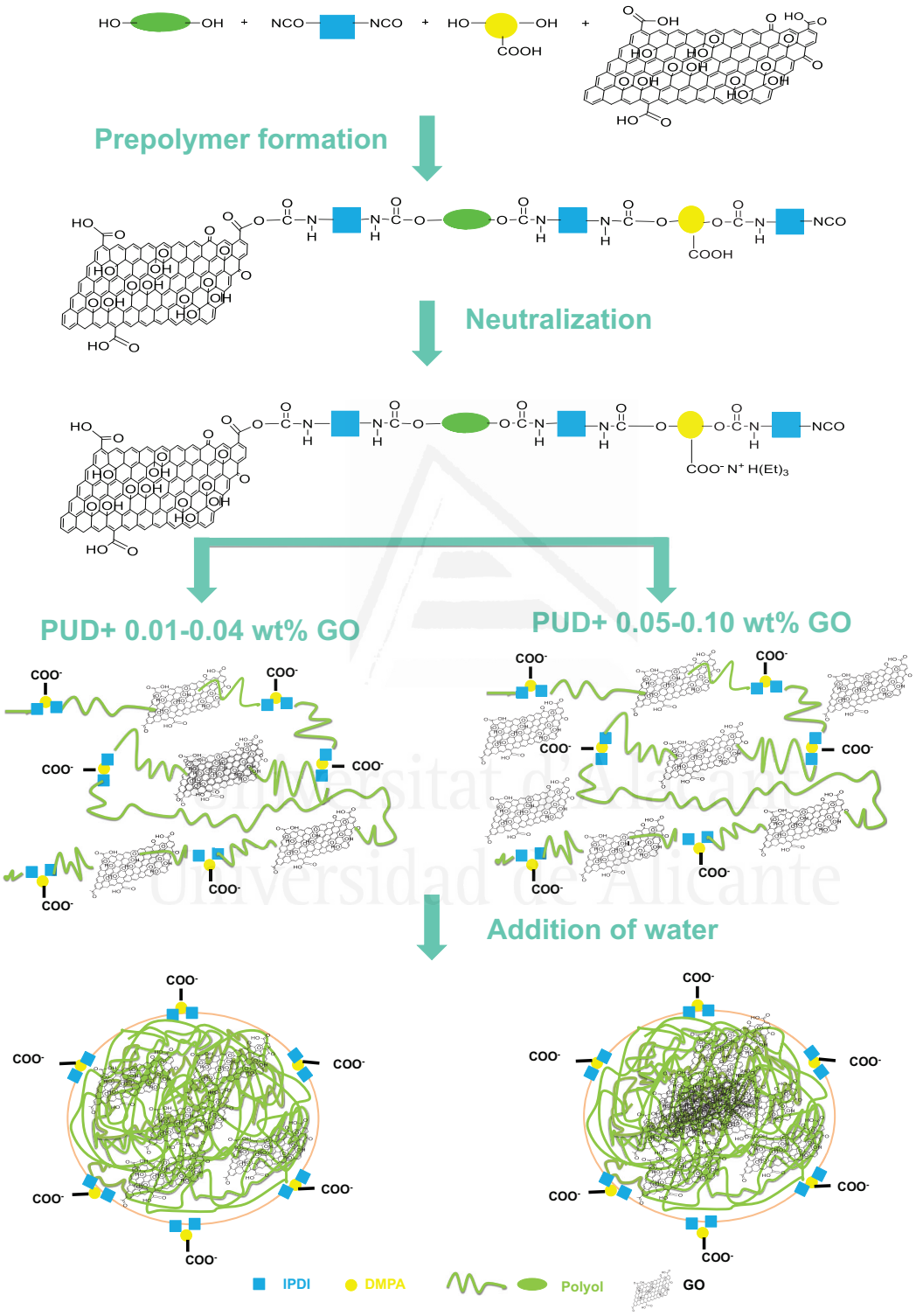

Figure 1.32. Scheme of the interactions between the GO sheets and the end NCO groups of the prepolymer, and the intercalation of the GO nano-sheets during the phase inversion stage.

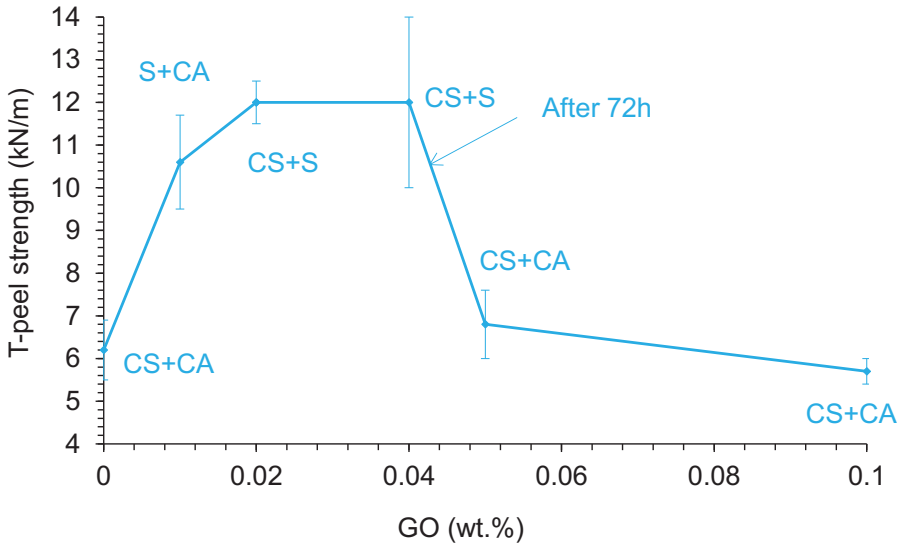

Figure 1.33. Variation of the T-peel strength of plasticized PVC/PUD or PUD+GO dispersion/plasticized PVC joints as a function of the amount of GO measured 72 hours after joint formation. Locus of failure: CS - Cohesion failure of the substrate surface; CA - Cohesion failure of the adhesive; S - Rupture of a substrate.

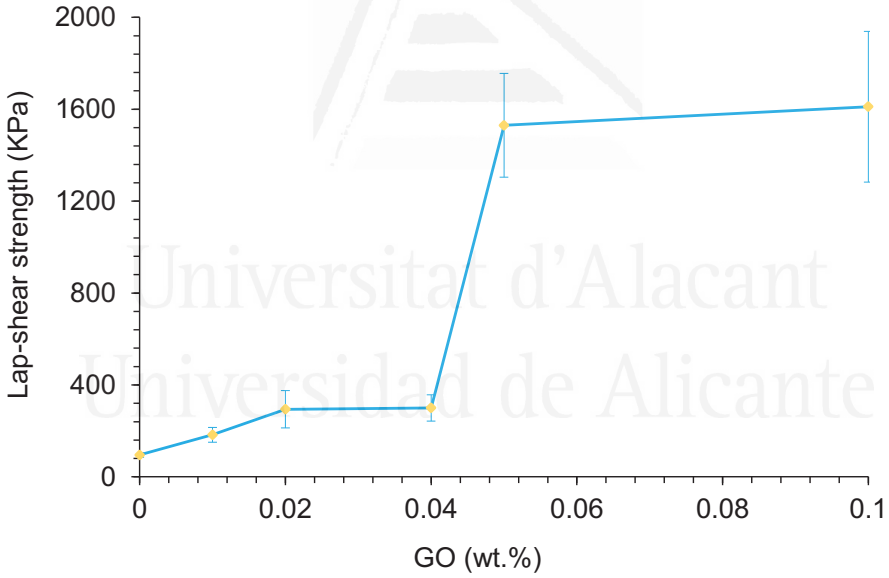

Figure 1.34. Variation of the single lap-shear strength of stainless steel 304/PUD or PUD+GO/stainless steel 304 joints as a function of the amount of GO after 120 hours of joint formation. All joints show an adhesion failure to the stainless steel 304 substrate.

Figure 1.34 shows the variation of the single lap-shear values of stainless steel 304/PUD or PUD+GO/stainless steel 304 adhesive joints obtained 5 days (120 hours) after joints formation. Whereas the lap-shear strength of the joint made with the PUD without GO is somewhat low, an increase in the single lap-shear strength is found in the joints made with

the PUDs containing GO. The lap-shear strength increases noticeably in the joints made with the PUDs containing 0.05-0.10 wt.% GO. Always an adhesion failure is obtained.

Influence of the stage of addition of GO during the synthesis of the PUDs on their properties

Considering that the addition of 0.01-0.05 wt.% GO produces the optimal properties of the PUDs and PUs, including T-peel strength, the influence of the stage of addition of GO during the synthesis of the PUDs (before prepolymer formation, after prepolymer formation, during the addition of water stage) on their properties was analyzed (Figure 1.35).

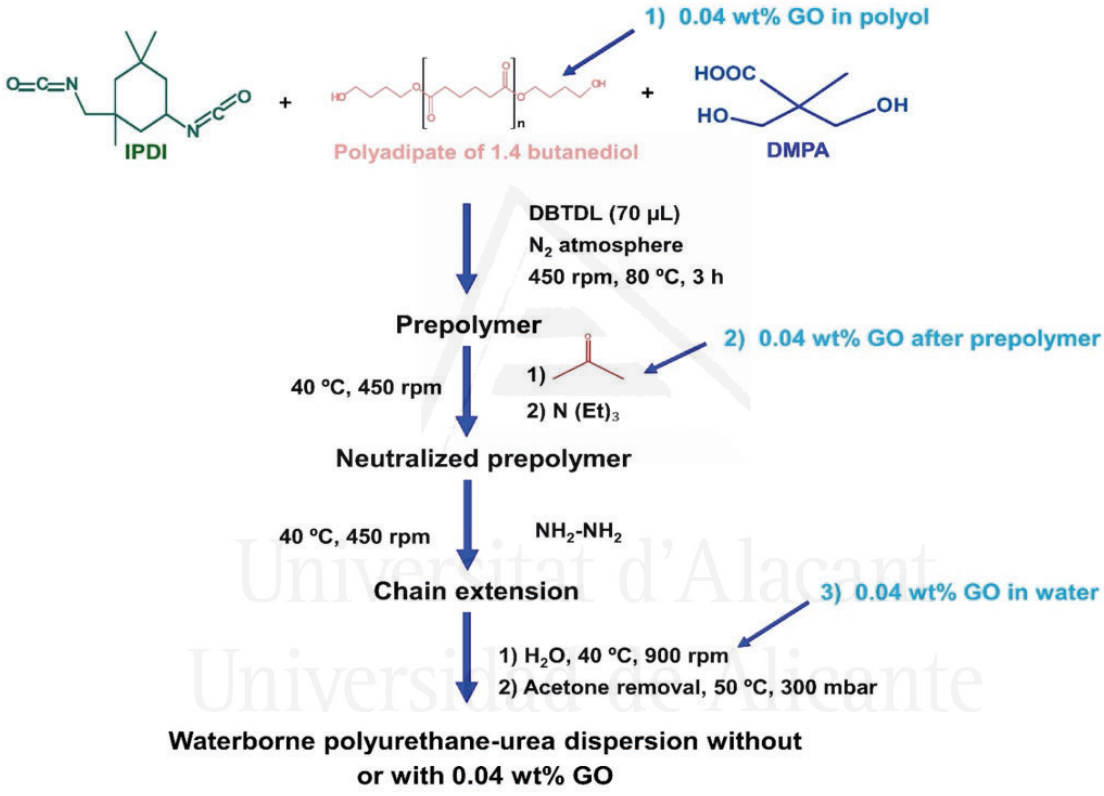

Figure 1.35. Synthesis of the waterborne poly(urethane urea) dispersions without and with 0.04 wt.% GO added in different stages of the synthesis.

The variation of the viscosity at 25 °C of the PUDs without and with 0.04 wt% GO added during different stages of the synthesis as a function of the shear rate is given in Figure 1.36. The viscosity of PUD without GO decreases by increasing the shear rate, i.e., non-Newtonian rheological behavior – shear thinning - is shown. The viscosity of PUD+0.04 wt% GO in water measured at a shear rate of 700 s^{-1} is higher than the one of PUD (Table 1.5), typical behavior of filled polyurethane in which the filler is intercalated among the polymer chains increasing the interactions between them; furthermore, the shear-thinning is much

less marked. Unexpectedly, the viscosities of the PUDs containing GO added before and after prepolymer formation are lower than the one of PUD (Table 1.5). The viscosities of the PUDs containing GO can be ascribed to the extent of the ionic interactions between the particles inside which the covalent interactions between GO and the poly(urethane urea) chains lead to changes on the particles surfaces decreasing the interactions between them. The extent of shear thinning of the PUDs has been coarsely estimated by the "pseudoplasticity index" which is obtained as the ratio of the viscosities measured at shear rates of 1 and 700 s^{-1}. The more shear thinning of the PUD, the higher pseudoplasticity index value. The highest pseudoplasticity index value corresponds to PUD (Table 1.5) in which the ionic interactions between the particles are stronger, and the lowest one corresponds to PUD+0.04 wt% after prepolymer.

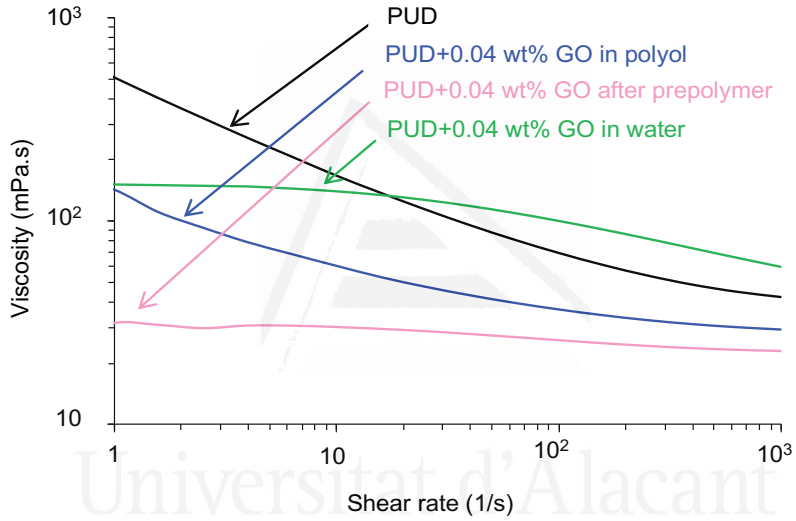

Figure 1.36. Variation of the viscosity of PUD and PUD+0.04 wt.% GO dispersions as a function of the shear rate.

Table 1.5. Viscosities at 25 °C at different shear rates and pseudoplasticity index values of the PUDs.

Poly(urethane urea) dispersion	Viscosity at 1 s^{-1} (mPa.s)	Viscosity at 700 s^{-1} (mPa.s)	Pseudoplasticity index*
PUD	505	42	12.0
PUD+0.04 wt.% GO in polyol	142	30	4.7
PUD+0.04 wt.% after prepolymer	31	23	1.3
PUD+0.04 wt.% GO in water	150	60	2.5

*Pseudoplasticity index = Viscosity at 1 s^{-1}/ Viscosity at 700 s^{-1}

Figure 1.37a shows the 3600-2700 cm^{-1} region of the ATR-IR spectra of PU and PU+0.04 wt% GO. The N-H stretching band at 3367 cm^{-1} in the PU without GO is displaced to 3354 cm^{-1} in PU+0.04 wt% GO in polyol, indicating the existence of interactions between the

functional groups on the GO nano-sheets and the hard segments of the poly(urethane urea). On the other hand, according to Figure 1.37b, the addition of GO displaces the C-O band from 1239 cm^{-1} (PU without GO) to 1256–1257 cm^{-1}, indicating different interactions between the soft segments caused by the GO nano-sheets; furthermore, the intensities of the bands at 1305 and 1370 cm^{-1} due to the absorption of the carboxylic acid of DMPA hard segments vary differently, because the GO-poly(urethane urea) interactions differ depending on the stage of addition of GO during the synthesis, the lowest intensity is obtained in PU+0.04 wt% GO in polyol.

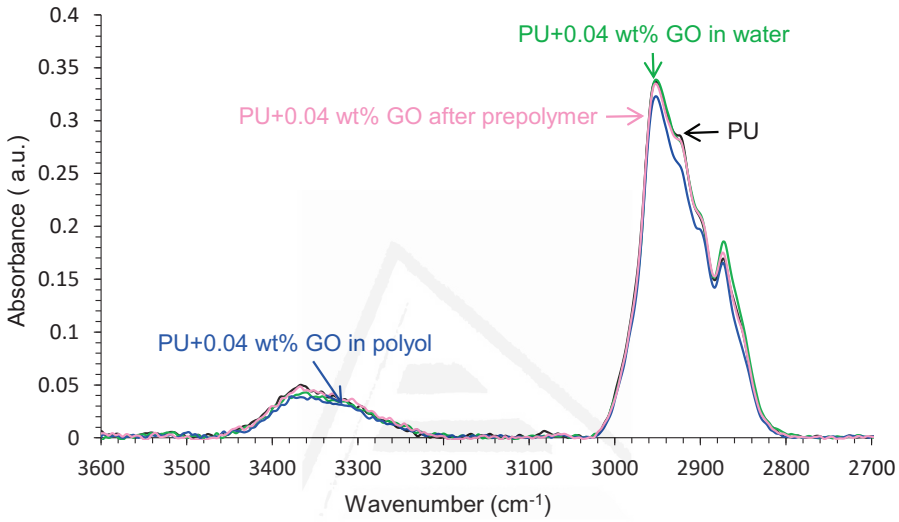

Figure 1.37a. 3600-2700 cm^{-1} region of the ATR-IR spectra of PU and PU+0.04 wt.% GO materials

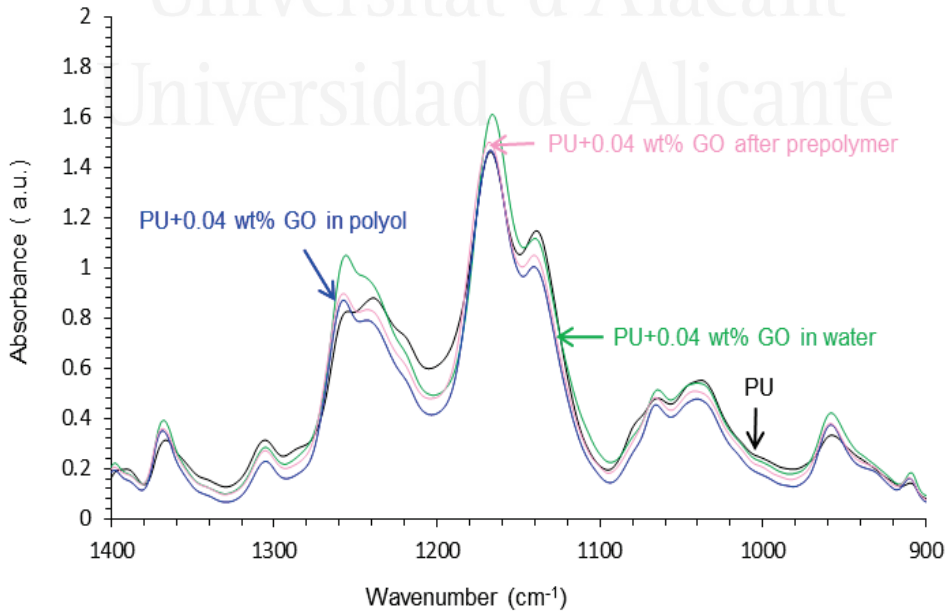

Figure 1.37b. 1400-900 cm^{-1} region of the ATR-IR spectra of PU and PU+0.04 wt.% GO materials.

Figure 1.38 shows the X-ray diffractograms of the PUs in which the characteristic diffraction peak of GO at 2Θ of 9.55° is not observed, indicating the interaction with the polymer chains. Additionally, three diffraction peaks of the PU+GO materials at 2Θ values of 21.3–21.7°, 21.9–22.4° and 24.0–24.2° can be distinguished, all these correspond to the crystalline structure of the polyester polyol. The diffraction peaks of the PUs appear at the same 2Θ values, except in PU+0.04 wt % GO in polyol, in which the diffraction peaks are displaced to lower 2Θ values. This is an indication of the increased interlayer spacing of the GO nano-sheets due to the interactions with the poly(urethane urea) chains. On the other hand, the intensities of the diffraction peaks of the PUs are similar except in PU+0.04 wt.% GO in polyol, in which the intensities are higher because of stronger interactions between the soft segments caused by the interactions between the functional groups on the GO nano-sheets and the poly(urethane urea) chains.

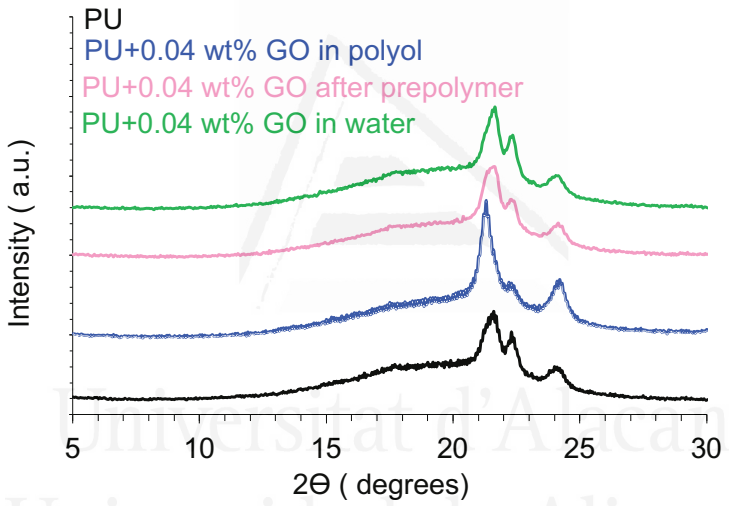

Figure 1.38. X-ray diffractograms of PU and PU+0.04 wt% GO materials.

The thermal data obtained from the TGA thermograms of the PU and PU+0.04 wt.% GO materials confirm their structural change by adding 0.04 wt.% GO in different stages of the synthesis. According to Table 1.6, PU and PU+0.04 wt % GO in water show a small thermal decomposition (2–4 wt.%) at 114-126 °C due to retained moisture. The PU without GO shows three thermal decompositions due to the urethane hard domains (270 °C), urea hard domains (315 °C), and soft domains (380 °C), the higher weight loss corresponds to the soft domains. The addition of GO maintains the temperatures and weight losses of the three thermal decompositions in the PUs, but the decomposition temperature of the urethane hard domains is higher in PU+0.04 wt% GO in polyol, and the one of the urea hard domains is lower in PU+0.04 wt% GO after prepolymer; additionally, both PU+0.04 wt% GO in polyol and PU+0.04 wt% GO after prepolymer show an additional decomposition (4–5 wt.%) at

196-211 °C, which can be ascribed to the thermal rupture of the GO-polyurethane urea interactions. Therefore, the addition of GO before or after prepolymer formation produces more noticeable changes in the degree of micro-phase separation than the one in PU+0.04 wt % GO in water.

Table 1.6. Some data obtained from the TGA thermograms of the PU and PU+0.04 wt% GO materials. At the end of TGA experiment, all PUs exhibit a residue of 2 wt.%.

Poly(urethane urea)	T_1 (ºC)	Weight $loss_1$ (%)	T_2 (ºC)	Weight $loss_2$ (%)	T_3 (ºC)	Weight $loss_3$ (%)	T_4 (ºC)	Weight $loss_4$ (%)
PU	114	2	270	10	315	24	380	62
PU+0.04 wt.% GO in polyol	196	4	275	10	312	21	376	63
PU+0.04 wt.% GO after prepolymer	211	5	271	11	304	18	377	64
PU+0.04 wt.% GO in water	126	4	270	10	312	21	377	63

The rheological and viscoelastic properties of the PUs are also modified by adding 0.04 wt% GO. Figure 1.39 shows the variation of the storage modulus (G´) as a function of the temperature for the PUs. The addition of 0.04 wt% GO in the polyol decreases the storage modulus of the PU, more markedly by increasing the temperature. Nevertheless, the G´ values are somewhat similar in the other PU+0.04 wt% GO materials, this indicates a different structure in PU+0.04 wt% GO in polyol than in the rest.

The mechanical properties of the PUs were assessed by stress-strain tests. According to Figure 1.40, all stress-strain curves show the elastic region followed by a marked yield point and the extended plastic deformation region, this one is less marked in PU+0.04 wt% GO in polyol. The highest yield stress and the lowest yield strain values correspond to PU+0.04 wt% GO in polyol. However, this PU exhibits lower tensile strength and elongation-at-break values than the rest (Table 1.7). The highest tensile strength without a decrease in the elongation-at-break corresponds to PU+0.04 wt% GO in water. Thus, the mechanical properties of the PUs are affected differently by adding GO at different stages of the synthesis.

Table 1.7. Some mechanical properties obtained from the stress-strain curves of the PU and PU+0.04 wt% GO materials.

Poly(urethane urea)	Yield stress (MPa)	Yield strain (%)	Tensile strength (MPa)	Elongation at-break (%)
PU	14 ± 1	7 ± 1	34 ± 4	725 ± 16
PU+0.04 wt.% GO in polyol	23 ± 1	3 ± 1	20 ± 5	637 ± 40
PU+0.04 wt.% GO after prepolymer	19 ± 5	11 ± 3	33 ± 5	728 ± 41
PU+0.04 wt.% GO in water	13 ± 1	13 ± 1	54 ± 3	695 ± 3

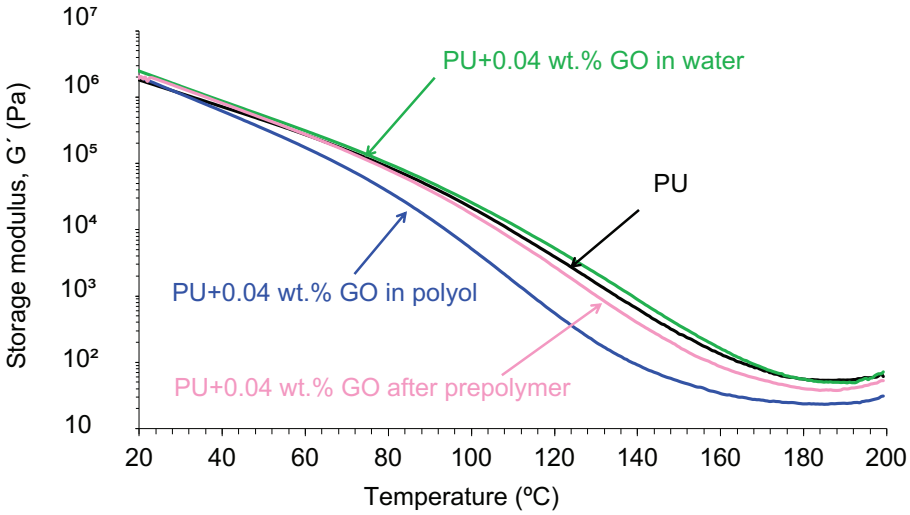

Figure 1.39. Variation of the storage modulus (G´) as a function of the temperature for PU and PU+0.04 wt% GO materials. Plate-plate rheology experiments.

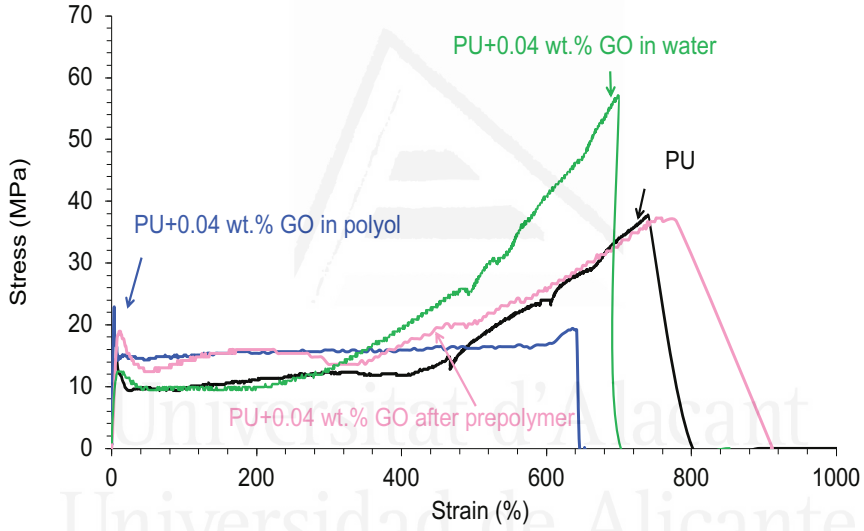

Figure 1.40. Stress-strain curves of the PU and PU+0.04 wt% GO materials.

Table 1.8 shows the T-peel strength values of the plasticized PVC/PUD or PUD+0.04 wt% GO/plasticized PVC joints measured 72 hours after joint formation. The T-peel strength values of the joints made with all PUDs containing GO are higher than the one made with the PUD without GO. The highest T-peel strength value corresponds to the joint made with PUD+0.04 wt% GO in polyol likely due to its particular structure, thermal and viscoelastic properties caused by the existence of more net GO-poly(urethane urea) interactions. Furthermore, a significantly higher T-peel strength value is obtained in the joint made with PU+0.04 wt% GO after prepolymer. The lower adhesion corresponds to the one made with PU+0.04 wt% GO in water in which only physical interactions between the GO nano-sheets and the polymeric chains can be expected.

Table 1.8. T-peel strength values of plasticized PVC/PUD or PUD+0.04 wt% GO/plasticized PVC joints. Locus of failure: CS - Cohesive failure of the substrate surface; CA - Cohesive failure of the adhesive; S - Rupture of a substrate.

Poly(urethane urea) dispersion	T-peel strength – 72h (kN/m)	Locus of failure
PUD	6.2 ± 0.7	CA+CS
PUD+0.04 wt.% GO in polyol	12.0 ± 2.0	S+CA
PUD+0.04 wt.% GO after prepolymer	9.3 ± 0.1	CS+CA
PUD+0.04 wt.% GO in water	7.1 ± 0.3	CS+CA

Influence of the surface chemistry of GO on the properties of the PUDs

The previous studies in this PhD work have shown that the addition of 0.04 wt.% GO in the polyol (i.e., before prepolymer formation) produces the best performance of the PUDs due to the creation of more net covalent interactions between the oxygen groups on the GO surface and the isocyanate groups of the prepolymer during synthesis. Therefore, to address the influence of the surface chemistry of GO on the structure-property relationship of the PUDs, the surface chemistry of GO was modified by grafting nitrogen functionalities (A-GO) and by removing some oxygen groups (r-GO), and the properties of the PUDs and PUs containing these GO derivatives were assessed.

The amounts of the surface functional groups on GO, A-GO, and r-GO obtained by XPS are shown in Table 1.9. GO contains the lowest amount of carbon and the highest amount of oxygen, while both r-GO and A-GO have similar amounts of carbon and oxygen, but the amount of nitrogen is somewhat higher in A-GO.

Table 1.9. Atomic percentages of elements on the surface of the GO derivatives. XPS experiments.

Graphene oxide derivative	Carbon (at.%)	Oxygen (at.%)	Nitrogen (at.%)
GO	64	35	<1
A-GO	84	14	2
r-GO	87	12	<1

The percentages of the different carbon species and their binding energies of GO, A-GO, and r-GO were assessed from their C1s spectra and they are given in Table 1.10. GO has the lowest percentage of C-C and the highest amount of C-O groups, the percentages of C-O groups are similar in r-GO and A-GO. On the other hand, r-GO shows the highest percentage of C=O groups. Therefore, all GO derivative surfaces show the same kind of carbon-oxygen functional groups, but in different amounts.

Table 1.10. Binding energies and percentages of species on the surface on the GO derivatives. C1s spectra.

GO derivative	Species	Percentage (at.%)	Binding energy (eV)
GO	C-C	62	284.6
	C-O	31	286.8
	C=O	5	288.5
	O-C=O	2	290.1
A-GO	C-C	72	284.6
	C-O, C-N	23	286.2
	C(O)OH	5	288.7
r-GO	C-C	67	284.6
	C-O	24	285.9
	C=O	8	288.4
	O-C=O	1	290.7

The variation of the viscosity at 25 ºC as a function of the shear rate for the PUDs without and with 0.04 wt.% GO derivatives with different surface chemistry are given in Figure 1.41. In general, at a low shear rate, the viscosities of the PUDs differ significantly, but at the high shear rate they are less different (19-34 mPa.s), this indicates the existence of non-Newtonian rheological behavior – shear thinning. The PUD without GO derivative shows the most noticeable shear thinning and the viscosity at a shear rate of 700 s^{-1} is 25 mPa.s. The addition of the GO derivative reduces the shear-thinning to a different extent depending on its functional chemistry. PUD+GO is the only one showing a Newtonian rheological behavior. Whereas PUD+A-GO shows some shear thinning and higher viscosity than PUD (34 mPa.s at a shear rate of 700 s^{-1}), PUD+r-GO has more noticeable shear-thinning but lower viscosity. Because the extent of the shear-thinning in the PUDs can be ascribed to the decrease of the ionic interactions between the particles, more net interactions between GO with the poly(urethane urea)chains are produced, likely due to the higher number of surface functional groups in this GO derivative.

Figure 1.42a shows that the addition of GO or A-GO displaces the N-H stretching band from 3364 cm^{-1} (PU without GO derivative) to 3351 or 3335 cm^{-1} respectively, due to the interactions between the OH and/or NH_2 functional groups on GO and A-GO surfaces with the end NCO groups of the prepolymer that lead to the formation of new urethane/urea hard segments. On the other hand, according to Figure 1.42b, the addition of GO and r-GO displaces the C-O band from 1240 cm^{-1} (PU without graphene derivative) to 1257 cm^{-1} indicating that the addition of r-GO affects differently the interactions between the soft segments of the poly(urethane urea).

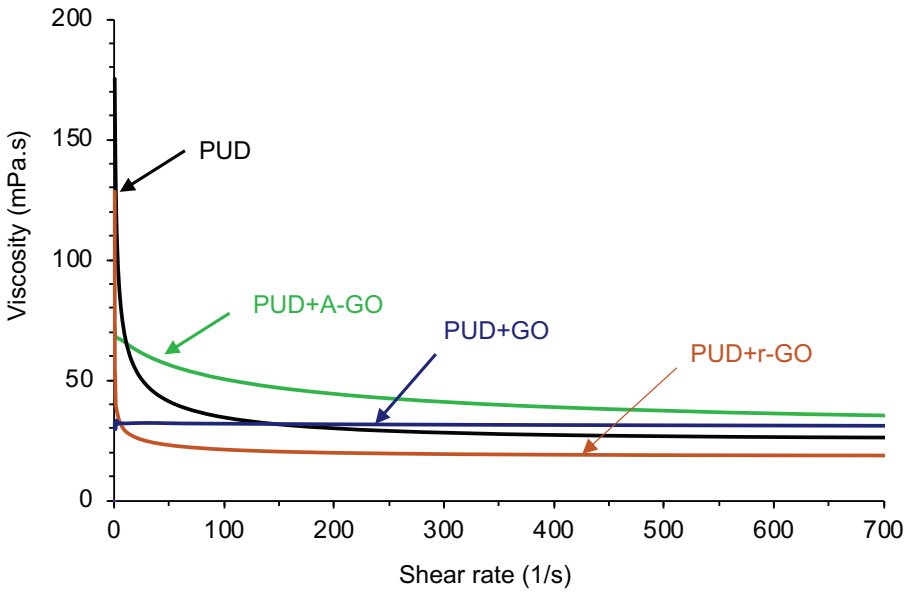

Figure 1.41. Variation of the viscosity of the PUDs without and with GO derivative as a function of the shear rate.

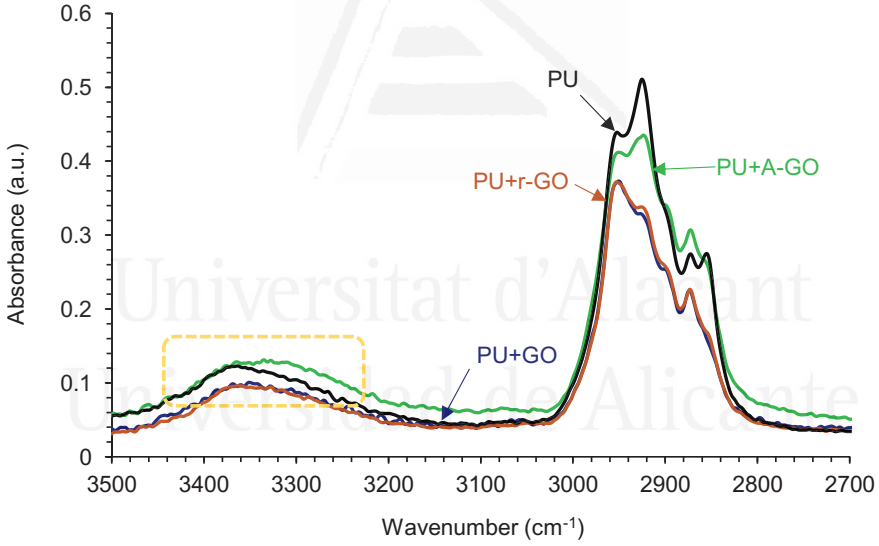

Figure 1.42a. 3500-2700 cm^{-1} region of the ATR-IR spectra of the PUs containing different GO derivatives.

Table 1.11 shows that the free urethane groups are dominant in all PUs. The addition of the GO derivative increases the percentage of the associated by hydrogen bond urethane groups, the increase is more important in PU+r-GO. This confirms the interactions between the hard segments in the PUs containing the GO derivatives. Furthermore, the percentage of free urea groups is lower in PU+r-GO. Therefore, the surface chemistry of the GO derivative determines the segmented structure and causes differences in the degree of micro-phase separation of the poly(urethane urea).

Table 1.11. Percentages of C=O species in the PUs containing different GO derivatives. Curve fitting of the carbonyl region of the ATR-IR spectra.

Wavenumber (cm^{-1})	Relative contribution of species (%)			
	PU	PU+GO	PU+A-GO	PU+r-GO
1727-1726 (free urethane)	54	43	43	40
1712-1708 (H-bonded urethane)	19	30	33	39
1693-1688 (free urea)	17	19	16	9
1657-1652 (H-bonded urea)	10	8	8	12

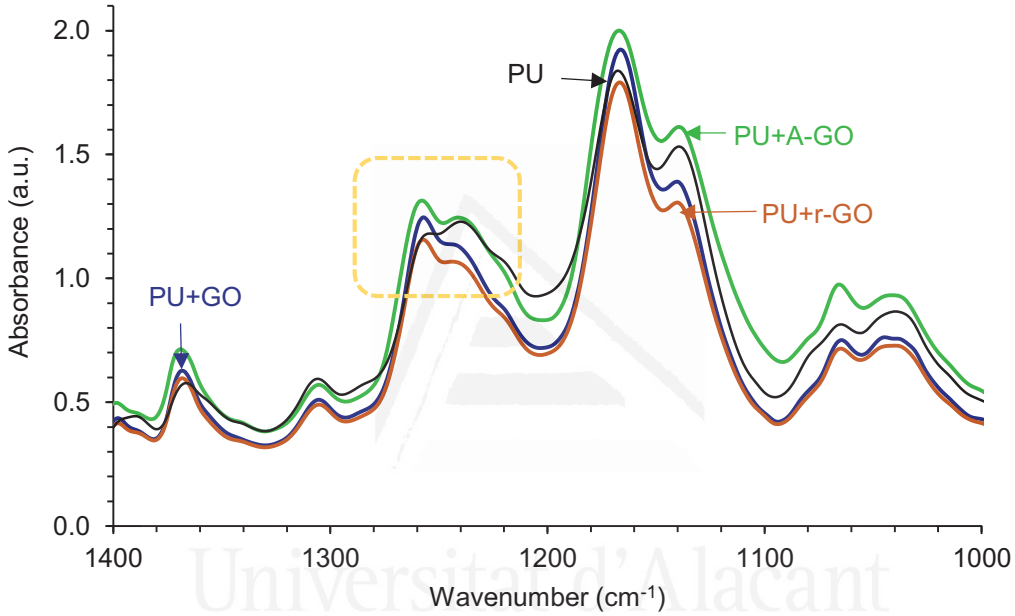

Figure 1.42b. 1400-1000 cm^{-1} region of the ATR-IR spectra of the PUs containing different GO derivatives.

Otherwise, according to Figure 1.43, some changes in the Raman shifts of the soft segments at 1124, 1090, and 1065 cm^{-1} (due to the C-N, C-O-C, and C-O groups respectively) are noticed, this indicates the existence of interactions between the soft segments of the poly(urethane urea) and the surface functional groups on the GO derivative.

Table 1.12 shows the thermal events of the DSC traces (second heating run) of the PUs containing different GO derivatives. The addition of 0.04 wt.% of any GO derivative doesn't change the glass transition temperatures of the soft segments – (-50) – (-53) ºC and 4-5 ºC -, but the T_g of the hard segments decreases, more noticeably in PU+r-GO. Furthermore, one melting peak at 45 ºC of the soft segments appears in PU+A-GO. Hence, the addition of the GO derivative changes the degree of micro-phase separation in the PU due to the

creation of GO derivative-polyurethane urea interactions, and the extent of these interactions depends on the functional groups of the GO derivative.

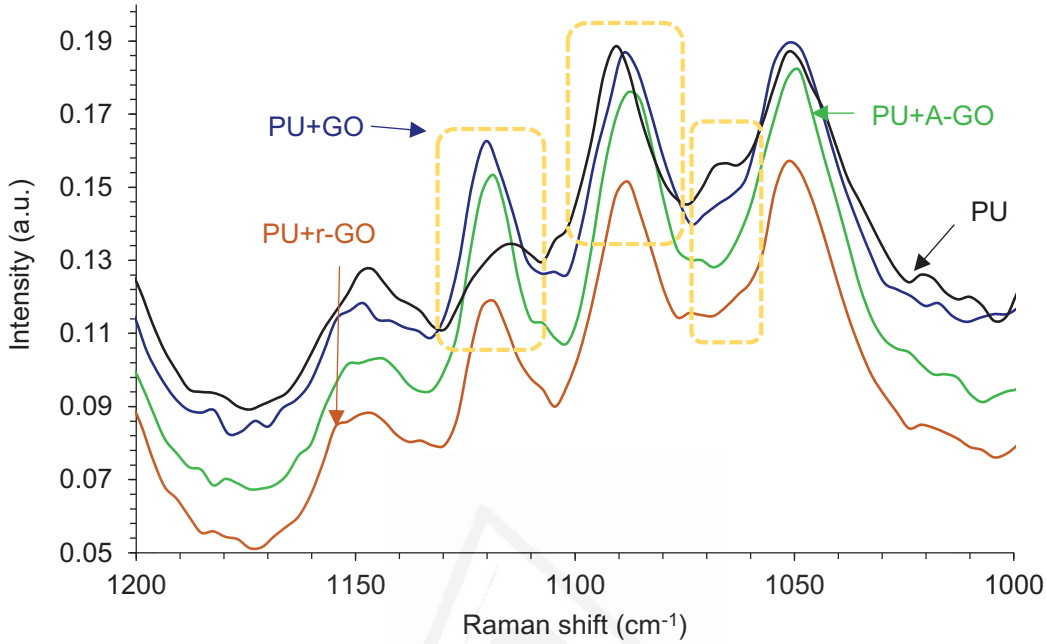

Figure 1.43. 1200-1000 cm^{-1} region of the Raman spectra of the PUs containing different GO derivatives.

Table 1.12. Some data obtained from the DSC traces of the PUs containing different GO derivatives. Second heating run.

Poly(urethane urea)	T_{g1} (°C)	T_{g2} (°C)	T_{g3} (°C)	T_m (°C)	ΔH_m (J/g)
PU	-53	5	193	-	-
PU+GO	-50	5	178	-	-
PU+A-GO	-52	5	179	45	1
PU+r-GO	-51	4	167	-	-

Figure 1.44a shows the variation of the weight as a function of the temperature for PU and PU+GO derivative materials. PU+GO shows lower thermal stability than PU and the other PU+GO derivative materials, likely due to more noticeable structural changes.

The structural changes in the PUs caused by adding GO derivatives can be better distinguished in the derivative TGA plots (Figure 1.44b). All PUs show one or two small thermal decompositions at 50-53 °C and 116-118 °C due to residual moisture.

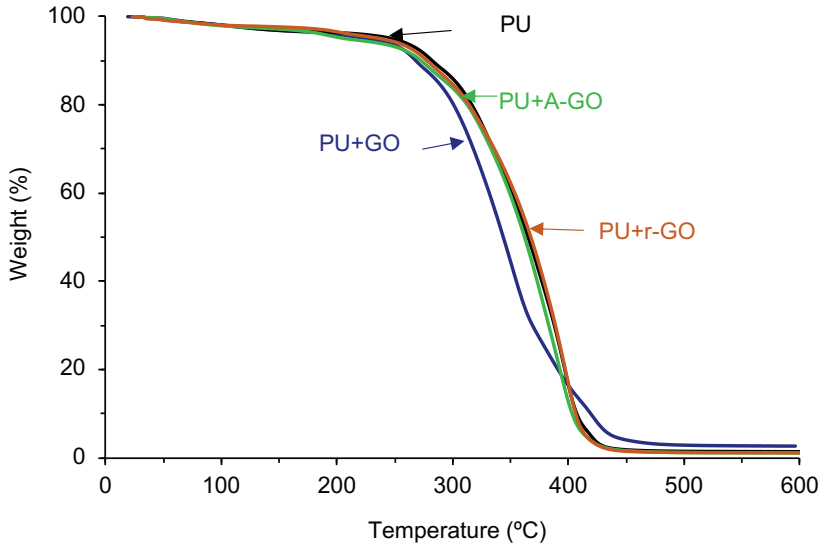

Figure 1.44a. Variation of the weight of the PUs containing different GO derivatives as a function of the temperature. TGA experiment.

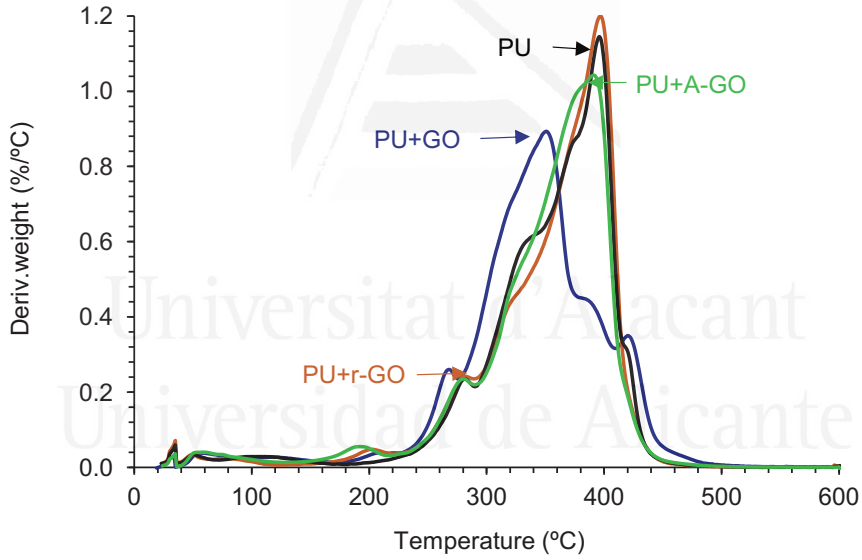

Figure 1.44b. Variation of the derivative of the weight of the PUs containing different GO derivatives as a function of the temperature. TGA experiment.

The PU without GO derivative shows five additional thermal decompositions due to the urethane (280 °C) and urea (329 °C) hard domains, and the soft domains (372, 396, and 422 °C). All PUs containing GO derivative show an additional thermal decomposition at 190-206 °C with weight losses of 2-3 wt.%, this can be ascribed to the existence of GO derivative-poly(urethane urea) interactions. This thermal decomposition is produced at lower temperatures in PU+A-GO, this indicates fewer interactions between A-GO and the

polymer chains. On the other hand, the temperature and the weight loss of the most thermal decompositions of the PU do not change by adding A-GO and r-GO, but the thermal decompositions of the soft domains at 372 and 422 °C do not appear as they are embedded in one unique thermal decomposition of the soft segments at 390-398 °C. Still, the temperature of decomposition and the amount of the urea hard domains decreases in PU+GO due to stronger GO-poly(urethane urea) interactions.

The viscoelastic properties of the PUs containing different GO derivatives have been assessed by DMA. In the glassy region, the storage modulus E´ of the PU increases by adding GO derivative, more noticeably in PU+GO and less markedly in PU+A-GO (Figure 1.45a). The glass transition and the rubbery plateau regions become steeper in the PUs containing GO derivative, except in PU+GO, and the melting is produced at a lower temperature. Therefore, the viscoelastic properties of the PUs are modified by adding GO derivatives. The viscoelastic behavior of PU+GO is similar to the one of the PU without GO derivative, but the values of E´ are higher, indicating that the covalently bonded GO nano-sheets contribute to increasing the storage modulus. However, r-GO and A-GO interact less effectively than GO with the poly(urethane urea) chains, leading to a steeper glass transition and rubbery plateau regions.

On the other hand, Figure 1.45b shows the existence of two relaxations in the tan δ vs temperature plots which can be associated with the glass transition temperatures of the PUs. The addition of the GO derivative decreases the temperatures of the two structural relaxations, and increases the value of the maximum tan delta, less noticeably in PU+GO, this indicates better interactions between the soft and the hard segments, i.e., a lower degree of phase separation, more noticeably in PU+r-GO and PU+A-GO. Furthermore, the value of the maximum of tan delta in PU+r-GO and PU+A-GO are significantly higher than in PU and PU+GO due to the intercalation of the GO derivative nano-sheets between the polymer chains that disturbs the interactions between the soft and the hard segments, and to the higher soft segments content in PU+A-GO. Therefore, the viscoelastic properties of the PUs are determined differently by adding GO derivative with different functional groups.

The addition of GO derivatives influences the morphology of the PU. The SEM micrographs of the fractured surfaces of the PU and PUs containing different GO derivatives are shown in Figure 1.46. All PUs containing the GO derivatives show rough fractured surfaces indicating some toughness. While a rough micro-fractured surface and some small cracks are seen in PU+r-GO, a rough wrinkled fractured surface with some nano-sheets and a few cracks are distinguished in PU+A-GO. The fractured surface of PU+GO is less rough and

the adhesion of the GO nano-sheets is good. Therefore, the addition of the GO derivatives with different functional groups causes different morphologies of the PUs.

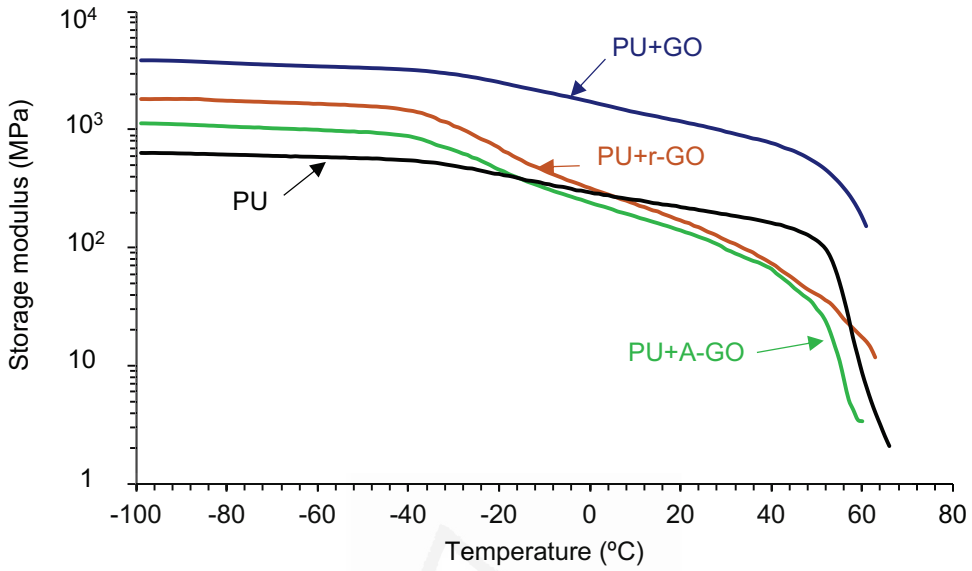

Figure 1.45a. Variation of the storage modulus (E′) as a function of the temperature for PUs containing different GO derivatives. DMA experiments.

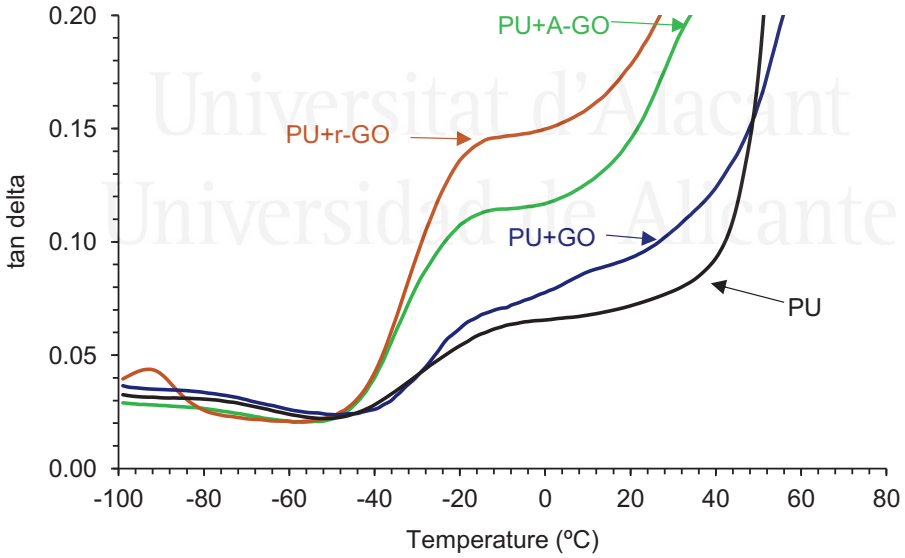

Figure 1.45b. Variation of tan delta as a function of the temperature for PUs containing different GO derivatives. DMA experiments.

The water contact angle values at 25 ºC on the PU and PU+0.04 wt.% GO derivative materials are given in Table 1.13. The addition of r-GO or GO does not change the

wettability on the PU surface (47-48º). Conversely, the addition of A-GO decreases the water contact angle value to 33º, likely due to the high polarity of the nitrogen groups on the A-GO surface.

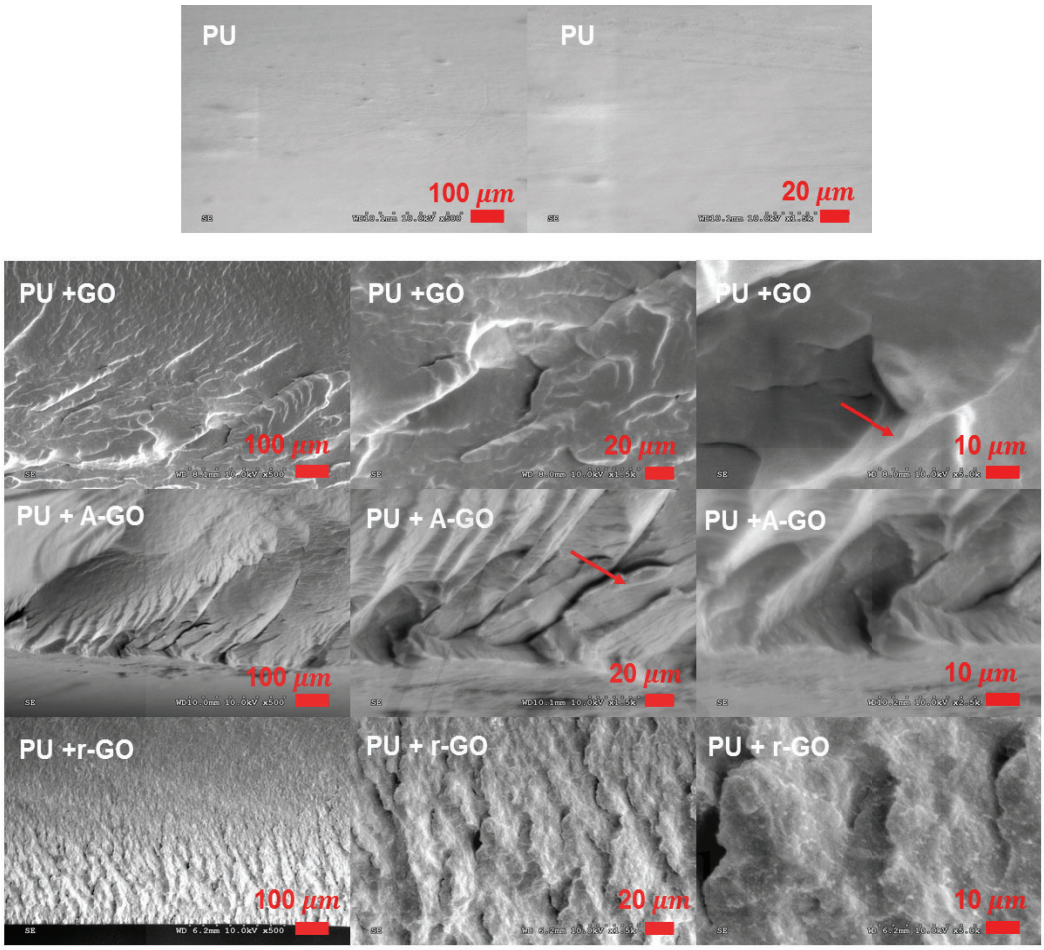

Figure 1.46. SEM micrographs of the fractured surfaces of the PUs containing different GO derivatives.

Table 1.13. Water contact angle values at 25 ºC on the PUs containing different GO derivatives.

Poly(urethane urea)	Water contact angle (º)
PU	47 ± 2
PU+GO	48 ± 0
PU+A-GO	33 ± 2
PU+r-GO	47 ± 2

The scheme of the covalent linkages between the functional groups on the GO derivative surface and the end NCO groups of the prepolymer produced during PUD synthesis are shown in Figure 1.47.

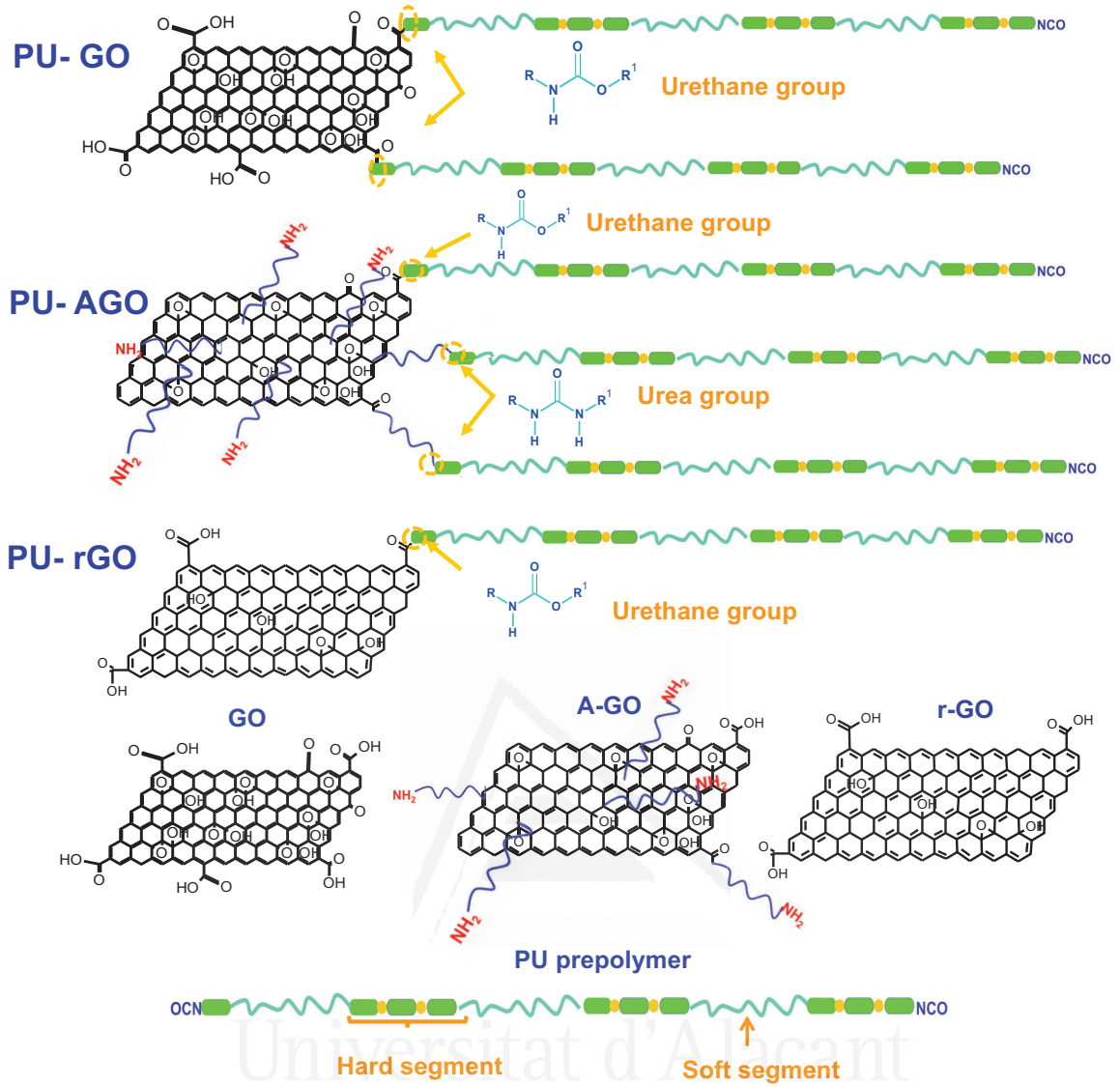

Figure 1.47. Scheme of the covalent linkages between the functional groups on the GO derivative surface and the end NCO groups of the prepolymer produced during PUD synthesis.

During PUD synthesis, the oxygen functional groups on GO and r-GO surface produce new urethane linkages by the reaction with the end –NCO groups of the prepolymer chain, to a greater extent in PU+GO than in PU+r-GO. Furthermore, the number of stacked graphene nano-sheets in r-GO is higher than in GO. Because the nano-sheets intercalate among the polymer chain, the degree of micro-phase separation will be different in PU+GO and PU+r-GO. However, GO has the highest number of functional groups and the thinnest graphene nano-sheets, so more net interactions with the polymer chains will be produced. Conversely, r-GO has the lowest content of functional groups and thicker graphene nano-sheets than GO, so the improvement of the properties of PU+r-GO should be less pronounced. The A-GO surface had a similar amount of oxygen functional groups than r-

GO and some amount of nitrogen functional groups. Because of the higher reactivity of amines with isocyanates, during PUD synthesis, the amine functional groups on the A-GO surface should react preferentially producing new urea hard domains; additionally, there is a chance that some oxygen functional groups on the A-GO surface may also react with the NCO groups. Furthermore, the number of stacked graphene nano-sheets is higher in A-GO than in GO, so the intercalation of the covalently A-GO nano-sheets will disturb differently the interactions between the poly (urethane urea) chains.

Table 1.14 shows the T-peel strength values of the plasticized PVC/PUD or PUD+GO derivative/plasticized PVC joints determined 72 hours after joint formation. The T-peel strength increases in the joints made with PUD+GO and PUD+r-GO and a cohesive failure of the PVC substrate is obtained, indicating a noticeable improvement in adhesion. On the other hand, similar lower T-peel strength values are obtained in the joints made with PUD and PUD+A-GO. The improvement in adhesion obtained with PUD+GO and PUD+ r-GO could be related to the more net covalent GO/PU derivative interactions. Due to the presence of thinner graphene nanosheets in GO, the adhesion is higher in the joints made with PUD+GO and PUD+r-GO, and is mainly determined by the covalent bonds between the oxygen functional groups on the surface of the GO derivative and the prepolymer chains. On the contrary, the lower adhesion of the joints made of PUD+A-GO can be ascribed to the higher content of the soft segments and the lower covalent bonds between the functional oxygen groups on the surface of A-GO and the prepolymer chains.

Table 1.14. T-peel strength values of the plasticized PVC/PUD or PUD+GO derivative/plasticized PVC joints obtained 72 hours after joint formation. Locus of failure: CS - Cohesion failure of the substrate surface; CA -Cohesion failure of the adhesive; S - Rupture of the PVC substrate.

Poly(urethane urea) dispersion	T-peel strength (kN/m)	Locus of failure
PUD	7.0 ± 1.0	CA+CS
PUD+GO	13.5 ± 0.7	S
PUD+A-GO	7.6 ± 2.1	CS+CA+S
PUD+r-GO	12.6 ± 2.0	CS

Influencia de la adición de diferentes derivados de grafeno en las propiedades de las poli(uretano urea)s (PUs)

Diferentes cantidades de distintos derivados de grafeno (0.04 % en peso de GO, 0.30 % en peso de nanoláminas de grafeno – GP -, 0.05 % en peso de grafito molido - MG) se dispersaron en el poliol antes de añadirse al reactor durante la síntesis de las dispersiones acuosas de poli(uretano urea) (PUDs).

Los grupos funcionales de los derivados del grafeno se han cuantificado mediante TGA (Tabla 1.15). GO tiene la mayor cantidad de grupos funcionales (61 %) y corresponden a grupos -C-OH (158, 231-257 °C) y -O-C=O (676-688 °C). GP muestra el contenido más bajo de grupos funcionales (3.5 %) y corresponden a grupos -C-OH (251 °C) y –O-C=O (590 °C), mientras que MG posee solamente 6 % de grupos C-O.

Tabla 1.15. Cantidades de grupos funcionales de los derivados del grafeno. Experimentos TGA.

Derivado del grafeno	Grupo	T (ºC)	Pérdida de peso (%)
GO	Humedad	59	14.0
	-C-OH	158, 231-257	41.0
	-O-C=O	676-688	6.0
GP	-C-OH	251	1.3
	-O-C=O	590	2.2
MG	Humedad	94	9.0
	-C-O	305	6.0

Las cantidades de grupos funcionales superficiales en GO, GP y MG se obtuvieron mediante XPS. Según la Tabla 1.16a, la superficie de GO contiene la mayor cantidad y la superficie de GP la menor cantidad de grupos funcionales de oxígeno, de acuerdo con los experimentos de TGA. Además, la superficie de GO posee una pequeña cantidad de nitrógeno.

Tabla 1.16a. Porcentajes de elementos atómicos en la superficie de los derivados del grafeno. Experimentos de XPS.

Derivado de grafeno	Carbono (at%)	Oxígeno (at%)	Nitrógeno (at%)
GO	64.0	35.0	1.0
GP	96.4	3.6	-
MG	91.4	8.6	-

El ajuste de los espectros C1s de alta resolución de las superficies de GO, GP y MG muestra la

existencia de grupos C–O principalmente, y contribuciones menores de grupos C=O y O-C=O (Tabla 1.16b). De acuerdo con la Tabla 1.16b, la superficie de GO posee el mayor porcentaje de grupos C-O y la superficie de MG contiene el mayor porcentaje de grupos C=O. Los porcentajes de grupos O-C=O son bajos y algo similares en todos los derivados del grafeno.

Tabla 1.16b. Energía de enlace y porcentajes de especies de carbono en las superficies de los derivados del grafeno. Espectros C1s.

Derivado de grafeno	Especie	Porcentaje (at%)	Energía de enlace (eV)
GO	C-C	62	284.6
	C-O	31	286.8
	C=O	5	288.5
	O-C=O	2	290.1
GP	C-C, C-H	74	284.6
	C-O	18	285.8
	C=O	5	287.9
	O-C=O	3	290.7
MG	C-C, C-H	76	284.6
	C-O	13	285.6
	C=O	9	286.6
	O-C=O	2	288.7

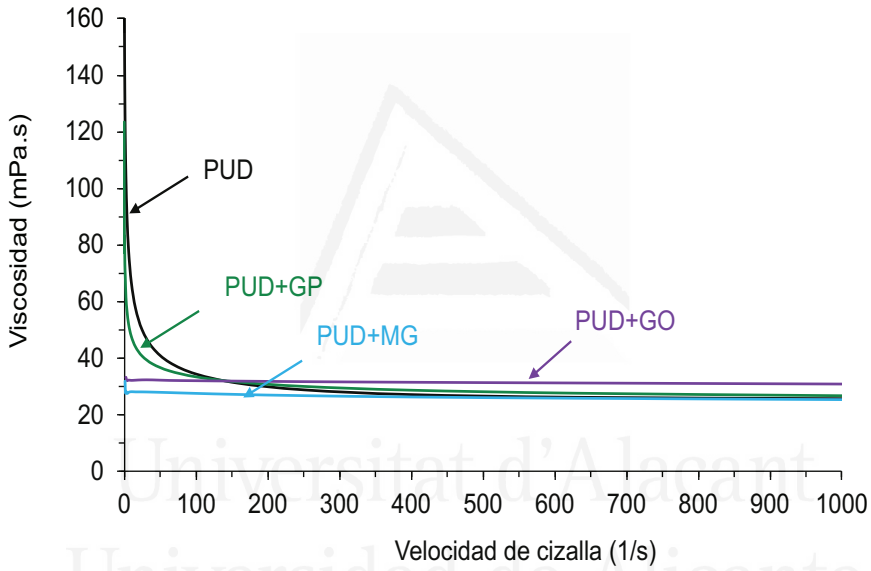

Figura 1.48. Variación de la viscosidad a 22 ºC de las PUDs que contienen diferentes derivados del grafeno en función de la velocidad de cizalla.

La variación de la viscosidad de los PUDs a 22 ºC en función de la velocidad de cizalla se muestra en la Figura 1.48 y las viscosidades a 22 ºC a diferentes velocidades de cizalla se dan en la Tabla 1.17.

El PUD sin derivado de grafeno muestra una disminución de la viscosidad al aumentar la velocidad de cizalla, es decir, exhibe un comportamiento reológico no newtoniano (comportamiento pseudoplástico), lo que se puede atribuir a interacciones entre las partículas. Sin embargo, la adición de pequeñas y casi similares cantidades (0.04-0-05 % en peso) de MG o GO no cambia la viscosidad de las dispersiones de poli(uretano urea) al aumentar la velocidad de cizalla, es decir, se obtiene un comportamiento reológico

newtoniano, lo que indica la existencia de interacciones entre el derivado del grafeno y las cadenas de poli(uretano urea). Además, la adición de GP en mayor cantidad (0.30 % en peso) que de GO o MG mantiene el comportamiento pseudoplástico de la PUD, lo que apunta a la existencia de menores interacciones netas con las cadenas de poli(uretano urea). Por lo tanto, la funcionalidad de la superficie, el número de láminas de grafeno apiladas y la cantidad de derivado de grafeno adicionada, determinan el comportamiento reológico de las PUDs.

El grado de pseudoplasticidad en las PUDs se puede cuantificar por la relación de las viscosidades a velocidades de cizalla de 1 y 100 s^{-1} ("índice de adelgazamiento por cizalla"). El índice de adelgazamiento por cizalla más alto corresponde a PUD seguido de PUD+GP, y los más bajos corresponden a PU+GO y PU+MG. Por tanto, la adición de distintos derivados del grafeno afecta de forma diferente a las interacciones iónicas entre las partículas de las dispersiones de poliuretano. Sin embargo, las viscosidades a altas velocidades de cizalla (10^3 s^{-1}) en todas las PUD son algo similares (25-31 mPa.s), independientemente de la naturaleza del derivado de grafeno, la cantidad adicionada y su morfología y polaridad superficial, lo que indica la ruptura de las interacciones entre las partículas.

Tabla 1.17. Valores de las viscosidades (η) a 22 ºC a diferentes velocidades de cizalla e índice de adelgazamiento por cizalla de las PUDs que contienen diferentes derivados del grafeno.

Dispersión de poli(uretano urea)	η a 1 s^{-1} (mPa.s)	η a 10^3 s^{-1} (mPa.s)	Índice de adelgazamiento por cizalla
PUD	132	25	5.3
PUD+GO	32	31	1.0
PUD+GP	73	26	2.8
PUD+MG	32	25	1.3

* Índice de adelgazamiento por cizallamiento = Viscosidad a 1 s^{-1}/Viscosidad a 10^3 s^{-1}.

La Figura 1.49a muestra que la adición del derivado de grafeno aumenta el número de onda de la banda C-H de los espectros IR-ATR desde 2925 (PU sin derivado de grafeno) a 2951 cm^{-1} y produce la desaparición de la banda C-H a 2855 cm^{-1}; estos cambios indican la existencia de interacciones entre los segmentos blandos de la PU debido a la intercalación/interacción con las nano-láminas de grafeno. De manera similar, la Figura 1.49b muestra que la adición del derivado de grafeno aumenta el número de onda de la banda C-O desde 1240 (PU sin derivado de grafeno) hasta 1255-1257 cm^{-1}, lo que confirma la existencia de interacciones entre los segmentos blandos de la PU.

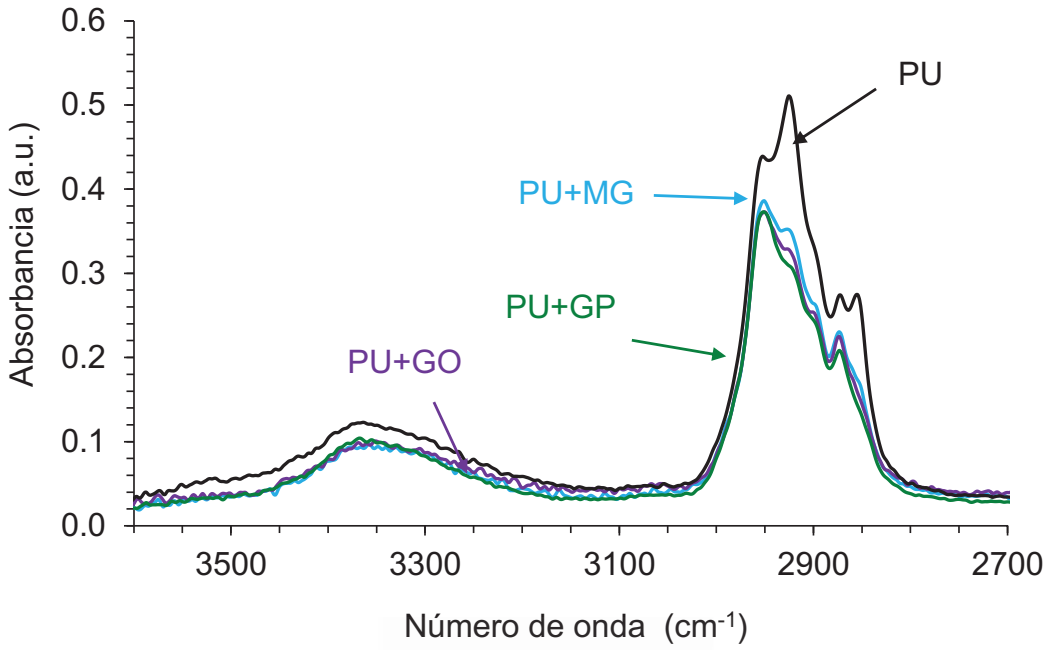

Figura 1.49a. Región de 3600-2700 cm^{-1} de los espectros IR-ATR de las PUs que contienen diferentes derivados del grafeno.

La adición de GO y MG disminuye el número de onda de la banda N-H de los segmentos duros desde 3364 (PU sin grafeno) hasta 3351 o 3358 cm^{-1}, lo que indica la existencia de interacciones con los segmentos duros (Figura 1.49a). Además, los números de onda a los que aparecen las diferentes especies C=O son algo similares en todas las PUs, pero los porcentajes de las diferentes especies C=O difieren (Tabla 1.18). La adición del derivado de grafeno disminuye el porcentaje de grupos uretano libre y aumenta el de grupos uretano enlazados por enlace de hidrógeno, más notablemente al añadir GP y MG, lo que indica un cambio en el grado de separación de microfases en las poli(uretano urea)s. Además, el porcentaje de grupos urea libre disminuye y el de los grupos urea enlazados por enlace de hidrógeno aumenta en las PUs que contienen GP y MG, siendo similares en PU y PU+GO. Por tanto, la polaridad de la superficie del derivado del grafeno determina de manera diferente las interacciones entre los segmentos duros de la poli(uretano urea) que conducen a diferentes estructuras y grados de separación de micro-fases. GP y MG contienen menos grupos funcionales de oxígeno y un mayor número de nano-láminas de grafeno apiladas que GO, por lo que el número de interacciones covalentes derivado de grafeno-poli(uretano urea) en PU+GP y PU+MG es menor, lo que unido al mayor espesor de las nano-láminas de grafeno intercalado, conduce a una mayor separación de micro-fases de las cadenas de poli(uretano urea).

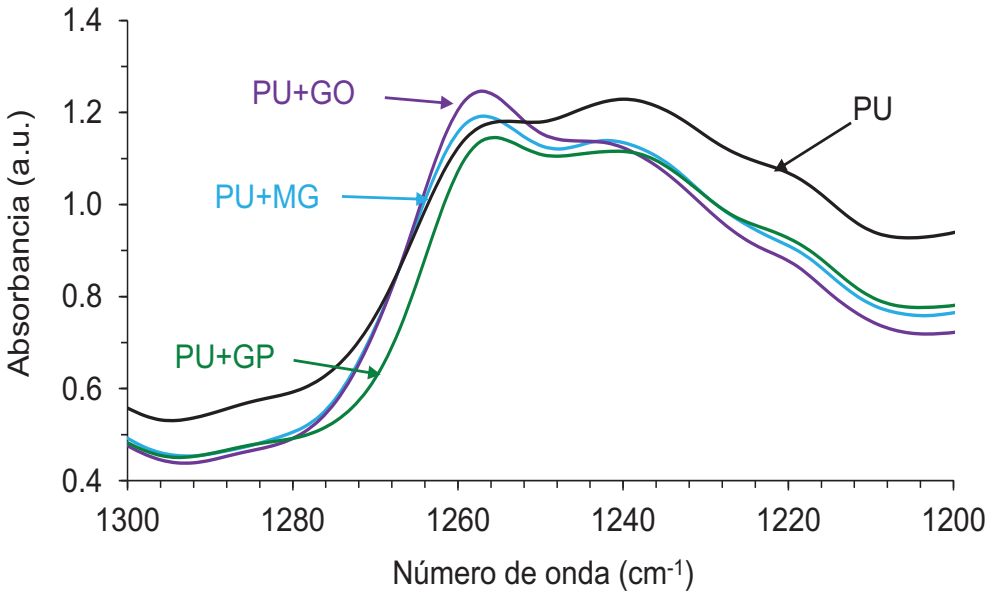

Figura 1.49b. Región de 1300-1200 cm^{-1} de los espectros IR-ATR de las PUs que contienen diferentes derivados del grafeno.

Tabla 1.18. Contribuciones relativas de los grupos uretano y urea libres y asociados en las PUs que contienen diferentes derivados del grafeno. Ajuste de la banda de carbonilo de los espectros IR-ATR.

Número de onda (cm^{-1})	Contribución relativa de especies (%)			
	PU	PU+GO	PU+GP	PU+MG
1727 (Uretano libre)	54	43	37	40
1712-1708 (Uretano enlazado)	19	30	37	35
1693-1689 (Urea libre)	17	19	9	13
1655-1653 (Urea enlazada)	10	8	17	12

La adición del derivado de grafeno crea nuevas bandas C-O-C en los espectros Raman de las PUs debidas a los segmentos blandos (Figura 1.50). La adición de GO y GP produce nuevas bandas C-O-C a 1120 y 1065 cm^{-1} respectivamente en los espectros Raman de las PUs, pero la adición de MG no produce cambios en el espectro Raman, lo que indica menores interacciones entre los segmentos blandos. Así, MG se intercala entre los segmentos blandos con pocas interacciones covalentes con las cadenas de poli(uretano urea), un comportamiento típico de un nanorrelleno. Aunque MG tiene una mayor cantidad de grupos funcionales de oxígeno en la superficie que GP y la cantidad adicionada es mayor que la de GO y GP, el número de nano-láminas de grafeno apiladas es mayor, lo que puede reducir la extensión de las interacciones covalentes. Sin embargo, las PUs que contienen GP y, particularmente, GO muestran un mayor número de interacciones covalentes con las cadenas de poli(uretano urea) debido a su mayor contenido de grupos superficiales C-O y al menor número de nano-láminas de grafeno apiladas, lo que provoca

interacciones diferentes entre los segmentos blandos y un diferente grado de separación de micro-fases.

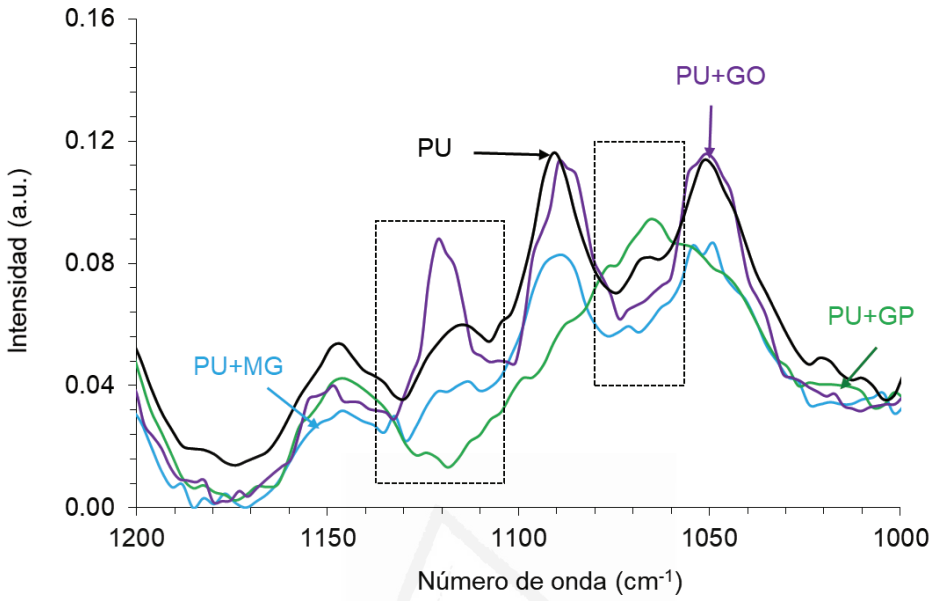

Figura 1.50. Región 1200-1000 cm^{-1} de los espectros Raman de las PUs que contienen diferentes derivados del grafeno.

Los eventos térmicos de las curvas DSC correspondientes al primer y segundo calentamiento de las PUs que contienen diferentes derivados del grafeno se dan en la Tabla 1.19. Las curvas DSC correspondientes al primer ciclo de calentamiento de las PUs muestran la transición vítrea de los segmentos blandos a baja temperatura y la fusión de los segmentos blandos a 46-48 ºC. Todas las PUs muestran dos temperaturas de transición vítrea (T_g) de los segmentos blandos a (-53) - (-50) ºC y 5 ºC, y una T_g de los segmentos duros a 175-193 ºC. La adición del derivado de grafeno disminuye la T_g de los segmentos duros de la PU, lo que indica un menor grado de separación de micro-fases entre los segmentos duros y blandos en las poli(uretano urea)s, independientemente de la morfología y la polaridad superficial del derivado de grafeno.

Tabla 1.19. Algunos datos obtenidos de las curvas DSC de las PUs que contienen diferentes derivados del grafeno.

Poli(uretano urea)	Primer ciclo de calentamiento		Segundo ciclo de calentamiento		
	T_{m1} (°C)	T_{m2} (°C)	T_{g1} (°C)	T_{g2} (°C)	T_{g3} (°C)
PU	46	-	-53	5	193
PU+GO	48	94	-50	5	178
PU+GP	48	122	-50	5	175
PU+MG	46	86	-50	5	175

La Figura 1.51a muestra que las curvas TGA de PU y PU+GP son algo similares y muestran mayor estabilidad térmica que PU+GO y PU+MG. En la literatura se ha establecido la mejora de la estabilidad térmica de los poliuretanos cuando contienen derivados de grafeno [68,74,84,85], pero en este estudio se encuentra una tendencia opuesta, lo que puede deberse a las pequeñas cantidades de derivado de grafeno que se han adicionado y al efecto dominante del grado de separación de micro-fases frente al grado de aglomeración/dispersión del derivado de grafeno en la matriz de la poli(uretano urea).

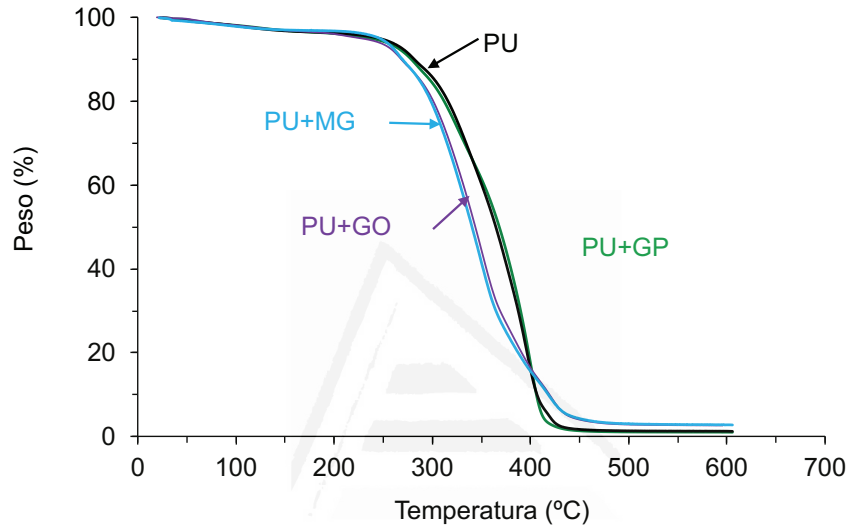

Figura 1.51a. Variación del peso de las PUs que contienen diferentes derivados del grafeno en función de la temperatura. Experimentos TGA.

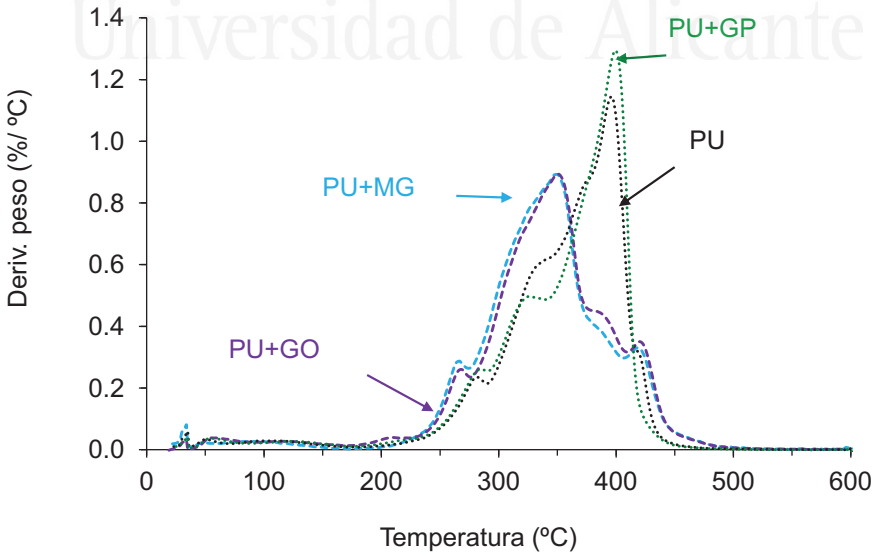

Figura 1.51b. Variación de la derivada del peso de las PUs que contienen diferentes derivados de grafeno en función de la temperatura. Experimentos TGA.

Los cambios estructurales en las PUs causados por la adición de los derivados de grafeno se pueden evaluar a partir de las curvas de la derivada del peso en función de la temperatura (curvas DTGA) (Figura 1.51b). Las curvas DTGA de PU y PU+GP son algo similares y diferentes a las de PU+GO y PU+MG. Todas las PUs presentan pequeñas pérdidas de peso (1-4 %) entre 48 y 118 ºC debidas a humedad residual. Adicionalmente, se distinguen las descomposiciones térmicas de los dominios duros de uretano (264-280 ºC), dominios duros de urea (315-329 ºC y 350-372 ºC), y dominios blandos (389-400 ºC y 421-422 ºC). La adición de GP aumenta la cantidad de dominios duros de uretano y de dominios blandos, y disminuye la de dominios duros de urea, lo que indica las interacciones entre las partículas de GP y las cadenas de poli(uretano urea). Sin embargo, en PU+GO y PU+MG se observan temperaturas más bajas de descomposición y mayores cantidades de dominios duros de uretano y de urea, así como de dominios blandos con respecto a PU y PU+GP, lo que indica interacciones más fuertes de GO y MG con los dominios duros y blandos de la poli(uretano urea).

Las propiedades viscoelásticas de las PUs que contienen diferentes derivados del grafeno han sido evaluadas mediante DMA. La variación del módulo de almacenamiento (E′) en función de la temperatura muestra la zona vítrea, seguida de la región de la transición vítrea y la región de meseta cauchosa, y, aproximadamente a 50 ºC, comienza la fusión de las PUs (Figura 1.52a). Los módulos de almacenamiento de las PUs que contienen diferentes derivados de grafeno aumentan al adicionar el derivado de grafeno, más notablemente en PU+MG y PU+GO. Por otro lado, la Figura 1.52b muestra la existencia de varias relajaciones estructurales en las PUs que contienen diferentes derivados del grafeno, y la temperatura de la relajación α se puede asociar a la temperatura de transición vítrea. Por debajo de -30 ºC, los valores de tan delta de todas las PUs son similares, pero la temperatura de relajación β se desplaza a menor temperatura al adicionar el derivado de grafeno, lo que confirma nuevamente las interacciones entre los segmentos blandos de la poli(uretano urea) y las nano-láminas de grafeno de los derivados de grafeno. Por encima de -30 ºC, PU+MG y PU+GO muestran valores de tan delta más altos que PU y PU+GP, lo que indica mejores propiedades de amortiguación debido a las interacciones covalentes más netas entre las cadenas del polímero y el derivado del grafeno. Por otro lado, la tan delta de PU+GP es menor que la de PU, lo que confirma un comportamiento típico de un nanorelleno. Además, aparece una relajación estructural adicional a 11-16 ºC en PU+GO y PU+MG debido a la existencia de una nueva estructura, y la temperatura de relajación α disminuye en todas las PUs que contienen derivado de grafeno. Por tanto, la adición del derivado del grafeno cambia las propiedades viscoelásticas de las poli(uretano urea)s, más

notoriamente al adicionar GO y MG, de acuerdo con las evidencias aportadas por espectroscopia IR-ATR, espectroscopia Raman, DSC y TGA.

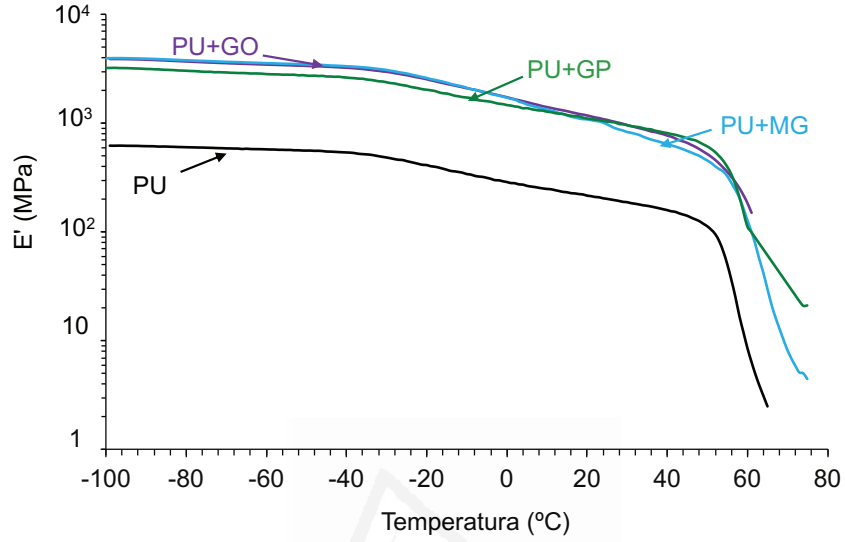

Figura 1.52a. Variación del módulo de almacenamiento (E ') en función de la temperatura para las PUs que contienen diferentes derivados del grafeno. Experimentos de DMA.

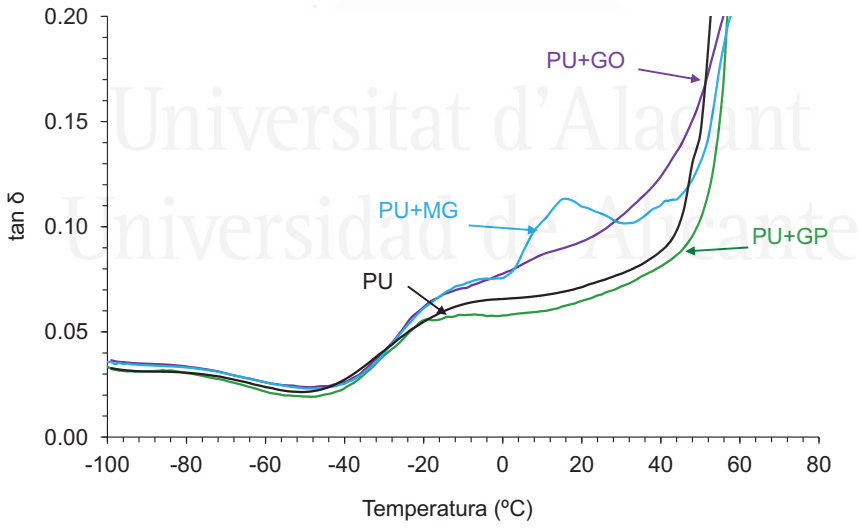

Figura 1.52b. Variación de tan delta en función de la temperatura para las PUs que contienen diferentes derivados del grafeno. Experimentos de DMA.

Las propiedades mecánicas de las PUs que contienen diferentes derivados de grafeno se evaluaron mediante ensayos tensión-deformación. Según la Figura 1.53, todas las curvas tensión-deformación muestran un marcado punto de fluencia seguido de la deformación

plástica hasta que se rompe la película de PU. Las propiedades mecánicas de PU+MG son ligeramente superiores a las de PU, probablemente debido a su mayor contenido de nanorelleno. Además, la tensión a rotura aumenta en todas las PUs que contienen derivado de grafeno, excepto en PU+GO. La adición de GP y, más notablemente, de GO disminuye el límite elástico del PU, pero aumenta la elongación a rotura. Estas evidencias apoyan la tenacidad impartida a la poli(uretano urea) al agregar GP y, en menor medida, GO, una propiedad que se relaciona con las interacciones entre el derivado del grafeno y la poli(uretano urea), así como con la mayor cantidad de GP añadido en PU+GP.

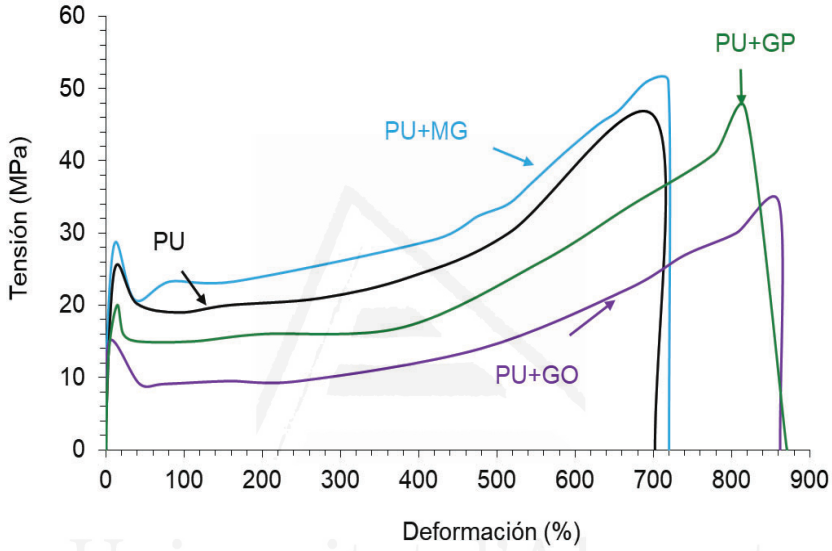

Figura 1.53. Curvas tensión-deformación de las PUs que contienen diferentes derivados del grafeno.

La dispersión de las partículas del derivado de grafeno en la matriz de PU se evaluó mediante microscopía láser confocal. La Figura 1.54 muestra un mayor grado de aglomeración de las partículas de MG en PU+MG, en el que las nano-láminas de grafeno están bastante desordenadas. En PU+GO y PU+GP se obtiene un menor grado de aglomeración de las nano-láminas de grafeno y se pueden distinguir varias partículas redondas bien dispersadas de tamaño menor a 5 µm, principalmente en PU+GP que posee mayor cantidad de nanorelleno.

Los cambios en la morfología de las PUs que contienen diferentes derivados del grafeno se evaluaron mediante micrografías SEM de las superficies fracturadas. Según la Figura 1.55, PU muestra una superficie lisa fracturada, mientras que en PU+MG se pueden distinguir algunos huecos y rugosidades, lo que indica la existencia de tensiones entre las

partículas de MG y la matriz de PU. Sin embargo, las superficies fracturadas PU+GO y PU+GP - que contiene una mayor carga de nanorelleno - muestran la morfología típica de un material tenaz, lo que confirma las interacciones covalentes más netas entre GO o GP y la poli(uretano urea).

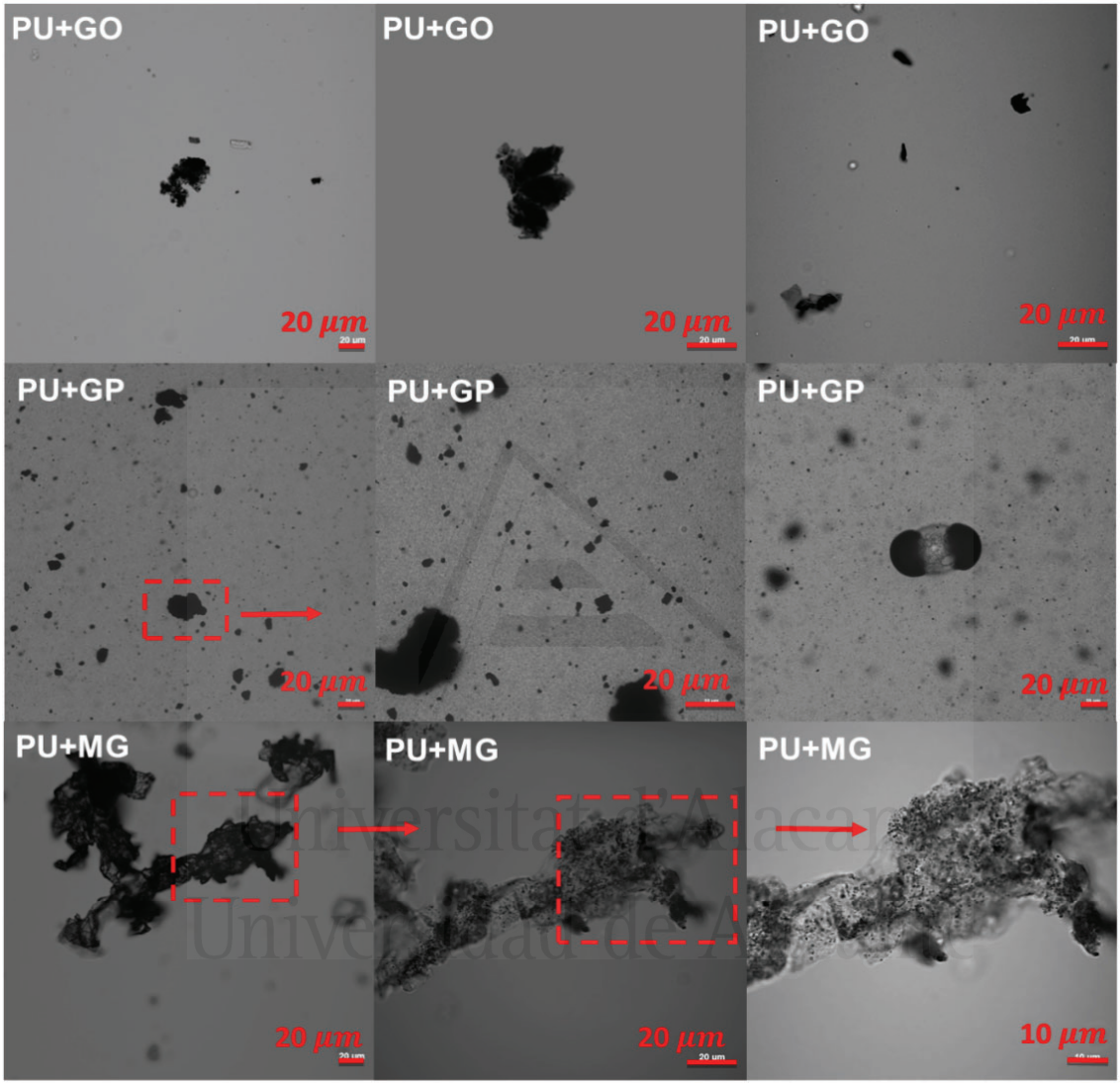

Figura 1.54. Micrografías de microscopía láser confocal de las PUs que contienen diferentes derivados del grafeno.

Las propiedades mejoradas de las PUs que contienen diferentes derivados del grafeno pueden explicarse por la existencia de interacciones entre los grupos funcionales en las superficies de las nano-láminas de grafeno y los segmentos blandos y duros de la poli(uretano urea). Debido a la mayor cantidad de grupos funcionales en GO, se puede esperar un mayor número de interacciones covalentes con los grupos NCO durante la formación del prepolímero, por lo que el grado de separación de micro-fases se verá

afectado de manera diferente que en PU+MG y PU+GP. Además, las nano-láminas de grafeno de GO están bien dispersadas entre los dominios blandos y duros de la poli(uretano urea) (Figura 1.56). Por otro lado, debido a la menor cantidad de grupos funcionales y mayor número de nano-láminas de grafeno apiladas en GP y MG, se favorece la formación de aglomerados de dichas nano-láminas, los cuales quedarán atrapados entre las cadenas de la poli(uretano urea), algunas de ellas covalentemente (Figura 1.56).

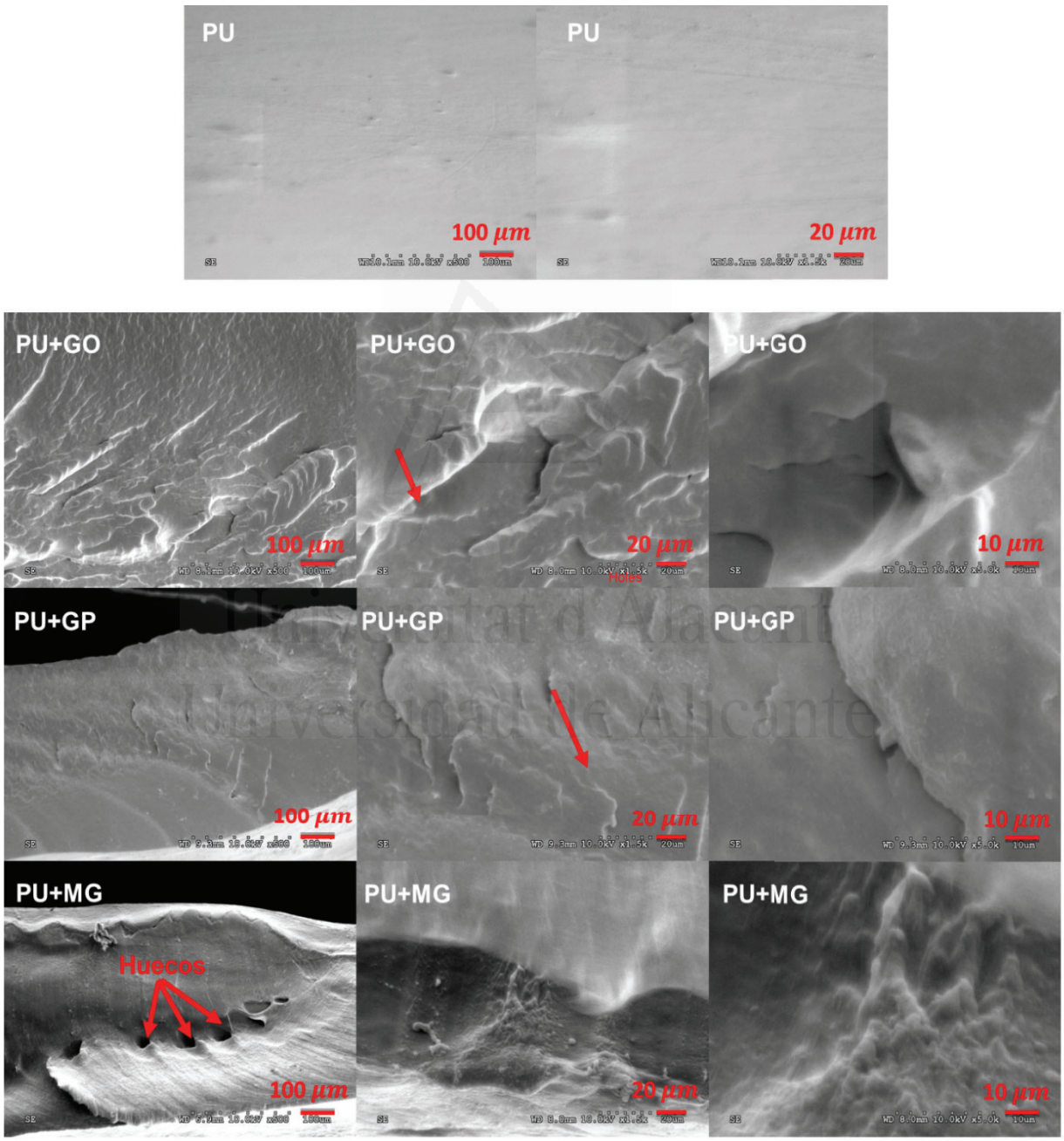

Figura 1.55. Micrografías SEM de las superficies fracturadas de las PUs que contienen diferentes derivados del grafeno.

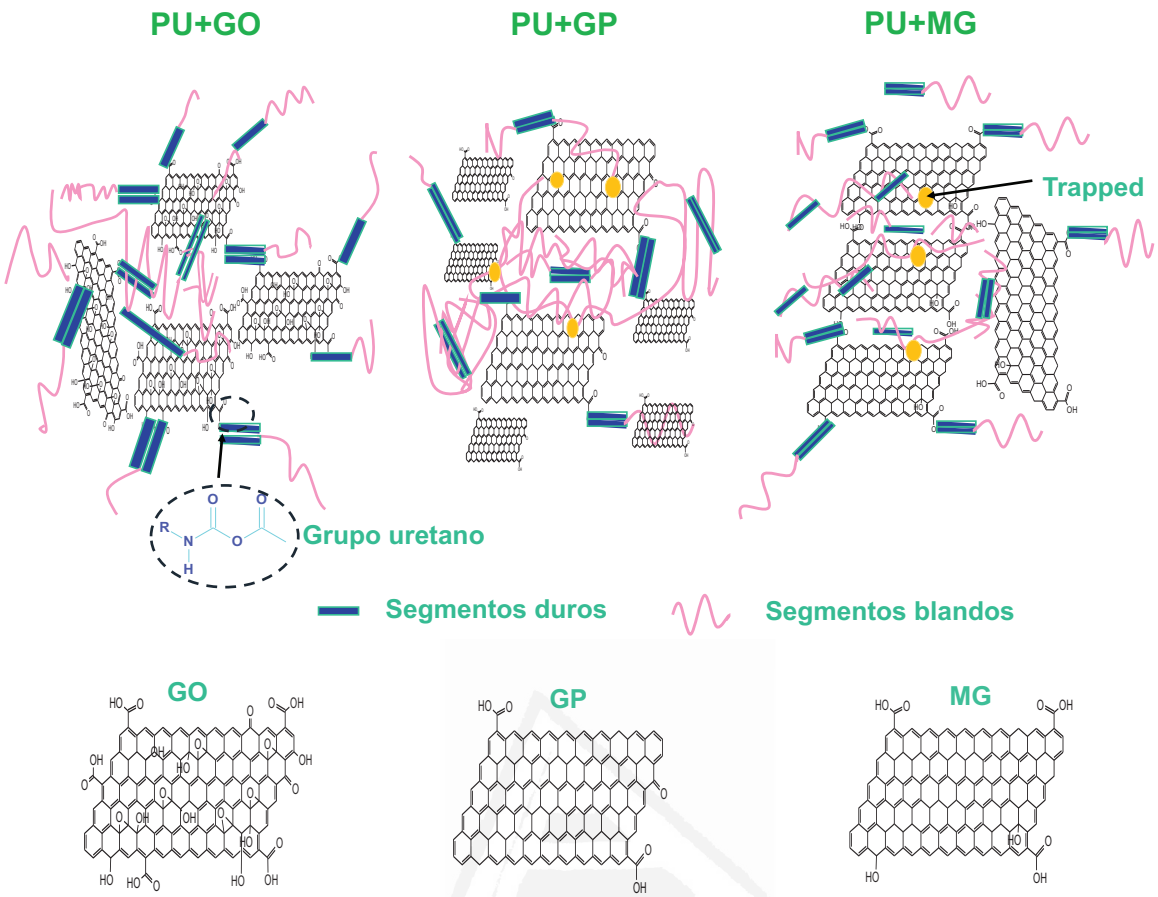

Figura 1.56. Esquema de las interacciones entre los distintos derivados del grafeno y los segmentos duros y blandos de las poli(uretano urea)s.

Tabla 1.20. Valores de fuerza de pelado de uniones PVC flexible/PUD/PVC flexible obtenidos 72 horas después de la formación de las uniones adhesivas. Tipos de fallos de las uniones: CS - Fallo de cohesión en la superficie del sustrato; CA - Fallo de cohesión del adhesivo; S - Rotura del sustrato.

Dispersión de poli(uretano urea)	Fuerza de pelado (kN/m)	Fallo de la unión
PUD	7.0 ± 1.0	CA+CS
PUD+GO	13.5 ± 0.7	S
PUD+GP	5.6 ± 0.7	CA
PUD+MG	7.1 ± 0.2	CA+CS

La Tabla 1.20 muestra los valores de fuerza de pelado de uniones PVC flexible/PUD o PUD+ derivado de grafeno/PVC flexible obtenidos 72 horas después de la formación de las uniones. Los valores de fuerza de pelado son relativamente similares en todas las uniones (5.6-7.1 kN/m) excepto en la realizada con PUD+GO que es mucho mayor (13.5 kN/m) y en la que se produce la rotura del PVC, lo que indica una notable mejora en la adherencia. En el resto de uniones adhesivas se obtienen fallos mixtos de cohesión del adhesivo y del PVC. Por lo tanto, la polaridad de la superficie y la morfología del derivado

del grafeno determinan las propiedades de adhesión de las PUDs, siendo el aumento de la adhesión más notable en PUD+GO debido a las interacciones covalentes más netas entre los grupos oxígeno de la superficie de las nano-láminas de GO y las cadenas de la poli(uretano urea).

6. Conclusions

El objetivo de este trabajo de tesis doctoral ha sido mejorar las propiedades de dispersiones acuosas de poli(uretano urea), particularmente las propiedades de adhesión, mediante la adición durante su síntesis de pequeñas cantidades (0.01-0.30 % en peso) de diferentes nanorellenos de derivados del grafeno que poseen diferentes morfologías y polaridades superficiales.

Los diferentes grupos funcionales, su cantidad, la composición química superficial y la morfología de los derivados del grafeno producen diferentes relaciones estructura-propiedades en las dispersiones acuosas de poli(uretano urea), debido a la diferente interacción química, física y químico-física entre ambos. La mayor cantidad de grupos funcionales superficiales de oxígeno del derivado de grafeno favorece la formación de interacciones covalentes entre la poli(uretano urea) y la superficie del derivado de grafeno. Por otro lado, el diferente método para incorporar el derivado de grafeno durante la síntesis de las dispersiones acuosas de poli(uretano urea) afecta de manera diferente a sus propiedades. Así, la adición de óxido de grafeno antes de la formación del prepolímero cambió de manera más eficiente la estructura de la poli(uretano urea) y produjo más enlaces covalentes netos entre las nano-láminas de GO y los grupos NCO del isocianato (los segmentos duros); estas interacciones generaron un menor porcentaje de grupos uretano libres, mayor cristalinidad, menores módulos de almacenamiento, mayor límite elástico y mayor fuerza de pelado en T. Además, la adición de óxido de grafeno en agua produjo interacciones físicas con las cadenas de poli(uretano urea), ya que las láminas de óxido de grafeno quedaban atrapadas entre las cadenas de poli(uretano urea) cuando se agregaban durante la etapa de adición de agua, lo que justifica sus propiedades mecánicas mejoradas y su alta fuerza de adhesión a cizalla.

Las pequeñas cantidades del derivado de grafeno añadidas durante la síntesis de las dispersiones acuosas de poli(uretano urea) condujeron a un menor cambio en la viscosidad debido a la disminución de las interacciones iónicas entre las partículas. La adición del derivado de grafeno mejoró las propiedades térmicas, reológicas, viscoelásticas y mecánicas de la poli(uretano urea), y estos cambios dependieron de la cantidad y método

de adición del derivado de grafeno durante la síntesis, pero de manera más eficiente al añadir el derivado de grafeno al inicio de la síntesis (polimerización in situ).

Dependiendo de la etapa de la síntesis de la PUD en la que se agrega el derivado de grafeno, el grado de separación de las micro-fases entre los segmentos duros y blandos cambió de manera diferente debido a la magnitud de las interacciones covalentes entre los grupos oxígeno superficiales en las nano-láminas de los derivados del grafeno y los segmentos duros de la poli(uretano urea), lo que se confirmó por el aumento de los porcentajes de grupos uretano y urea asociados por enlace de hidrógeno. De esta forma, dependiendo del equilibrio entre el número de interacciones covalentes entre los grupos superficiales de las nano-láminas de grafeno y los grupos isocianato, y el número de láminas de grafeno de tamaño nanométrico apiladas, se obtuvieron diferentes propiedades y morfologías en las poli(uretano urea)s.

En general, todos los derivados del grafeno se dispersaron bien en la matriz de poli(uretano urea), pero al aumentar el número de nano-láminas apiladas de grafeno se produjo aglomeración de las partículas del derivado de grafeno, por lo que el color de la dispersión acuosa de poli(uretano urea) se hacía más oscuro.

Por otro lado, debido a la diferente polaridad de los derivados de grafeno y la poli(uretano urea), la mojabilidad cambió y aumentó la hidrofobicidad superficial. Los diferentes derivados de grafeno utilizados en este estudio formaron enlaces covalentes con los grupos isocianato finales de la cadena del prepolímero produciendo nuevos segmentos duros de uretano y segmentos duros de urea (solo cuando se agregó óxido de grafeno funcionalizado con amina), lo que hizo que la poli(uretano urea) se rigidizara y que disminuyera la adherencia. Además, debido a que el óxido de grafeno funcionalizado con amina contenía nano-láminas de grafeno apiladas más gruesas, se produjo un mayor porcentaje de segmentos blandos.

El descenso de la cantidad de grupos oxígeno superficiales y el mayor número de nano-láminas apiladas de grafeno en el derivado de grafeno produjeron interacciones menos netas con la poli(uretano urea), ya que las láminas de grafeno atrapadas entre las cadenas de poli(uretano urea) producían interacciones físicas. Debido a las interacciones covalentes, se incrementaron las propiedades mecánicas en las poli(uretano urea)s, aumentando el alargamiento a la rotura, lo que indicaba un incremento de la tenacidad.

Finalmente, la mejora de las propiedades de adhesión y la impartición de tenacidad a las poli(uretano urea)s que contenían pequeñas cantidades de diferentes derivados de grafeno están relacionados con la cantidad de grupos oxígeno en la superficie del derivado de

grafeno que generan enlaces covalentes con las cadenas de la poli(uretano urea). Sin embargo, la adición de algunos de derivados del grafeno (MG, GP) no mejoraron las propiedades de adhesión debido a una aglomeración de las nanoláminas de grafeno en la matriz de poli(uretano urea), obteniéndose la mayor adhesión al agregar óxido de grafeno, debido a su mayor cantidad de grupos C-O superficiales y a su pequeña cantidad de nano-láminas apiladas de grafeno.

Las conclusiones específicas obtenidas en los diferentes estudios realizados en esta tesis doctoral se resumen a continuación.

Adición de pequeñas cantidades de óxido de grafeno en el poliol durante la síntesis de las dispersiones acuosas de poli(uretano urea) (PUDs)

1. Los valores de pH de las PUDs fueron básicos, la adición de 0.01-0.05 % en peso de GO disminuyó la viscosidad y la pseudoplasticidad fue mucho menos marcada; sin embargo, la adición de 0.10 % en peso de GO aumentó notablemente la viscosidad y la pseudoplasticidad de la PUD debido a la aglomeración de las partículas de GO en las micelas de poli(uretano urea).
2. La adición de hasta 0.04 % en peso de GO incrementó los porcentajes de grupos uretano y urea asociados por enlace de hidrógeno, debido a las interacciones entre los grupos oxígeno en la superficie de las nano-láminas de GO y los segmentos duros de la poli(uretano urea). Por otro lado, la adición de 0.05-0.10 % en peso de GO produjo menos grupos uretano asociados por enlaces de hidrógeno, la existencia de cristalización fría y la formación de nuevas bandas en los espectros Raman, indicando la aglomeración de las partículas de GO. Las interacciones entre los grupos superficiales del GO y las cadenas de poli(uretano urea) también se evidenciaron por el aumento de las temperaturas de las descomposiciones térmicas de las poli(uretano urea)s, y por la existencia de una descomposición térmica adicional a 198-229 ºC, la cual se desplazó a menor temperatura al aumentar la cantidad de GO.
3. En los PUs que contienen 0.01-0.04 % en peso de GO, el aumento de la cantidad de GO aumentó los módulos y disminuyó las temperaturas en el cruce de los módulos de almacenamiento y de pérdida, lo que indicó un mayor grado de separación de micro-fases inducido por las interacciones GO-poli(uretano urea).
4. Las nano-láminas de GO se dispersaron bien en la matriz de PU y el tamaño de los dominios de las partículas de GO fue similar en todos los materiales PU+GO (10-15 µm). Además, también se observaron nano-láminas de GO con un tamaño inferior a

1 µm bien dispersadas en la matriz de PU, más abundantes al aumentar el contenido de GO. El número de partículas de GO más pequeñas es más importante en PU+0.04 % en peso de GO, lo que justifica sus diferentes propiedades evidenciadas por espectroscopia IR-ATR, DSC, TGA y difracción de rayos X.

5. La adición de 0.02-0-04 % en peso de GO aumentó los valores de fuerza de pelado en T de las uniones PVC/PUD, pero las realizadas con PUDs conteniendo 0.05-0.10 % en peso de GO eran menores y similares a los de la unión realizada con la PUD sin GO, lo que se atribuyó a la existencia de aglomerados de nano-láminas de GO. Por otro lado, la fuerza de cizalla de las uniones acero inoxidable/PUD fue mayor cuando se usaron las dispersiones acuosas de poli(uretano urea) con 0.05-0.10 % en peso de GO.
6. La mejora de las propiedades de las poli(uretano urea)s que contienen GO se ha explicado por las interacciones covalentes entre los grupos oxígeno superficiales del GO y los grupos NCO del prepolímero durante la síntesis de las PUDs. Durante la formación del prepolímero, algunos grupos NCO reaccionaron con los grupos OH superficiales en los bordes de las nano-láminas de GO creando nuevos grupos uretano unidos covalentemente. Durante la etapa de inversión de fases, las nano-láminas de GO unidas covalentemente se intercalaron entre las cadenas de poli(uretano urea), lo que provocó cambios en el grado de separación de micro-fases entre los segmentos duros y blandos. Sin embargo, para cantidades de GO superiores al 0.04 % en peso, algunas nano-láminas de GO no se unieron covalentemente al prepolímero y quedaron físicamente “atrapadas” entre las cadenas de poli(uretano urea). Como consecuencia, las propiedades de las poli(uretano urea)s fueron diferentes cuando contenían 0.01-0.04 % y 0.05-0.10 % en peso de GO.

Adición de 0.04 % en peso de óxido de grafeno (GO) en diferentes etapas de la síntesis de las dispersiones acuosas de poli(uretano urea)

1) La adición de 0.04 % en peso de GO en diferentes etapas de la síntesis de las PUDs determinó de manera diferente su estructura, propiedades viscoelásticas y de adhesión.
2) La adición de GO antes de la formación del prepolímero cambió de manera más eficiente la estructura de la poli(uretano urea), es decir, las nano-láminas de GO unidas covalentemente alteraron las interacciones entre los segmentos duros

causando un menor porcentaje de grupos uretano libres, mayor cristalinidad, menor módulo de almacenamiento, mayor límite elástico y mayor fuerza de pelado en T.

3) La adición de GO en agua produjo interacciones físicas con las cadenas de poli(uretano urea), es decir, el GO actuaba como un nanorrelleno, lo que justificó las propiedades mecánicas mejoradas y la alta fuerza de cizalla.
4) La adición de 0.04 % en peso de GO disminuyó la viscosidad de las PUDs, siendo una excepción la dispersión PUD+0.04 % en peso de GO en agua. Además, la adición de GO antes de la formación del prepolímero produjo interacciones entre el GO y la poli(uretano urea) provocando cambios en el grado de separación de micro-fases entre los segmentos duros y blandos que se evidenció por una disminución de los porcentajes de grupos uretano y urea libre, y por una disminución de la cantidad de grupos uretano asociados por enlace de hidrógeno. Las interacciones GO-poli(uretano urea) en las PUs que contenían GO añadido antes y después de la formación del prepolímero también se evidenciaron por la disminución de los valores de la T_g de los segmentos blandos y duros, por la ausencia del pico de difracción del GO a $2\Theta=9.55^{o}$, y por la existencia de una descomposición térmica adicional (4-5 % en peso) a 196-211 °C.
5) Las nano-láminas de GO se dispersaron bien en la matriz de poli(uretano urea) sin formarse aglomerados, pudiendo distinguirse nano-láminas de GO de aproximadamente 5-15 μm de longitud, independientemente de la etapa de la síntesis en la que se añadió el GO. Además, el valor más alto del ángulo de contacto medido con agua correspondió a PU+0.04 % en peso de GO en agua.
6) La fuerza de pelado en T aumentó en las uniones a PVC hechas con todos las PUDs que contenían GO, y la mayor fuerza de pelado se obtuvo en la union hecha con PUD-0.04 % en peso de GO en poliol, probablemente debido a la existencia de un mayor número de enlaces covalentes GO-poli(uretano urea). Además, se obtuvo una alta fuerza de pelado en T en la union hecha con PU+0.04 % en peso de GO después del prepolímero. La menor fuerza de pelado en T se obtuvo cuando se usó PU+0-04 % en peso de GO en agua en la que se únicamente se generaron interacciones físicas GO-poli(uretano urea).

Influencia de la química superficial del óxido de grafeno en las propiedades de las dispersiones acuosas de poli(uretano urea)

1) La adición de óxido de grafeno funcionalizado con amina (A-GO) cambió el pH de la PUD debido al tratamiento con dodecil amina y, por lo tanto, las diferencias en el pH de las PUD se pueden atribuir a los grupos funcionales en el derivado de GO.

2) La PUD sin derivado de GO mostró una pseudoplasticidad más notable y la adición del derivado de GO redujo de manera diferente la pseudopalsticidad dependiendo de su química superficial, mientras que PUD+GO mostró un comportamiento reológico newtoniano.
3) La adición de GO y A-GO desplazó el número de onda de la banda de estiramiento NH y la adición de GO y r-GO desplazó el número de onda de la banda CO, confirmando el cambio estructural de los segmentos duros de la poli(uretano urea).
4) Los nuevos grupos uretano se formaron por reacción de los grupos C-O en la superficie GO y r-GO con los grupos NCO finales del prepolímero, y las nano-láminas de GO y r-GO se unieron covalentemente a los segmentos duros de uretano. Como consecuencia, se obtuvieron menores grados de separación de fases en PU+GO y en PU+r-GO que en PU.
5) Los grupos funcionales amina en la superficie de A-GO reaccionaron preferentemente con los grupos isocianato produciendo nuevos dominios duros de urea y, debido a que A-GO tenía nano-hojas de grafeno apiladas más gruesas, se produjo un mayor porcentaje de segmentos blandos que en el PU sin derivado de GO.
6) Los derivados de GO se dispersaron bien en la matriz de poli(uretano urea), pero cambiaron su morfología de manera diferente. Mientras que en PU+r-GO y PU+A-GO se observó una superficie arrugada y fracturada, en PU+GO aparecía una morfología típica de un polímero rígido.
7) La adición de A-GO aumentó más el porcentaje de los segmentos blandos en PU+A-GO que en los otros PUs.
8) La estabilidad térmica de PU se afectó de manera diferente al agregar el derivado de GO con diferentes grupos funcionales.
9) En la región vítrea, el módulo de almacenamiento de PU aumentó y la fusión se produjo a menor temperatura al agregar el derivado de GO, más notoriamente en PU+GO y menos notablemente en PU+A-GO debido a su mayor porcentaje de segmentos blandos.
10) La adición del derivado GO impartió cierta tenacidad a la PU, en diferente medida dependiendo de la cantidad de grupos funcionales y el número de nano-láminas de grafeno apiladas en el derivado de GO.
11) Se obtuvieron los valores más altos de resistencia al pelado en T en las uniones realizadas con PUD+GO y PUD+r-GO, en las que se obtuvo una rotura del sustrato de PVC, lo que indicaba una adherencia óptima.

Influencia de la adición de pequeñas cantidades de diferentes derivados del grafeno (GO, MG, GP) en las propiedades de las dispersiones acuosas de poli(uretano urea)

1) La adición de los distintos derivados de grafeno cambió de manera diferente el grado de separación de micro-fases de la poli(uretano urea) debido al equilibrio de las interacciones covalentes entre la superficie del derivado de grafeno y los grupos isocianato de la poli(uretano urea), y el número de nano-láminas apiladas de grafeno.
2) La adición de MG o GO no cambió la viscosidad de las PUDs, y la pseudoplasticidad de las dispersiones de PUD y PUD+GP se atribuyó a la creación de interacciones iónicas más fuertes entre las partículas de PUD.
3) La adición del derivado de grafeno disminuyó la T_g de los segmentos duros de PU, lo que indicaba un menor grado de separación de micro-fases entre los segmentos duros y blandos en la poli(uretano urea). Además, la adición del derivado de grafeno aumentó los porcentajes de grupos uretano y urea asociados por enlace de hidrógeno, más notablemente al agregar GP y MG. Por otro lado, la adición de GP aumentó la cantidad de dominios duros y blandos de uretano, y disminuyó la cantidad de dominios duros de urea.
4) Se encontraron temperaturas más bajas de descomposición y mayor cantidad de dominios duros de uretano y urea, y de dominios blandos en PU+GO y PU+MG con respecto a PU y PU+GP, lo que indicaba interacciones más fuertes de GO y MG con los dominios duros de urea y dominios blandos de las cadenas de poli(uretano urea).
5) Puesto que GP y MG contenían menos grupos oxígeno superficiales y mayor número de nano-láminas apiladas de grafeno que GO, formaron menor número de interacciones covalentes derivado de grafeno-poli(uretano urea), lo que causó un grado diferente de separación de micro-fases en PU+GO que en PU+GP y PU+MG. Mientras que MG se intercaló entre los segmentos blandos con interacciones covalentes reducidas con las cadenas de poli(uretano urea) mostrando un comportamiento típico de nanorrelleno, GP y, en particular, GO mostraron un mayor número de interacciones covalentes con las cadenas de poli(uretano urea).
6) Los valores de E´ de las PUs aumentaron al adicionar el derivado de grafeno, más notoriamente en PU+MG y PU+GO, y por debajo de -30 ºC, la temperatura de la relajación estructural β disminuyó, debido a las interacciones entre los segmentos blandos y las nano-láminas de grafeno. Por encima de -30 ºC, PU+MG y PU+GO mostraron valores de tan delta más altos que PU y PU+GP, lo que indicó mejores

propiedades de amortiguación, y ambos mostraron una relajación estructural adicional a 11-16 ºC.

7) PU y PU+GP eran más estables térmicamente que PU+GO y PU+MG, y la resistencia a la tracción aumentó en todas las PUs que contenían derivados de grafeno, excepto en PU+GO. La adición de GP y, más marcadamente, GO disminuyó el límite elástico de la PU pero aumentó el alargamiento a la rotura, lo que mostró la tenacidad impartida al agregar GP y, en menor medida GO, a la poli(uretano urea). La tenacidad también se confirmó en las micrografías SEM de las superficies fracturadas.
8) Se encontró mayor grado de aglomeración y partículas de MG altamente desordenadas en PU+MG, y menor grado de aglomeración de las nano-láminas de grafeno en PU+GO y PU+GP. La superficie fracturada de PU mostró una superficie de fractura lisa, mientras que en PU+MG se distinguieron algunos huecos y rugosidades debidas a tensiones entre las partículas de MG y la matriz de PU.
9) Los valores de fuerza de pelado en T fueron similares en todas las uniones (5.6-7.1 kN/m) excepto en la realizada con PUD+GO que era mucho mayor (13.5 kN/m), debido a las interacciones covalentes más netas entre la superficie de las nano-láminas de GO y las cadenas de poli(uretano urea). Por lo tanto, la polaridad de la superficie y la morfología del derivado del grafeno determinaron las propiedades, incluida la adhesión, de las PUDs.

7. References

1. Frisch, K.C. Chemistry and technology of polyurethane adhesives. Adhesion Science and Engineering. 2002, 16, 759–812, doi:10.1016/b978-044451140-9/50016-0
2. Patel, M.R.; Shukla, J.M.; Patel, N.K.; Patel, K.H. Biomaterial based novel polyurethane adhesives for wood to wood and metal to metal bonding. Materials Research. 2009, 12 (4), 385–393, doi:10.1590/s1516-14392009000400003.
3. Bao, L.H.; Lan, Y.J.; Zhang, S.F. Synthesis and properties of waterborne polyurethane dispersions with ions in the soft segments. Journal of Polymer Research. 2006, 13 (6), 507–514, doi:10.1007/s10965-006-9073-7.
4. Lin, S.B.; Hwang, K.S.; Tsay, S.Y.; Cooper, S.L. Segmental orientation studies of polyether polyurethane block copolymers with different hard segment lengths and

distributions. Colloid and Polymer Science. 1985, 263 (2), 128–140, doi:10.1007/bf01412787.

5. Xiao, Y.; Jiang, L.; Liu, Z.; Yuan, Y.; Yan, P.; Zhou, C.; Lei, J. Effect of phase separation on the crystallization of soft segments of green waterborne polyurethanes. Polymer Testing. 2017, 60, 160–165, doi:10.1016/j.polymertesting.2017.03.029.
6. García-Pacios, V.; Costa, V.; Colera, M.; Martín-Martínez, J.M. Waterborne polyurethane dispersions obtained with polycarbonate of hexanediol intended for use as coatings. Progress in Organic Coatings. 2011, 71 (2), 136–146, doi:10.1016/j.porgcoat.2011.01.006.
7. Arán-Aís, F.; Torró-Palau, A. M.; Orgilés-Barceló, A. C.; Martín-Martínez, J.M. Characterization of thermoplastic polyurethane adhesives with different hard/soft segment ratios containing rosin as an internal tackifier. Journal of Adhesion Science and Technology. 2002, 16 (11), 1431–1448, doi:10.1163/156856102320252886.
8. Rahman, M.M.; Kim, H.D. Characterization of waterborne polyurethane adhesives containing different soft segments. Journal of Adhesion Science and Technology. 2007, 21 (1), 81–96, doi:10.1163/156856107779976088.
9. Cantos Delegido, B. Nuevas dispersiones acuosas de poliuretano obtenidas empleando co-solventes ecológicos: Síntesis, characterization y aplicación como adhesivos. Doctoral Thesis. University de Alicante (Spain). 2015.
10. Cakić, S.M.; Špírková, M.; Ristić, I.S.; B-Simendić, J.K.; M-Cincović, M.; Poręba, R. The waterborne polyurethane dispersions based on polycarbonate diol: Effect of ionic content. Materials Chemistry and Physics. 2013, 138 (1), 277–285, doi:10.1016/j.matchemphys.2012.11.057.
11. Jiang, X.; Li, J.; Ding, M.; Tan, H.; Ling, Q.; Zhong, Y.; Fu, Q. Synthesis and degradation of nontoxic biodegradable waterborne polyurethanes elastomer with poly(ε-caprolactone) and poly(ethylene glycol) as soft segment. European Polymer Journal. 2007, 43 (5), 1838–1846, doi:10.1016/j.eurpolymj.2007.02.029.
12. Guo, Y.; Guo, J.; Miao, H.; Teng, L.; Huang, Z. Properties and paper sizing application of waterborne polyurethane emulsions synthesized with isophorone diisocyanate. Progress in Organic Coatings. 2014, 77 (5), 988–996, doi:10.1016/j.porgcoat.2014.02.003.
13. Lee, S.Y.; Wu, S.C.; Chen, H.; Tsai, L.L.; Tzeng, J.J.; Lin, C.H.; Lin, Y.M. Synthesis and characterization of polycaprolactone-based polyurethanes for the fabrication of elastic guided bone regeneration membrane. BioMed Research International. 2018, Article ID 3240571, 1–13, doi:10.1155/2018/3240571.

14. Džunuzović, J.V.; Stefanović, I.S.; Džunuzović, E.S.; Dapčević, A.; Šešlija, S.I.; Balanč, B.D.; Lama, G.C. Polyurethane networks based on polycaprolactone and hyperbranched polyester: Structural, thermal and mechanical investigation. Progress in Organic Coatings. 2019, 137, 105305, doi:10.1016/j.porgcoat.2019.105305.
15. Fuensanta, M.; Jofre-Reche, J.A.; Rodríguez-Llansola, F.; Costa, V.; Martín-Martínez, J.M. Structure and adhesion properties before and after hydrolytic ageing of polyurethane urea adhesives made with mixtures of waterborne polyurethane dispersions. International Journal of Adhesion and Adhesives. 2018, 85, 165–176, doi:10.1016/j.ijadhadh.2018.06.002.
16. Li, S.; Zhao, J.; Zhang, Z.; Zhang, J.; Yang, W. Aliphatic thermoplastic poly(urethane urea)s and polyureas synthesized through a non-isocyanate route. RSC Advances. 2015, 5 (9), 6843–6852, doi:10.1039/c4ra12195c.
17. Wang, K.; Peng, Y.; Tong, R.; Wang, Y.; Wu, Z. The effects of isocyanate index on the properties of aliphatic waterborne polyurethaneureas. Journal of Applied Polymer Science. 2010,118, 920-927, doi:10.1002/app.32454.
18. Pérez Limiñana, M.A. Síntesis y caracterización de dispersiones acuosas de poliuretano como alternativa a los adhesivos en base disolvente orgánico usados en calzado. Doctoral thesis. University de Alicante (Spain). 2004.
19. Kim, B. K. Aqueous polyurethane dispersions. Colloid & Polymer Science. 1996, 274 (7), 599–611, doi:10.1007/bf00653056
20. Zhu, Y.; Hu, J.; Yeung, K.; Choi, K.; Liu, Y.; Liem, H. Effect of cationic group content on shape memory effect in segmented polyurethane cationomer. Journal of Applied Polymer Science. 2006, 103 (1), 545–556, doi:10.1002/app.24820.
21. Cao, J.; Yang, M.; Lu, A.; Zhai, S.; Chen, Y.; Luo, X. Polyurethanes containing zwitterionic sulfobetaines and their molecular chain rearrangement in water. Journal of Biomedical Materials Research Part A. 2012, 101A (3), 909–918, doi:10.1002/jbm.a.34384
22. Rahman, M.M.; Kim, H.D. Synthesis and characterization of waterborne polyurethane adhesives containing different amount of ionic groups (I). Journal of Applied Polymer Science. 2006, 102 (6), 5684–5691. doi:10.1002/app.25052.
23. Fuensanta, M.; Khoshnood, A.; Martín-Martínez, J.M. Structure–properties relationship in waterborne poly(urethane-urea)s synthesized with dimethylolpropionic acid (DMPA) internal emulsifier added before, during and after prepolymer formation. Polymers. 2020, 12 (11), 2478, doi:10.3390/polym12112478.

24. Xu, H.; Qiu, F.; Wang, Y.; Yang, D.; Wu, W.; Chen, Z.; Zhu, J. Preparation, mechanical properties of waterborne polyurethane and crosslinked polyurethane-acrylate composite. Journal of Applied Polymer Science. 2011, 124 (2), 958–968, doi:10.1002/app.35127.
25. Tawa, T.; Ito, S. The role of hard segments of aqueous poly(urethane urea) dispersion in determining the colloidal characteristics and physical properties. Polymer Journal. 2006, 38 (7), 686–693, doi:10.1295/polymj.pj2005193.
26. Pandya, H.; Mahanwar, P. Fundamental insight into anionic aqueous polyurethane dispersions. Advanced Industrial and Engineering Polymer Research. 2020, 3, 102-110, doi:10.1016/j.aiepr.2020.07.003.
27. Touchet, T.J.; Cosgriff-Hernandez, E.M. Hierarchal structure–property relationships of segmented polyurethanes. Advances in Polyurethane Biomaterials. 2016, 3–22, doi:10.1016/b978-0-08-100614-6.00001-9.
28. Ramesh, S.; Rajalingam, P.; Radhakrishnan, G. Chain-extended polyurethanes—Synthesis and characterization. Polymer International. 1991, 25 (4), 253–256, doi:10.1002/pi.4990250409
29. Sakurai, S.; Okamoto, Y.; Sakaue, H.; Nakamura, T.; Banda, L.; Nomura, S. Structure and properties of segmented poly(urethaneurea)s with relatively short hard-segment chains. Journal of Polymer Science Part B: Polymer Physics. 2000, 38 (13), 1716–1728, doi:10.1002/1099-0488(20000701)38:13<1716::aid-polb50>3.0.co;2-x
30. Orgilés-Calpena, E.; Arán-Aís, F.; Torró-Palau, A. M.; Orgilés-Barceló, C. Influence of the chain extender nature on adhesives properties of polyurethane dispersions. Journal of Dispersion Science and Technology. 2012, 33 (1), 147–154, doi:10.1080/01932691.2010.54825.
31. Lei, L.; Zhong, L.; Lin, X.; Li, Y.; Xia, Z. Synthesis and characterization of waterborne polyurethane dispersions with different chain extenders for potential application in waterborne ink. Chemical Engineering Journal. 2014, 253, 518–525, doi:10.1016/j.cej.2014.05.044.
32. Pérez-Limiñana, M.A.; Arán-Aís, F.; Torró-Palau, A. M.; Orgilés-Barceló, C.; Martín-Martínez, J.M. Structure and properties of waterborne polyurethane adhesives obtained by different methods. Journal of Adhesion Science and Technology. 2006, 20 (6), 519–536, doi:10.1163/156856106777213320
33. Welham, N.; Berbenni, V.; Chapman, P. Effect of extended ball milling on graphite. Journal of Alloys and Compounds. 2003, 349 (1-2), 255–263, doi:10.1016/s0925-8388(02)00880-0.

34. Hermann, H.; Schubert, T.; Gruner, W.; Mattern, N. Structure and chemical reactivity of ball-milled graphite. Nanostructured Materials. 1997, 8 (2), 215–229, doi:10.1016/s0965-9773(97)00010-x.
35. Bonaccorso, F.; Lombardo, A.; Hasan, T.; Sun, Z.; Colombo, L.; Ferrari, A.C. Production and processing of graphene and 2D crystals. Materials Today. 2012, 15 (12), 564–589, doi:10.1016/s1369-7021(13)70014-2.
36. Balan, A.; Kumar, R.; Boukhicha, M.; Beyssac, O.; Bouillard, J.C.; Taverna, D.; Shukla, A. Anodic bonded graphene. Journal of Physics D: Applied Physics. 2010, 43 (37), 374013, doi:10.1088/0022-3727/43/37/374013.
37. Miyamoto, Y.; Zhang, H.; Tománek, D. Photoexfoliation of graphene from graphite: AnAb Initio study. Physical Review Letters. 2010, 104 (20), 208302, doi:10.1103/physrevlett.104.208302.
38. Hernandez, Y.; Nicolosi, V.; Lotya, M.; Blighe, F.M.; Sun, Z.; De, S.; Coleman, J.N. High-yield production of graphene by liquid-phase exfoliation of graphite. Nature Nanotechnology. 2008, 3 (9), 563–568, doi:10.1038/nnano.2008.215.
39. Emtsev, K.V.; Bostwick, A.; Horn, K.; Jobst, J.; Kellogg, G.L.; Ley, L.; Seyller, T. Towards wafer-size graphene layers by atmospheric pressure graphitization of silicon carbide. Nature Materials. 2009, 8 (3), 203–207, doi:10.1038/nmat2382.
40. Bartelt, N.C.; McCarty, K.F. Graphene growth on metal surfaces. MRS Bulletin. 2012, 37 (12), 1158–1165, doi:10.1557/mrs.2012.237.
41. Kern, W.; Schnable, G.L. Low-pressure chemical vapor deposition for very large-scale integration processing—A review. IEEE Transactions on Electron Devices. 1979, 26 (4), 647–657, doi:10.1109/t-ed.1979.19473.
42. Saeed, M.; Alshammari, Y.; Majeed, S.A.; Al-Nasrallah, E. Chemical vapour deposition of graphene—Synthesis, characterisation, and applications: A review. Molecules. 2020, 25(17), 3856(1-62), doi:10.3390/molecules25173856.
43. Wu, J.; Pisula, W.; Muellen, K. Graphenes as potential material for electronics. ChemInform. 2007, 107 (3), 718–747, doi:10.1002/chin.200726225.
44. Zhi, L.; Müllen, K. A bottom-up approach from molecular nanographenes to unconventional carbon materials. Journal of Materials Chemistry. 2008, 18 (13), 1472, doi:10.1039/b717585j.
45. Staudenmaier, L. Verfahren zur Darstellung der Graphitsäure. Berichte Der Deutschen Chemischen Gesellschaft. 1898, 31 (2), 1481–1487, doi:10.1002/cber.18980310237.
46. Hummers, W.S.; Offeman, R.E. Preparation of graphitic oxide. Journal of the American Chemical Society. 1958, 80 (6), 1339–1339, doi:10.1021/ja01539a017.

47. Aliyev, E.; Filiz, V.; Khan, M.M.; Lee, Y.J.; Abetz, C.; Abetz, V. Structural characterization of graphene oxide: Surface functional groups and fractionated oxidative debris. Nanomaterials. 2019, 9 (8), 1180, doi.org/10.3390/nano9081180.
48. Khan, Z.U.; Kausar, A.; Ullah, H. A review on composite papers of graphene oxide, carbon nanotube, polymer/GO, and polymer/CNT: Processing strategies, properties, and relevance. Polymer-Plastics Technology and Engineering. 2015, 55 (6), 559–581, doi:10.1080/03602559.2015.1098693.
49. McAllister, M.J.; Li, J.L.; Adamson, D.H.; Schniepp, H.C.; Abdala, A.A.; Liu, J.; Herrera-Alonso, M.; Milius, D.L.; Car, R.R.K.; Prud'homme, R.K.; Aksay, I.A. Single sheet functionalized graphene by oxidation and thermal expansion of graphite, Chem. Mater. 2007, 19, 4396–4404, doi:10.1021/cm0630800.
50. Ferreira, F.V.; Cividanes, L.D.S.; Brito, F.S.B.; Menezes, R.C.; Franceschi, W.; Simonetti, E.A.N.; Thim. G.P. Functionalizing of graphene and applications: review. 1st ed. Springer. 2016, 1-29, doi:10.1007/978-3-319-35110-0_1.
51. Ramanathan, T.; Abdala, A.; Stankovich, S.; Dikin, D.A.; Herrera-Alonso, M.R.D. Piner, R.D.; Adamson, D.H.; Schniepp, H.C.; Chen, X.; Ruoff, R.S.; Nguyen, S.T.; Aksay, I. A.; Prud'Homme, R.K.; Brinson, L.C. Functionalized graphene sheets for polymer nanocomposites. Nat. Nanotechnol. 2008, 3, 327–331, doi:10.1038/nnano.2008.96.
52. Rohini, R.; Katti, P.; Bose. S. Tailoring the interface in graphene/thermoset polymer composites: a critical review. Polymer. (Guildf). 2015, 70, A17–A34, doi:10.1016/j.polymer.2015.06.016.
53. Compton, O.C.; Jain, B.; Dikin, D.A.; Abouimrane, A.; Amine, K.; Nguyen, S.T. Chemically active reduced graphene oxide with tunable C/O ratios. ACS. Nano. 2011, 5, 4380–4391, doi:10.1021/nn1030725.
54. Dideikin, A.T.; Vul, A.Y. Graphene oxide and derivatives: The place in graphene family. Frontiers in Physics. 2019, 6, 1-13, doi:10.3389/fphy.2018.00149.
55. Chua, C.K.; Pumera, M. The reduction of graphene oxide with hydrazine: Elucidating its reductive capability based on a reaction-model approach. Chemical Communications. 2016, 52 (1), 72–75, doi:10.1039/c5cc08170j.
56. Farah, S.; Farkas, A.; Madarász, J.; László, K. Comparison of thermally and chemically reduced graphene oxides by thermal analysis and Raman spectroscopy. Journal of Thermal Analysis and Calorimetry. 2020, 142, 331–337, doi:10.1007/s10973-020-09719-3.

57. Yu, W.; Sisi, L.; Haiyan, Y.; Jie, L. Progress in the functional modification of graphene/graphene oxide: a review. RSC Advances. 2020, 10 (26), 15328–15345. doi:10.1039/d0ra01068e.
58. Georgakilas, V.; Otyepka, M.; Bourlinos, A.B.; Chandra, V.; Kim, N.; Kemp, K. C., Kim, K.S. Functionalization of graphene: Covalent and non-covalent approaches, derivatives and applications. Chemical Reviews. 2012, 112 (11), 6156–6214, doi:10.1021/cr3000412.
59. Duan, X.; Ao, Z.; Sun, H.; Indrawirawan, S.; Wang, Y.; Kang, J.; Wang, S. Nitrogen-doped graphene for generation and evolution of reactive radicals by metal-free catalysis. ACS Applied Materials & Interfaces. 2015, 7 (7), 4169–4178, doi:10.1021/am508416n.
60. Xu, Z.; Zhang, J.; Shan, M.; Li, Y.; Li, B.; Niu, J.; Qian, X. Organosilane-functionalized graphene oxide for enhanced antifouling and mechanical properties of polyvinylidene fluoride ultrafiltration membranes. Journal of Membrane Science. 2014, 458, 1–13, doi:10.1016/j.memsci.2014.01.050.
61. Navaee, A.; Salimi, A. Efficient amine functionalization of graphene oxide through the Bucherer reaction: an extraordinary metal-free electro catalyst for the oxygen reduction reaction. RSC Advances. 2015, 5 (74), 59874-59880, doi:10.1039/c5ra07892j.
62. Chiou, Y.C.; Chou, H.Y.; Shen, M.Y. Effects of adding graphene nanoplatelets and nanocarbon aerogels to epoxy resins and their carbon fiber composites. Materials & Design. 2019,178, 107869, doi:10.1016/j.matdes.2019.107869.
63. Jiménez-Suárez, A.; Prolongo, S.G. Graphene nanoplatelets. Applied Sciences. 2020, 10 (5), 1753, doi:10.3390/app10051753.
64. Menes, O.; Cano, M.; Benedito, A.; Giménez, E.; Castell, P.; Maser, W.K.; Benito, A.M. The effect of ultrathin graphite on the morphology and physical properties of thermoplastic polyurethane elastomer composites. Compos. Sci. Technol. 2012, 72, 1595–1601, doi:10.1016/j.compscitech.2012.06.016.
65. Gaidukovs, S.; Kampars, V.; Bitenieks, J.; Bochkov, I.; Gaidukova, G.; Cabulis, U.; Kampars, V.; Bitenieks, J.; Bochkov, I.; Gaidukova, G. Thermo-mechanical properties of polyurethane modified with graphite oxide and carbon nanotube particles. J. Renew. Mat. 2016, 4587, 1–11, doi:10.1080/10584587.2016.1182394.
66. Pokharel, P.; Lee, D.S. High performance polyurethane nanocomposite films prepared from a masterbatch of graphene oxide in polyether polyol. Chem. Eng. J. 2014, 253, 356–365, doi:10.1016/j.cej.2014.05.046.

67. Zhang, F.; Liu, W.; Liang, L.; Wang, S.; Shi, H.; Xie, Y.; Yang, M.; Pi, K. The effect of functional graphene oxide nanoparticles on corrosion resistance of waterborne polyurethane. Colloids Surf. A Physicochem. Eng. Asp. 2020, 591, 124565, doi:10.1016/j.colsurfa.2020.124565.
68. Cai, D.; Jin, J.; Yusoh, K.; Rafiq, R.; Song, M. High performance polyurethane/functionalized graphene nanocomposites with improved mechanical and thermal properties. Compos. Sci. Technol. 2012, 72, 702–707, doi:10.1016/j.compscitech.2012.01.020.
69. Ding, J.N.; Fan, Y.; Zhao, C.X.; Liu, Y.B.; Yu, C.T.; Yuan, N.Y. Electrical conductivity of waterborne polyurethane/graphene composites prepared by solution mixing. J. Compos. Mater. 2011, 46, 747–752, doi:10.1177/0021998311413835.
70. Wu, S.; Shi, T.; Zhang, L. Preparation and properties of amine-functionalized reduced graphene oxide/waterborne polyurethane nanocomposites. High Perform Polym, 2016, 28 (4), 453–65, doi:10.1177/0954008315587124.
71. Kim, Y.J.; Kim, B.K. Synthesis and properties of silanized waterborne polyurethane/graphene nanocomposites. Colloid Polym Sci. 2014, 292, 51–8, doi: 10.1007/s00396-013-3054-2.
72. Kaur, G.; Adhikari, R.; Cass, P.; Bown, M.; Evans, M.D.M., Vashi, A.V.; Gunatillake, P. Graphene/polyurethane composites: fabrication and evaluation of electrical conductivity, mechanical properties and cell viability. RSC Advances. 2015, 5 (120), 98762–98772, doi:10.1039/c5ra20214k.
73. Lee, Y.R.; Raghu, A.V.; Jeong, H.M.; Kim, B.K. Properties of waterborne polyurethane/functionalized graphene sheet nanocomposites prepared by an in situ method. Macromol. Chem. Phys. 2009, 210, 1247– 1254, doi:10.1002/macp.200900157.
74. Zhang, F.; Liu, W.; Wang, S.; Jiang, C.; Xie, Y.; Yang, M.; Shi, M. A novel and feasible approach for polymer amine modified graphene oxide to improve water resistance, thermal, and mechanical ability of waterborne polyurethane. Appl. Surf. Sci. 2019, 491, 301–312, doi:10.1016/j.apsusc.2019.06.148.
75. Christopher, G.; Anbu Kulandainathan, M.; Harichandran, G. Comparative study of effect of corrosion on mild steel with waterborne polyurethane dispersion containing graphene oxide versus carbon black nanocomposites. Prog. Org. Coatings. 2015, 89, 199–211, doi:10.1016/j.porgcoat.2015.09.022.
76. Hu, L.; Jiang, P.; Zhang, P, Bian, G.; Sheng, S.; Huang, M.; Bao, Y.; Jialiang Xia, J. Amine-graphene oxide/ waterborne polyurethane nanocomposites : Effects of

different amine modifiers on physical properties. J. Mater. Sci. 2016, 51(18), 8296–8309, doi:10.1007/s10853-016-9993-5.

77. Yadav, S.K.; Cho, J.W. Functionalized graphene nanoplatelets for enhanced mechanical and thermal properties of polyurethane nanocomposites. Appl. Surf. Sci. 2013, 266, 360–367, doi: 10.1016/j.apsusc.2012.12.028.
78. Nine, M.J.; Tran, D.N.H.; El Mekawy, A.; Losic, D. Interlayer growth of borates for highly adhesive graphene coatings with enhanced abrasion resistance, fire-retardant and antibacterial ability. Carbon. 2017, 117, 252–262, doi:10.1016/j.carbon.2017.02.064.
79. Kale, M.B.; Luo, Z.; Zhang, X.; Dhamodharan, D.; Divakaran, N.; Mubarak, S.; Wu, L.; Xu, Y. Waterborne polyurethane/graphene oxide-silica nanocomposites with improved mechanical and thermal properties for leather coatings using screen printing. Polymer. 2019, 170, 43–53, doi:10.1016/j.polymer.2019.02.055.
80. Marami, G.; Adib Nazari, S.; Ali Faghidian, S.; Vakili-Tahami, F.; Etemadi, S. Improving the mechanical behavior of the adhesively bonded joints using RGO additive. Int J. Adh. Adh. 2016, 70, 277–86, doi:10.1016/j.ijadhadh.2016.07.014.
81. Zhao, Z.; Guo, L.; Feng, L.; Lu, H.; Xu, Y.; Wang, J.; Xianga, B.; Zoud, X. Polydopamine functionalized graphene oxide nanocomposites reinforced the corrosion protection and adhesion properties of waterborne polyurethane coatings. Eur Polym J. 2019, 120, 1–13, doi:10.1016/j.eurpolymj.2019.109249.
82. Yang, F.; Wu, Y.; Zhang, S.; Zhang, H.; Zhao, S.; Zhang, J.; Fei, B. Mechanical and thermal properties of waterborne polyurethane coating modified through one-step cellulose nanocrystals/graphene materials sols method. Coatings. 2020, 10, 1–12, doi:10.3390/coatings10010040.
83. Cristofolini, L.; Guidetti, G.; Morellato, K.; Gibertini, M.; Calvaresi, M.; Zerbetto, F.; Montalti, M.; Falini, G. Graphene materials strengthen aqueous polyurethane adhesives. ACS Omega. 2018, 3, 8829−8835, doi:10.1021/acsomega.8b01342.
84. Strankowski, M. Effect of variation of hard segment content and graphene-based nano filler concentration on morphological, thermal, and mechanical properties of polyurethane nanocomposite. Int J Polym Sci. 2018; Article ID:1090753, 1-20, doi:10.1155/2018/1090753.
85. Wang, X.; Hu, Y.; Song, L.; Yang, H.; Xing, W.; Lu, H. In situ polymerization of graphene nanosheets and polyurethane with enhanced mechanical and thermal properties. J Mater Chem. 2011, 21(12), 4222-4227. doi: 10.1039/C0JM03710A.

8. Future work

Based on this work and with the aim of continuing the research in this field, various challenges are proposed, as well as new studies and possibilities for better knowledge that would provide suitable plans for future work. The future work is summarized below.

- Determine the corrosion resistance of waterborne poly(urethane urea) coatings containing small amounts of graphene derivatives.
- Determine the influence of the addition of GO on the poly(urethane urea) structure made with different soft segments (i.e. different polyols) and different chain extenders.
- Improve the dispersion of the GO in the waterborne poly(urethane urea) dispersion by adding different surfactants.
- Synthesis of waterborne poly(urethane urea) dispersions with small amounts of graphene oxide quantum dots paying particular attention to their dispersion and stabilization over time.
- Mixing different graphene derivatives with different polarity and functional groups for controlling the adhesion of waterborne poly(urethane urea) dispersions.
- Adding inorganic oxide + graphene derivative blends to waterborne poly(urethane urea) to improve their thermal stability without affecting their adhesion.

Second part. Copy of the published articles

First article

Tounici, Abir; Martín-Martínez, José Miguel. *Addition of small amounts of graphene oxide in the polyol during the synthesis of waterborne polyurethane urea adhesives for improving their adhesion properties*. Int. J. Adh. Adh. 2020; 104:102725.

doi:10.1016/j.ijadhadh.2020.102725

Summary: Mixtures of polyadipate of 1,4-butanediol polyol and different small amounts (0.01–0.10 wt%) of graphene oxide (GO) were added during the synthesis of waterborne polyurethane urea dispersions (PUDs) carried out with the acetone method. The addition of 0.02–0.04 wt% GO increased the T-peel strength of plasticized poly (vinyl chloride)/PUD/plasticized poly (vinyl chloride) joints whereas the addition of 0.05–0.10 wt% GO increased the single lap-shear strength of stainless steel/PUD/stainless steel joints. The improved adhesion of the PUDs containing GO was ascribed to the creation of covalent interactions between the surface groups on the GO surface and the NCO groups of the isocyanate during prepolymer formation, creating new urethane groups; during the phase inversion, the covalently bonded GO sheets were embedded between the polyurethane urea chains inside the PUD particles, this changed the degree of phase separation between the hard and the soft segments. When more than 0.04 wt% GO was added, some GO particles cannot be covalently bonded to the prepolymer during the PUD synthesis but they agglomerated and physically “trapped” between the polyurethane urea chains. As a consequence, the adhesion properties of the PU+GO films were different in the PU films containing 0.01–0.04 wt% GO and the ones containing 0.05–0.10 wt% GO.

Keywords: Polyurethane; water based; thermal analysis; infrared spectra; viscoelasticity.

Second article

Tounici, Abir ; Martín-Martínez, José Miguel. *Addition of graphene oxide in different stages of the synthesis of waterborne poly(urethane urea) adhesives and its influence on their structure, thermal, viscoelastic and adhesion properties*. Materials. 2020; 13(13):2899.

doi:10.3390/ma13132899

Summary: In this study, 0.04 wt % graphene oxide (GO) was added in different stages (before and after prepolymer formation, and during water addition) of the synthesis of waterborne polyurethane-urea dispersions (PUDs) prepared by using the acetone method. The structural, thermal, mechanical, viscoelastic, surface and adhesion properties of the polyurethane-ureas (PUUs) containing 0.04 wt % GO were studied. The addition of GO before and after prepolymer formation produced covalent bonds between the GO sheets and the NCO groups of the isocyanate, whereas the GO sheets were trapped between the polyurethane chains when added during water addition step. As a consequence, depending on the stage of the PUD synthesis in which GO was added, the degree of micro-phase separation between the hard and soft segments changed differently. The addition of GO before prepolymer formation changed more efficiently the polyurethane-urea structure, i.e., the covalently bonded GO sheets disturbed the interactions between the hard segments causing lower percentage of free urethane groups, higher crystallinity, lower storage modulus, higher yield stress and T-peel strength. The interactions between the GO sheets and the polymeric chains have been evidenced by plate-plate rheology, thermal gravimetric analysis and spectroscopy. On the other hand, physical interactions between GO and the polyurethane-urea chains were produced when GO was added in water during the synthesis, i.e., GO was acting as a nanofiller, which justified the improved mechanical properties and high lap-shear strength, but poor T-peel strength.

Keywords: waterborne polyurethane-urea adhesive; graphene oxide; structure-property relationship; adhesion; thermal properties; viscoelastic properties.

Third article

Tounici, Abir; Martín-Martínez, José Miguel. *Influence of the surface chemistry of graphene oxide on the structure–property relationship of waterborne poly(urethane urea) adhesive*. Materials. 2021, 14:4377.

doi:10.3390/ma14164377

Summary: Small amounts—0.04 wt.%—graphene oxide derivatives with different surface chemistry (graphene oxide—GO-, amine-functionalized GO—A-GO-, reduced GO—r-GO) were added during prepolymer formation in the synthesis of waterborne poly(urethane urea) dispersions (PUDs). Covalent interactions between the surface groups on the graphene oxide derivatives and the end NCO groups of the prepolymer were created, these interactions differently altered the degree of micro-phase separation of the PUDs and their structure–properties relationships. The amine functional groups on the A-GO surface reacted preferentially with the prepolymer, producing new urea hard domains and higher percentage of soft segments than in the PUD without GO derivative. All GO derivatives were well dispersed into the PU matrix. The PUD without GO derivative showed the most noticeable shear thinning and the addition of the GO derivative reduced the extent of shear thinning differently depending on its functional chemistry. The free urethane groups were dominant in all PUs and the addition of the GO derivative increased the percentage of the associated by hydrogen bond urethane groups. As a consequence, the addition of GO derivative caused a lower degree of micro-phase separation. All PUs containing GO derivatives exhibited an additional thermal decomposition at 190–206 ◦C which was ascribed to the GO derivative-poly(urethane urea) interactions, the lowest temperature corresponded to PU+A-GO. The PUs exhibited two structural relaxations, their temperatures decreased by adding the GO derivative, and the values of the maximum of tan delta in PU+r-GO and PU+A-GO were significantly higher than in the rest. The addition of the GO derivative increased the elongation-at-break, imparted some toughening, and increased the adhesion of the PUD. The highest T-peel strength values corresponded to the joints made with PUD+GO and PUD+r-GO, and a rupture of the substrate was obtained.

Keywords: Waterborne poly(urethane urea); graphene oxide derivative; surface chemistry; adhesion; micro-phase separation; structure-property relationship.

Fourth article

Tounici, Abir; Martín-Martínez, José Miguel. *Structure and adhesion properties of waterborne poly(urethane ureas)s containing small amounts of different graphene derivatives*. J. Adhes. Sci. Technol. 2021; 35(24),2758-2789.

doi: 10.1080/01694243.2021.1970371

Summary: Waterborne poly(urethane urea)s (PUDs) containing graphene derivatives with different morphologies and surface polarities were synthesized via in situ polymerization by using the acetone method. Small amounts (0.04–0.30 wt.%) of graphene oxide (GO), graphite nanoplatelets (GP) or milled graphite (MG) were mixed with polyadipate of 1,4-butanediol polyol and added during synthesis of the PUDs. The addition of graphene derivatives changed differently the degree of micro-phase separation of the poly(urethane urea)s (PUs) depending on the balance between the extent of covalent interactions between the surface functional groups on the graphene sheets and the isocyanate groups, and the number of stacked graphene sheets. Whereas MG mainly intercalated between the soft segments showing a typical behavior of nanofiller, GP and, particularly, GO showed different degrees of micro-phase separation due to more net covalent interactions with the poly(urethane urea) chains which caused higher crystallinity. The addition of graphene derivative decreased the glass transition temperature of the hard segments and increased the percentages of associated by hydrogen bond urethane and urea groups, more noticeably by adding GP and MG. Lower temperatures of decomposition and higher amounts of urethane and urea hard domains, and soft domains were found in PU+GO and PU+MG, and they showed an additional structural relaxation at 11–16 C. PU and PU+GP had higher thermal stabilities than PU+GO and PU+MG and the addition of GP and, more markedly, GO imparted toughening to the poly(urethane urea). The T-peel strength values were higher in the joints made with PUD+GO due to the more net covalent interactions between the surface functional groups on the GO sheets and the poly(urethane urea) chains. On the other hand, the lap-shear strength of the joints made with PUD+MG and, in less extent, with PUD+GP noticeably increased.

Keywords: Waterborne poly(urethane urea), adhesion, graphene derivative, micro-phase separation, viscoelastic properties.

Third part. Unpublished work

Electrical conductivities composites containing small amounts (less than 0.30 wt.%) of different graphene derivatives

1. Abstract

To enhance the electrical conductivity of the poly(urethane urea)s (PUs), small amounts (0.01-0.30 wt.%) of graphene derivatives with different surface chemistry and morphology - graphene oxide (GO), reduced GO (r-GO), amine-functionalized GO (A-GO), graphite nanoplatelets (GP), milled graphite (MG)- were added during their syntheses. The PU/graphene derivative composites were prepared by the in-situ polymerization and solution mixing methods. The electrical conductivity of the PU/graphene derivative composites was measured at room temperature using the four-probe method. The addition of all graphene derivatives improved the electrical conductivity of the PUs, more notably by adding MG (19.9×10^{-5} S/cm). The increase of the amount of GO increased the electrical conductivity, and the highest value corresponded to PU+0.10 wt% GO. In addition, depending on the stage of addition of GO during the synthesis of the PU, the electrical conductivity of the PU/graphene derivative composites changed. The highest one corresponded to PU+0.04 wt% GO in water due to the higher physical interactions between GO and the poly(urethane urea). The electrical conductivities of PU+GO and PU+A-GO are somewhat similar and lower than the ones of PU+r-GO. The reduction of GO enhanced the transfer of pi electrons between the nanosheets and the poly(urethane urea). The stability of the electrical conductivity of the PU/graphene derivative composites over time was not sufficient and declined after 1 month. PU/graphene derivative compounds were good candidates for new applications in the electrochemical field.

2. Introduction and objectives

The electrical conductivity of a material is mainly governed by its electronic structure, which is determined by the gap between the valence and conduction bands. When the valence band overlaps the conduction band, the conductivity occurs [1].

In the polyurethane structure, the urethane group has a strong proton donor group (NH group) and also a strong proton acceptor group (C=O group), and is an insulator. Semiconductor polyurethanes have potential in electric charging, digital printing, imaging, electronics, biomedicine, and safe and effective floor static build-up [2,3]. Conductive

polyurethane can also play a major role in electromechanical devices requiring superior properties and electrical charge transfer [4].

The electrical conductivity of the polyurethane can be improved by adding conductive materials such as conducting polymers, carbon blacks, carbon nanotubes, graphite, and graphene derivatives. The nature and amount added to the conductive material will determine the level of conductivity of the polyurethane. According to the existing literature, the electrical conductivity of the polymer/graphene materials ranges from 10^{-19} to 1 S/cm [5], the electrical conductivity depends on the methods of preparation, the most commonly used are the solution mixing, the melting process, and the in-situ polymerization. The graphene is the best conductive material known to date, due to the presence of highly mobile pi (π) electrons located above and below the graphene sheet. Basically, the electronic properties of the graphene are dictated by the bonding structure (valence and conduction bands) of the pi orbitals. However, the conductivity of the graphene oxide (GO) depends on the degree of graphite exfoliation and the number of sheets, the amount of oxygen surface groups, and, especially, the level of impurities. The strong oxidation of the graphite leads to a decrease of the electrical conductivity due to disrupted π conjugation; however, the reduction of the graphene oxide results in a partial recovery of π-π coupling, so it may show increased electrical conductivity. On the other hand, single-layer graphene has a thermal conductivity between 3500 and 5000 W/mK [6]. Liu et al. [7] prepared flexible polyurethane composites containing multi-walled carbon nanotubes by in-situ polymerization, they showed high electrical conductivity (up to 16.67 S/cm) and thermal conductivity (up to 5.31 W/m.K); the highest electrical conductivity was obtained by adding 48.1 wt.% multi-walled carbon nanotubes. Abdullah et al. [8] synthesized waterborne polyurethane-oxidized graphite composites containing 5-30 wt.% oxidized graphite with improved electrical conductivity (up to 10^{-4} S/cm), the conductivity starts when 20 wt.% oxidized graphite is added.

In order to increase the electrical conductivity of the polyurethanes by adding less amount of carbon-based fillers, some studies have considered the effect of adding less than 15 wt.% graphene derivatives to waterborne polyurethanes (PUD) on their electrical conductivity. Thus, Cunha and Paiva [9] mixed commercial waterborne polyurethane with up to 10 wt.% few-layer graphene (FLG) aqueous suspensions using ultrasounds and improved electrical conductivity of the resulting materials was obtained (up to 10^{-5} S/m). The highest one was obtained by adding 3.5 wt.% FLG. Velayutham et al. [10] prepared polyurethanes with NCO/OH ratios of 2.0, 2.2, and 2.4 and up to 12.5 wt.% graphite powder was added, they found that the PU composites became electro-conductive when filled with 9-10 wt.% graphite (2.56×10^{-9} S/cm), and that the NCO/OH ratio did not influence the

electrical conductivity. Kaur et al. [11] synthesized PU/graphene composites by using different methods (melt processing, solution mixing, and in-situ polymerization), the mixing solution imparted the highest electrical conductivity (5.96×10^{-2} S/cm). In the same direction, Ding et al. [12] prepared waterborne polyurethane/graphene materials by solution mixing, and they found high electrical conductivity ($8.30\ x10^{-4}$ S/cm). The conductivity increased by adding higher amounts of graphene. On the other hand, Du et al. [13] prepared graphene urethane-based oxide (FGO) by in situ polymerization and improved thermal conductivity was found by adding 0.5 wt.% FGO.

In some studies, the functionalization of the graphene derivatives has been carried out for increasing the properties of the PUDs, including their electrical conductivity. Thus, N-doped reduced graphene oxide/waterborne polyurethane (NRGO/PUD) compounds were prepared by in situ chemical reduction of graphene oxide in aqueous solution; when the NRGO content increased from 1 to 2 wt.%, the electrical conductivity of the NRGO/PUD compound notably increased (from 10^{-10} to 10^{-7} S/cm), and a value of 10^{-1} S/cm was obtained in the PUD containing 12 wt.% NRGO [14]. On the other hand, Fan et al. [15] have synthesized a functionalized graphene oxide-functionalized nanocellulose (FGO-FNC) and have prepared PUDs containing 2-4 wt.% FGO-FNC that exhibit good electrical conductivity and high-water resistance, electrical conductivity up to 10^{-3} S/cm was obtained.

In our previous studies [16-19], different waterborne poly(urethane urea)s (PUDs) containing different amounts of graphene derivatives of different nature, polarity and morphology, have been characterized and they have excellent mechanical, viscoelastic, and adhesion properties. The innovation of those studies relies on the addition of less than 0.10 wt.% graphene derivative. This amount is substantially lower than the one commonly used in the existing literature. The improvement of the properties of the PUDs obtained by adding graphene derivatives with oxygen functional groups was ascribed to the existence of interactions between the functional groups on the nano-sheets surface and the NCO groups of the isocyanate which produced new urethane groups covalently bonded to the graphene derivative surface during their syntheses. As a consequence, the degree of micro-phase separation between the hard and the soft segments in the PUDs changed, more noticeably in the PU+GO composites that contain 0.01-0.04 wt.% GO and 0.05-0.10 wt.% GO. Because some graphene derivative nano-sheets are chemically bonded to the PU structure and some of them are physically trapped between the polymer chains, it is feasible to consider the existence of electrical conductivity in PUs containing an extremely low content of graphene derivatives. Therefore, the objective of this study is the measurement of the electrical conductivity of PUDs containing small amounts of graphene derivatives of different nature, polarity, and morphology. Thus, PUDs containing graphene oxide, reduced

graphene oxide, amine-functionalized graphene oxide, graphite nanoplatelets, and milled graphite have been synthesized and their electrical conductivity has been measured.

3. Experimental

Materials

Different reagents were used for synthesizing the waterborne poly(urethane urea)s (PUDs). Polyadipate of 1,4-butanediol polyol of molecular weight 2000 Da – Hoopol F-501 (Synthesia, Barcelona, Spain) - was used, its residual moisture was removed by heating at 80 °C under reduced pressure (300 mbar) for 2 hours. Isophorone diisocyanate (IPDI, 98 wt% purity), 2,2 bis(hydroxymethyl) propionic acid (DMPA, 98 wt%) internal emulsifier, triethylamine (TEA, 99 wt% purity) neutralizing agent, monohydrated hydrazine (HZ, 60 wt% purity) chain extender, and dibutyltin dilaurate (DBTDL, 95 wt% purity) catalyst were used. All these reagents were supplied by Sigma Aldrich (Barcelona, Spain). Acetone (99.5 wt% purity) – Sigma Aldrich, St Louis, MO, USA – and de-ionized water were also used.
The following graphene derivatives were added during the PUD synthesis:

- Graphene oxide (GO) containing 95 % single graphene sheets was supplied by Graphenea (San Sebastián, Spain).
- Reduced graphene oxide (r-GO) powder was supplied by Graphenea (San Sebastián, Spain).
- Amine-functionalized graphene oxide (A-GO) powder obtained by treatment of GO with dodecyl amine was supplied by Graphenea (San Sebastián, Spain).
- Graphene nanoplatelets (GP) with more than 97 wt.% carbon, a BET surface area of 500 m^2/g, and graphene sheets with a length of 5-10 μm and lateral size of 0.04-0.2 μm were supplied by GrapheneTech (Zaragoza, Spain).
- Milled graphite (MG) was supplied by zEroCor/Carbon Upcycling (Calgary, Canada).

All graphene derivatives were dried in the oven at 80 ºC overnight and kept at this temperature until use.

Preparation of the PUD/graphene derivative composites

The synthesis of the PUD/graphene derivative composites has been detailed in previous studies [16-19]. The acetone method was used, the NCO/OH ratio was 1.5, 5 wt.% DMPA (with respect to the amount of prepolymer) was added, and they had about 40 wt.% solids content. The graphene derivative was dispersed in the polyol before being added to the

reactor. Then, the mixture was heated on a heat plate at 70 °C for 30 min to remove residual water.

The synthesis of the PUD/graphene derivative composites follows different sequential steps (Figure 3.1) involving the synthesis of the prepolymer by reacting the polyol + graphene derivative mixture, DMPA, and catalyst at 80°C for 30 minutes, followed by the addition of the isocyanate at 80 °C for 150 min. Then, the prepolymer was dissolved in the acetone and the neutralization of the protons of DMPA in the prepolymer was carried out with triethylamine at 40°C for 30 minutes. The next steps were the chain extension with hydrazine, the dispersion in water, and the acetone distillation.

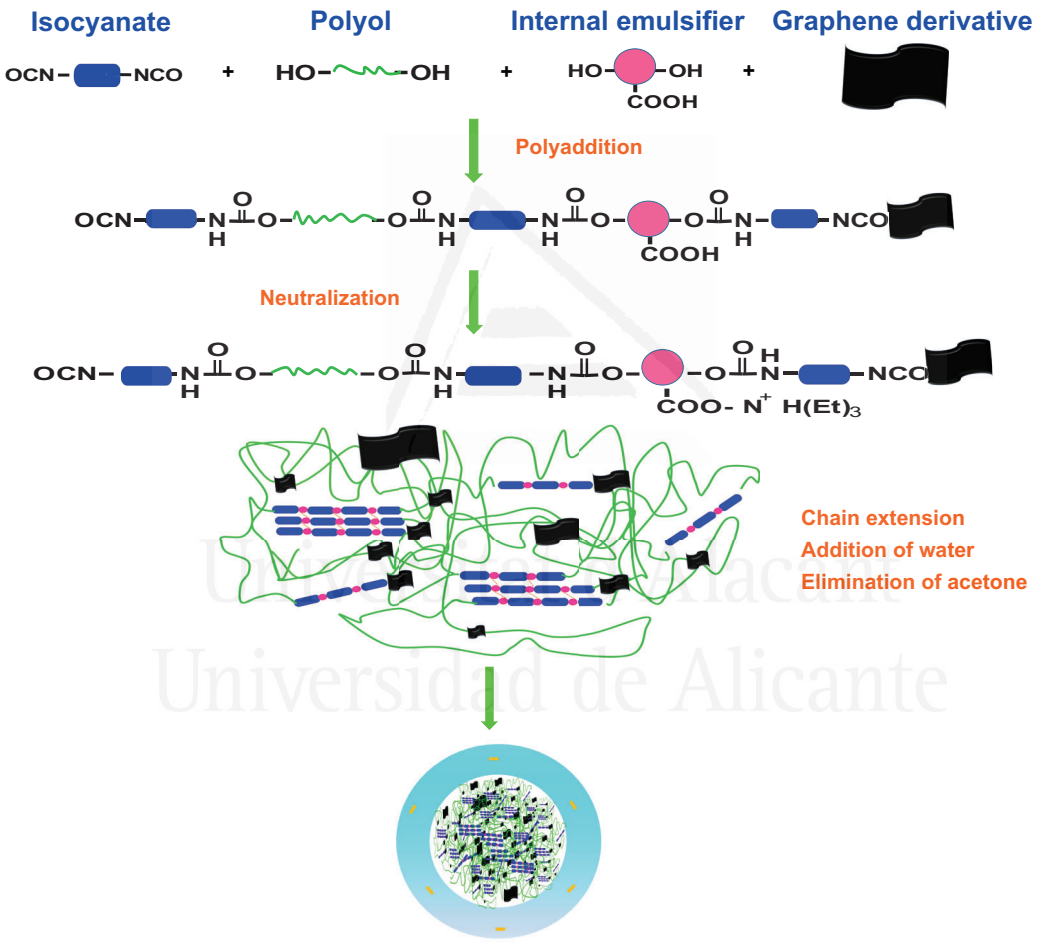

Figure 3.1. Scheme of the synthesis of the PUD/graphene derivative composites [16-19].

Thin PU/graphene derivative composites films were prepared by placing the PUDs on a glass-coated Teflon® substrate, the thickness was adjusted with pieces of double-sided tape applied to the sides of the mould; then, the water was allowed to evaporate under atmospheric pressure and room temperature for 24 hours.

Experimental techniques

The surface resistance (RC) of the PU/graphene derivative composites was measured at room temperature by using a four-probe method in a Signatone Quad ProII Process equipment (Pro4-440N, Gilroy, CA, USA) (Figure 3.2). The use of the four metal points aligned and spaced at a distance of 1mm allows the measurement of the electrical current between the two central points. These measurements allow a fast determination of the surface resistance according to equation 3.1.:

$$RC = 4.53\ (\Delta V/I) \qquad \text{(Eq 3.1)}$$

Where ΔV is the change in the voltage measured between the inner probes and I is the current applied between the outer probes.

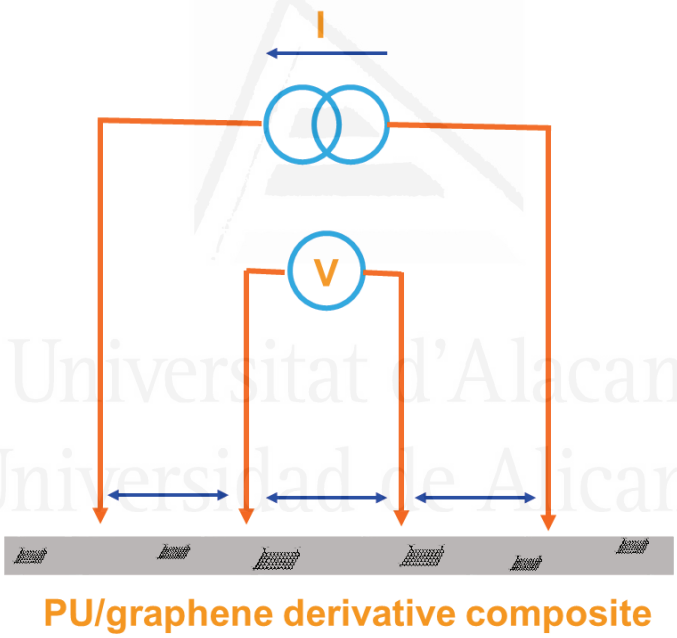

Figure 3.2. Scheme of the four-point probe method for measuring the surface resistivity of the PU/graphene derivative composites.

The electrical conductivity or specific conductance is the reciprocal of the surface resistance.

The thicknesses of the PU/graphene derivative composites were 0.06-0.20 μm. At least six measurements were obtained and averaged.

4. Results and discussion

Electrical conductivity of PU/graphene derivative composites containing different amounts (0.01-0.10 wt.%) of graphene oxide

The addition of a conductive material such as graphite/graphene derivative to polyurethane may impart electrical conductivity [8,20]. Table 3.1 shows the electrical resistivity and the conductivity values of the PU/graphene derivative composites containing different small amounts (0.01–0.10 wt.%) of GO – PU/GO. Whereas the PU without graphene derivative is an insulator (RG = 2.94 x 10^6 Ohm.cm), the addition of GO decreases the RC to a greater extent by increasing its content. The highest electrical conductivity (3.47 x 10^{-5} S/cm) corresponds to the composite containing 0.10 wt.% GO. According to Figure 3.3, the addition of 0.01 wt.% GO only increases the electrical conductivity to 1.67 x 10^{-5} S/cm and an almost linear increase in the electrical conductivity is obtained by increasing the GO content in the composite. As a result, the addition of GO increases steadily the electrical conductivity of the PU/GO composites in two orders of magnitude.

Table 3.1. Values of the electrical resistivity and the conductivity of the PU/graphene oxide composites containing different amounts of GO.

Composite	Resistivity x 10^4(Ohm cm)	Conductivity x 10^{-5} (S/cm)
PU	294.00 ± 61.00	0.03 ± 0.01
PU+0.01 wt.% GO	5.98 ± 0.84	1.67 ± 0.30
PU+0.02 wt.% GO	5.52 ± 1.10	1.81 ± 0.08
PU+0.04 wt.% GO	4.02 ± 1.60	2.49 ± 0.40
PU+0.05 wt.% GO	3.98 ± 1.30	2.51 ± 0.30
PU+0.10 wt.% GO	2.88 ± 0.96	3.47 ± 0.40

The increase of the electrical conductivity of the PU/GO composites results from the good dispersion of the GO nano-sheets into the PU matrix which causes a good network connection between the GO nano-sheets. The addition of less than 0.10 wt.% GO to the waterborne polyurethane-urea changes the degree of micro-phase separation due to the interactions between the NCO groups and the OH groups on the edges of the GO nano-sheet during the synthesis of the composites, thus covalently bonded urethane groups are produced. Furthermore, the addition of GO produces a higher percentage of the H-bonded urethane and urea groups, this is an indication of the improved interactions between the oxygen surface groups on the GO nano-sheets and the hard segments of the poly(urethane urea) (Table 3.2). Hence, these interactions lead to an enhanced transfer of electrons and

an increase in electrical conductivity (Figure 3.3). On the other hand, for amounts of GO higher than 0.04 wt.%, some GO nano-sheets are trapped between the poly(urethane urea) chains, which also contributes to the increase of the electrical conductivity.

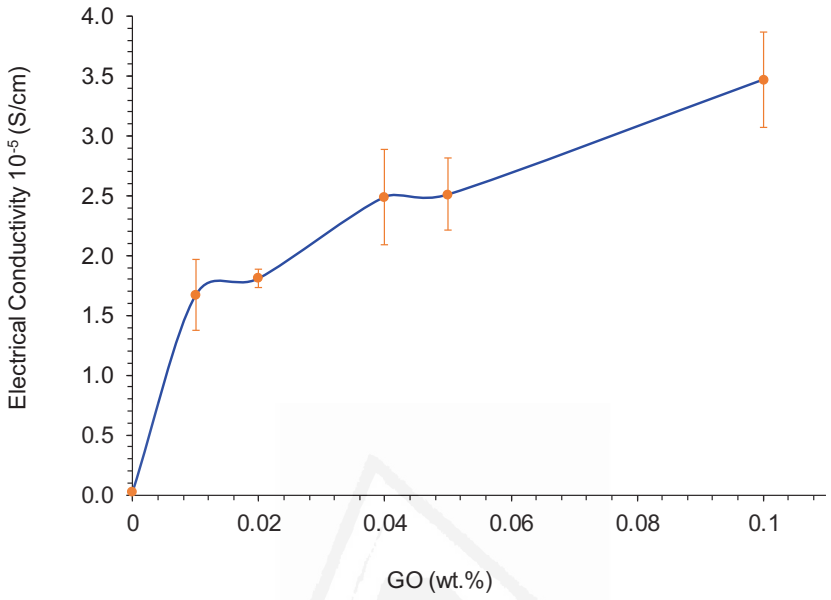

Figure 3.3. Variation of the electrical conductivity of the PU/graphene oxide composites containing different amounts of GO as a function of the amount of GO.

Table 3.2. The percentage of associated urethane and urea groups in the PU/graphene oxide composites containing different amounts of GO. Curve fitting of the carbonyl band of the ATR-IR spectra [17].

Composite	H-bonded urethane (%)	H-bonded urea (%)
PU	9	11
PU+0.01 wt% GO	20	27
PU+0.02 wt% GO	29	19
PU+0.04 wt% GO	35	11
PU+0.05 wt% GO	31	19
PU+0.10 wt% GO	23	19

Electrical conductivity of PU/graphene derivative composites containing 0.04 wt.% graphene oxide added in different steps of the synthesis

The electrical conductivity of the PU/GO composites can also be affected by the stage of the synthesis at which GO is added. Therefore, the electrical conductivity of the PU/graphene derivative composites containing 0.04 wt.% GO added in different stages of

the synthesis (PU+0.04 wt.% GO in polyol, PU+0.04 wt.% after prepolymer and PU+0.04 wt.% GO in water) was measured.

Table 3.3 shows that the values of the electrical resistivity of PU+0.04 wt.% GO in polyol and PU+0.04 wt.% after prepolymer are somewhat similar and lower than in PU+0.04 wt.% GO in water (Figure 3.4). This trend is in agreement with previous studies which demonstrated the highest electrical conductivity of polyurethane-graphene composites made by solution mixing with respect to the ones made by using melt processing and in situ polymerization methods [11]. Consequently, the electrical conductivity of the PU/GO composites is affected differently by the stage of the synthesis at which GO is added. The highest electrical conductivity is obtained when the physical interactions between GO and the poly(urethane urea) are dominant. In other words, the existence of covalent bonds between GO and the NCO groups at the end of the prepolymer in the PU/GO composite imparts lower electrical conductivity because of the inhibited mobility of the GO nano-sheets in the polymer matrix.

Table 3.3. Values of the electrical resistivity and conductivity of the PU/GO composites. Influence of the stage of addition of GO during synthesis.

Composite	Resistivity x 10^4 (Ohm cm)	Conductivity x 10^{-5}(S/cm)
PU	294.00 ± 61.00	0.03 ± 0.01
PU+0.04 wt.% GO in polyol	4.02 ± 1.60	2.49 ± 0.40
PU+0.04 wt.% GO after prepolymer	5.02 ± 0.84	1.99 ± 0.45
PU+0.04 wt.% GO in water	2.21 ± 0.75	4.51 ± 0.72

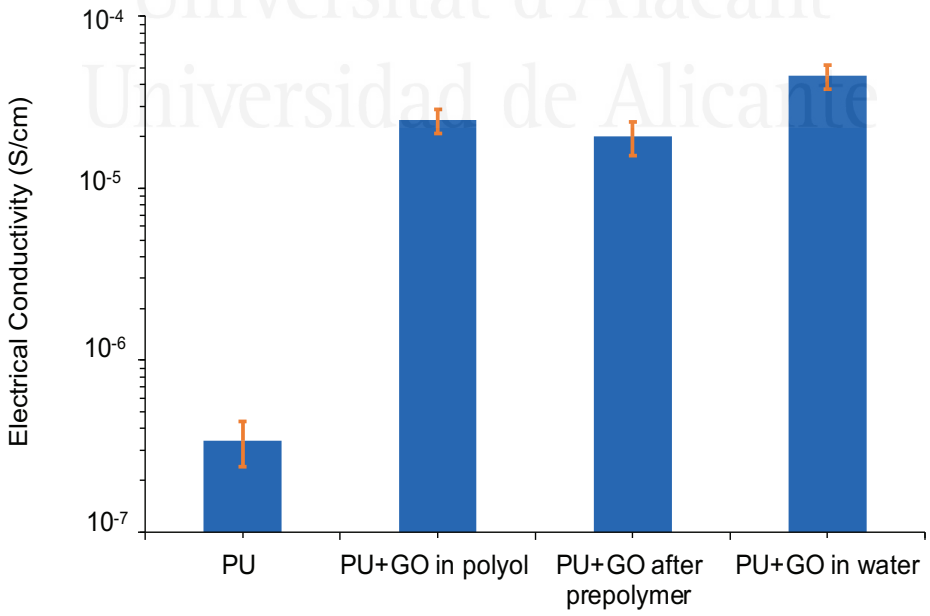

Figure 3.4. Electrical conductivity of the PU/0.04 wt.% GO composites. Influence of the stage of addition of GO during synthesis.

Electrical conductivity of PU/graphene derivative composites containing 0.04 wt.% graphene oxide with different surface chemistry

The surface chemistry of GO should affect the electrical conductivity of PU/GO composites because of the different extent of covalent interactions between the GO nano-sheets and the NCO groups of the prepolymer during the synthesis. Therefore, the electrical conductivity of the composites made with GO having a different surface chemistry (reduced GO – r-GO, amine-functionalized GO – A-GO) was measured.

Table 3.4. Values of the electrical resistivity and conductivity of the PU/0.04 wt.% GO with different surface chemistry composites.

Composite	Resistivity x 10^4 (Ohm cm)	Conductivity x 10^{-5} (S/cm)
PU	11.10 ± 2.00	0.90 ± 0.03
PU+0.04 wt.% GO	6.54 ± 0.60	1.53 ± 0.25
PU+0.04 wt.% A-GO	9.13 ± 0.78	1.09 ± 0.20
PU+0.04 wt.% r-GO	1.14 ± 0.91	8.75 ± 0.11

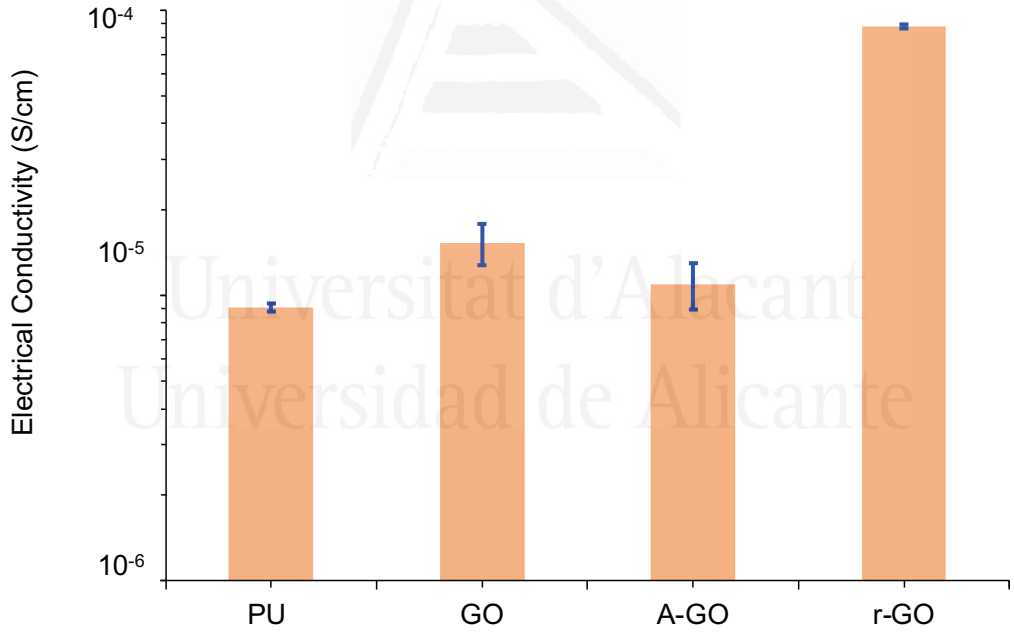

Figure 3.5. Electrical conductivity of the PU/0.04 wt.% GO with different surface chemistry composites.

Table 3.4 shows the values of the electrical resistivity and conductivity of the PU/GO with different surface chemistry composites. The addition of 0.04 wt.% GO increases the electrical conductivity of all composites (Figure 3.5). The electrical conductivities of PU+GO and PU+A-GO are somewhat similar and lower than the one of PU+r-GO. The presence of

functional groups on the GO surface enhances the electron transfer to the polymer inhibiting its mobility [21]. During the reduction of the GO, the amount of the oxygen functional groups on the nano-sheets decreases, the relative percentage of sp^2 carbon atoms increases (as evidenced by XPS) [18], and, as a consequence, the electrical conductivity of PU+r-GO is higher than in the other composites.

Electrical conductivity of PU/graphene derivative of different nature composites

The GO surface has a high amount of oxygen functional groups, which seems detrimental to the electrical conductivity of the PU/GO composites [22]. Therefore, additional PU composites were synthesized with graphene derivatives of different nature and lower amounts of oxygen surface groups (milled graphite – MG -, graphite nanoplatelets - GP); both GP and MG have a higher number of stacked graphene sheets than GO. The addition of the graphene derivatives of different nature changes differently the degree of micro-phase separation of the poly(urethane urea)s due to the different interactions between the surface functional groups on the graphene sheets and the isocyanate groups. When MG is added, it mainly intercalates physically between the polymer chains, but the addition of GP and GO produces more covalent interactions with the poly(urethane urea) chains than when MG is added.

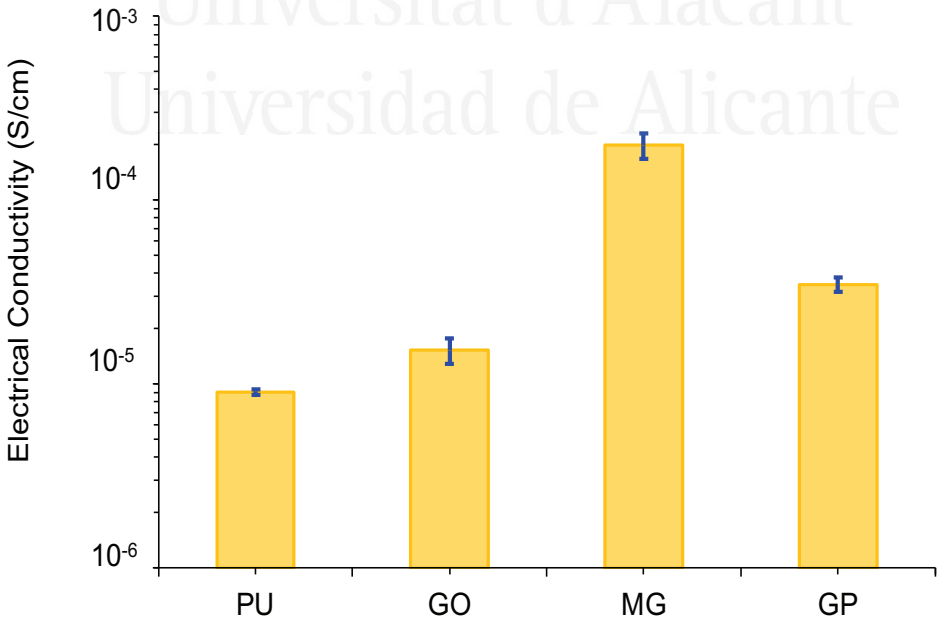

Figure 3.6. Electrical conductivity of the PU/graphene derivative composites.

According to Table 3.5, the addition of MG significantly increases the electrical conductivity of the PU/graphene derivative composites, and the electrical conductivities of PU+GP and PU+GO are lower and similar between them (Figure 3.6). The C-H/C=O ratio in the ATR-IR spectra is an estimation of the soft to hard segments ratio, the values corresponding to the different PU/graphene derivatives are given in Table 3.5; the intensity of the methylene band at 2873 cm^{-1} of the soft segments with respect to the intensity of the C=O band at 1727 cm^{-1} of the hard segments has been used for the calculation [19]. The C-H/C=O ratios are lower and somewhat similar in the PU/graphene composites than in PU, this justifies the higher electrical conductivity. However, the highest electrical conductivity of PU+MG cannot be justified on the basis of different soft/hard segments ratio but on the physical interactions between the MG nano-sheets in the PU composite.

Table 3.5. Values of the electrical resistivity, the conductivity, and the ratios of the intensities of the C-H stretching band with respect to the one of the C=O stretching (ATR-IR spectra) of the PU/graphene derivative composites.

Composite	$I_{C-H}/I_{C=O}$	Resistivity $x10^4$ (Ohm cm)	Conductivity $x10^{-5}$ (S/cm)
PU	0.13	11.1 ± 2.00	0.90 ± 0.03
PU+GO	0.11	6.54 ± 0.60	1.53 ± 0.25
PU+MG	0.11	0.50 ± 0.16	19.9 ± 3.07
PU+GP	0.10	2.86 ± 0.35	3.49 ± 0.31

Comparison of the electrical conductivities of the PU/graphene derivative composites with the values reported in the literature

For comparison, the electrical conductivities of several waterborne polyurethane-graphene derivative composites obtained by using different methods and different graphene derivatives were compiled from different publications [23-29] and they are summarized in Table 3.6. The electrical conductivities of the already published waterborne polyurethane-graphene derivative composites range between 10^{-1} and 10^{-6} S/cm (Table 3.6), these values are within the range of the electrical conductivities obtained in this study. Furthermore, in the existing literature, the highest electrical conductivities of the waterborne polyurethane-graphene derivative composites are obtained by adding 6.5 wt.% GP, 30 wt.% CB, and 10 wt.% CNT, and they are synthesized by using the solution mixing or the in-situ methods. In this study, the electrical conductivities of the PU/graphene derivative composites ranged between 10^{-4} and 10^{-5} S/cm, but the amount added of the graphene derivative was lower than 0.30 wt.%. As a consequence, the addition of small amounts of graphene derivatives

is a promising strategy for improving the electrical conductivity of the waterborne polyurethanes.

Table 3.6. Electrical conductivities of the PU/graphene composites in the existing literature and in this study.

Polyurethane	Filler	Method	Filler content (wt.%)	Electrical conductivity (S/cm)	Ref
TPU	FG	Solution blending	7	4.92×10^{-4}	[23]
WPU	FG	Solution mixing	6	2.75×10^{-4}	[24]
WPU	FG	In-situ method	4	7.87×10^{-4}	[25]
TPU	CNT	Solution mixing	10	1.76×10^{-1}	[26]
PU	G	Solution preparing-electrospinning	10	8.95×10^{-6}	[27]
PU	GP	In-situ method	6.5	10^{-2}	[28]
PU	CB	Solution mixing	30	3.20×10^{-2}	[29]
PU	r-GO	In situ method	0.04	8.75×10^{-5}	This work
	MG	In situ method	0.30	1.99×10^{-4}	
	GO	In situ method	0.10	3.47×10^{-5}	
	GO	Solution mixing	0.04	4.51×10^{-5}	

TPU: Thermoplastic polyurethane, WPU: Waterborne polyurethane, PU: Polyurethane, FG: Functionalized graphene, CNT: Carbon nanotube, GP: Graphite nanoplatelets, G: Graphene, CB: Carbon black.

Stability of the electrical conductivity of the PU/graphene derivative composites

The stability of the electrical conductivity of the PU/graphene derivative composites was analyzed one month after being measured. Table 3.7 shows the decrease in the electrical conductivity of the PU/graphene derivative composites after one month. This is an indication of the collapse of the graphene nano-sheets during the measurement of the electrical conductivity.

The stability of the electrical conductivity of the PU/graphene derivative composites was also analyzed by placing them at -4 ºC for 1h. Table 3.7 shows that the electrical conductivity of the PU/graphene derivative composites is not affected after being cooling down at -4 ºC.

Table 3.7. Variation of the electrical conductivities of the PU/graphene derivative composites with the time and temperature.

Composite	Conductivity x 10^{-5} (S/cm)		
	Initial	After 1 month at room T	After 1 month at room T +1 hour at -4 °C
PU+0.04 wt.% r-GO	8.75 ± 0.11	0.70 ± 0.16	0.48 ± 0.01
PU+MG	19.9 ± 3.07	1.27 ± 0.12	2.63 ± 0.80
PU+0.04 wt.% GO in water	4.51 ± 0.72	0.47 ± 0.12	0.40 ± 0.07
PU+0.10 wt.% GO	3.47 ± 0.40	0.72 ± 0.05	0.69 ± 0.08

5. Conclusions

The addition of less than 0.30 wt.% different graphene derivatives imparted electrical conductivity to waterborne poly(urethane rea)s. The electrical conductivities ranged between 10^{-4} and 10^{-5} S/cm.

The electrical conductivity of the PU/graphene derivative composites increased by increasing the amount of GO. Furthermore, the stage of the synthesis at which the GO was added determined the electrical conductivity of the PU/graphene derivative composites. The highest electrical conductivity corresponded to PU+0.04 wt.% GO in water because of the dominance of the physical interactions between the GO nano-sheets and the polymer chains. The reduction of GO enhanced the transfer of pi electrons between the nano-sheets and the polymer, and, thus, enhanced electrical conductivity was obtained in the poly(urethane urea) containing 0.04 wt.% r-GO. On the other hand, the presence of oxygen groups on the GO surface reduced the electrical conductivity of the PU/graphene derivative composites. Furthermore, the addition of the graphene derivatives of different nature also determined the electrical conductivity of the PU/graphene derivative composites. The highest electrical conductivity was obtained by adding 0.05 wt.% milled graphite. Finally, the electrical conductivities of the PU/graphene derivative composites decreased over time but were not affected by the exposure to low temperatures.

6. References

1. Le, T.H.; Kim, Y.; Yoon, H. Electrical and electrochemical properties of conducting polymers. Polymers, 2017, 9(12), 1-32. doi:10.3390/polym9040150.
2. Alfahed, R.K.F.; Ajeel, K.I.; Shakir, S. Synthesis and Characterization of Polyurethane/POT Dopant and Study Its Electrical Properties. Journal of Materials Science and Engineering, 2015, A 5 (11-12), 391–397. doi: 10.17265/2161-6213/2015.11-12.002.
3. Luo, J.; Zhao, Y.; Chen, M.; Yao, Y. Electrically conductive adhesives based on thermoplastic polyurethane filled with carbon nanotubes. China Semiconductor Technology International Conference (CSTIC) 2016. 1-3. doi:10.1109/cstic.2016.7463946.
4. Song, B.; Tuan, C.C.; Li, L.; Zhu, Y.; Moon, K.S.; Wong, C.P. Highly Conductive Polyurethane/Polyaniline-Based Composites for Wearable Electronic Applications.

IEEE 66th Electronic Components and Technology Conference (ECTC). 2016. 2424-2429. doi:10.1109/ectc.2016.54

5. Zhang, J.; Qiu, J.; Liu, J. Electrical conductivity of graphene/polymer nanocomposites. Rev. Adv. Sci. Eng., 2014, 3, 48–65. doi:10.1166/rase.2014.1052.
6. Lee, Y. S.; Yu, J.; Shim, S. E.; Yang, C. M. Synergistic effects of hybrid carbonaceous fillers of carbon fibers and reduced graphene oxides on enhanced heat-dissipation capability of polymer composites. Polymers, 2020, 12(4), 1-14. doi:10.3390/polym12040909.
7. Liu, W.; Yao, T.; Jia, K.; Gu, J.; Wang, D.; Wei, X. Flexible and thermal conducting multi-walled carbon nanotubes/waterborne polyurethane composite film from in situ polymerization for efficient electromagnetic interference shielding. J. Mater. Sci: Mater Electron, 2021, 32, 4393–4403. doi: 10.1007/s10854-020-05182-w.
8. Abdullah, N.M.; MohdRus, A.Z.; Abdullah, M.F.L. Functionalized waterborne polyurethane-based graphite-reinforced composites. Advances in Materials Science and Engineering, 2019, Article ID 8710370, 1–13. doi:10.1155/2019/8710370.
9. Cunha, E.; Paiva, M.C. Composite films of waterborne polyurethane and few-layer graphene—enhancing barrier, mechanical, and electrical properties. J. Compos. Sci. 2019, 3, 1-14. doi:10.3390/jcs3020035.
10. Velayutham, T.S.; Ahmad, A.B.; Abd Majid, W.H.; Neon, G.S. Electrical properties of polyurethane graphite composites. J Fizik Malaysia, 2008, 29, 25–28.
11. Kaur, G.; Adhikari, R.; Cass, P.; Bown, M.; Evans, M.D.M.; Vashi, A.V.; Gunatillake, P. Graphene/polyurethane composites: Fabrication and evaluation of electrical conductivity, mechanical properties and cell viability. RSC Advances, 2015, 5(120), 98762–98772. doi:10.1039/c5ra20214k.
12. Ding, J.N.; Fan, Y., Zhao, C.X.; Liu, Y.B.; Yu, C.T.; Yuan, N.Y. Electrical conductivity of waterborne polyurethane/graphene composites prepared by solution mixing. J. Compos. Mater. 2011, 46(6), 747–752. doi:10.1177/0021998311413835.
13. Du, W.; Zhang, Z.; Su, H.; Lin, H.; Li, Z. Urethane-functionalized graphene oxide for improving compatibility and thermal conductivity of waterborne polyurethane composites. Industrial & Engineering Chemistry Research, 2018, 57 (21), 7146–7155, doi:10.1021/acs.iecr.8b00656
14. Tian, K.; Su, Z.; Wang, H.; Tian, X.; Huang, W.; Xiao, C. N-doped reduced graphene oxide/waterborne polyurethane composites prepared by in situ chemical reduction of graphene oxide. Composites Part A: Applied Science and Manufacturing, 2017, 94, 41–49. doi:10.1016/j.compositesa.2016.11.020.

15. Fan, W.; Wang, J.; Zhang, Z.; Li, Z. Synergistic enhancement of UV-resistance and electrical conductivity of waterborne polyurethane composite with combination of functionalized 2D graphene oxide and 1D nanocellulose. Progress in Organic Coatings, 2021,151, 106017. doi:10.1016/j.porgcoat.2020.106017.
16. Tounici, A.; Martín-Martínez J.M. Addition of graphene oxide in different stages of the synthesis of waterborne poly(urethane urea) adhesives and its influence on their structure, thermal, viscoelastic and adhesion properties. Materials. 2020, 13(13), 2899. doi:10.3390/ma13132899
17. Tounici, A.; Martín-Martínez, J.M. Addition of small amounts of graphene oxide in the polyol during the synthesis of waterborne polyurethane urea adhesives for improving their adhesion properties. Inter. J. Adh. Adh. 2020, 104,102725. doi:10.1016/j.ijadhadh.2020.102725.
18. Tounici, A.; Martín-Martínez, J. M. Influence of the surface chemistry of graphene oxide on the structure–property relationship of waterborne poly(urethane urea) adhesive. Materials. 2021, 14, 4377. doi:10.3390/ma14164377.
19. Tounici, A.; Martín-Martínez, J. M. Structure and adhesion properties of waterborne poly(urethane ureas)s containing small amounts of different graphene derivatives. J. Adhes. Sci. Technol. 2021. doi: 10.1080/01694243.2021.1970371.
20. Mohan, V.B.; Brown, R.; Jayaraman, K.; Bhattacharyya, D. Characterisation of reduced graphene oxide: Effects of reduction variables on electrical conductivity. Materials Science and Engineering: B, 2015, 193, 49–60. doi:10.1016/j.mseb.2014.11.002
21. Punckt, C.; Muckel, F.; Wolff, S.; Aksay, I.A.; Chavarin, C.A.,Bacher, G., Mertin, W. The effect of degree of reduction on the electrical properties of functionalized graphene sheets. Applied Physics Letters, 2013, 102(2), 023114. doi:10.1063/1.4775582.
22. Sreeprasad, T.S., Berry, V. How do the electrical properties of graphene change with its functionalization? Small, 2012, 9(3), 341–350. doi:10.1002/smll.201202196.
23. Nguyen, D.A.; Lee, Y.R.; Raghu, A. V.; Jeong, H. M.; Shin, C. M.; Kim, B.K. Morphological and physical properties of a thermoplastic polyurethane reinforced with functionalized graphene sheet. Polymer International, 2009, 58(4), 412–417. doi:10.1002/pi.2549.
24. Raghu, A.V.; Lee, Y.R.; Jeong, H.M.; Shin, C.M. Preparation and physical properties of waterborne polyurethane/functionalized graphene sheet nanocomposites. Macromolecular Chemistry and Physics, 2008, 209(24), 2487–2493. doi:10.1002/macp.200800395

25. Lee, Y.R.; Raghu, A.V.; Jeong, H.M.; Kim, B.K. Properties of waterborne polyurethane/functionalized graphene sheet nanocomposites prepared by an in situ method. Macromolecular Chemistry and Physics, 2009, 210(15), 1247–1254. doi:10.1002/macp.200900157.
26. Luo, J.; Cheng, Z.; Li, C.; Wang, L.; Yu, C.; Zhao, Y.; Yao, Y. Electrically conductive adhesives based on thermoplastic polyurethane filled with silver flakes and carbon nanotubes. Composites Science and Technology, 2016, 129, 191–197. doi:10.1016/j.compscitech.2016.04.026.
27. Bahrami, S.; Solouk, A.; Mirzadeh, H.; Seifalian, A.M. Electroconductive polyurethane/graphene nanocomposite for biomedical applications. Compos. B 2019, 168, 421–431. doi:10.1016/j.compositesb.2019.03.044.
28. Puri, P.; Mehta, R.; Rattan, S. Synthesis of conductive polyurethane/graphite composites for electromagnetic interference shielding. Journal of Electronic Materials, 2015, 44(11), 4255–4268. doi:10.1007/s11664-015-4004-1.
29. Li, F.; Qi, L.; Yang, J.; Xu, M.; Luo, X.; Ma, D. Polyurethane/conducting carbon black composites: Structure, electric conductivity, strain recovery behavior, and their relationships. J Appl Pol Sci, 2000, 75(1), 68–77. doi:10.1002/(sici)1097-4628(20000103)75:1<68::aid-app8>3.0.co;2-i.